T · H · E

OHIO STATE UNIVERSITY

Automated Composite Ellipsoid Modelling for High Frequency GTD Analysis

K.Y. Sze, R.G. Rojas, F.T. Klevenow and J.T. Scheick

The Ohio State University

ElectroScience Laboratory

NASA/Langley Research Center
Hampton, Virginia 23665-5225

A. Approved for public release; Distribution is unlimited

NOTICES

When Government drawings, specifications, or other data are used for any purpose other than in connection with a definitely related Government procurement operation, the United States Government thereby incurs no responsibility nor any obligation whatsoever, and the fact that the Government may have formulated, furnished, or in any way supplied the said drawings, specifications, or other data, is not to be regarded by implication or otherwise as in any manner licensing the holder or any other person or corporation, or conveying any rights or permission to manufacture, use, or sell any patented invention that may in any way be related thereto.

50272-101

REPORT DOCUMENTATION PAGE	1. REPORT NO.	2.	3. Recipient's Accession No.

4. Title and Subtitle	5. Report Date
	September 1991
Automated Composite Ellipsoid Modelling for High Frequency GTD Analysis	6.

7. Author(s)	8. Performing Org. Rept. No.
K.Y. Sze, R.G. Rojas, F.T. Klevenow and J.T. Scheick	722792-2

9. Performing Organization Name and Address	10. Project/Task/Work Unit No.
The Ohio State University	
ElectroScience Laboratory	11. Contract(C) or Grant(G) No.
1320 Kinnear Road	(C) NAG-1-1058
Columbus, OH 43212	(G)

12. Sponsoring Organization Name and Address	13. Report Type/Period Covered
	Technical Report
NASA/Langley Research Center	14.
Hampton, Virginia 23665-5225	

15. Supplementary Notes

16. Abstract (Limit: 200 words)

This report discusses the prelimary results of a scheme currently being developed to fit a composite ellipsoid to the fuselage of a helicopter in the vicinity of the antenna location under the assumption that the antenna is mounted on the fuselage. The parameters of the close-fit composite ellipsoid would then be utilized as inputs into NEWAIR3, a code programmed in FORTRAN 77 for high frequency GTD analysis of the radiation of airborne antennas.

17. Document Analysis   a. Descriptors

HIGH FREQUENCY ANALYSIS   ANTENNA

COMPOSITE ELLIPSOID MODELLING   HELICOPTER FUSELAGE CROSS-SECTIONS

NUMERICAL RESULTS

b. Identifiers/Open-Ended Terms

c. COSATI Field/Group

18. Availability Statement	19. Security Class (This Report)	21. No. of Pages
A. Approved for public release;	Unclassified	183
Distribution is unlimited.	20. Security Class (This Page)	22. Price
	Unclassified	

Contents

List of Figures

List of Tables

Chapter 1

Introduction

In the world of electromagnetics, high frequency radiation and scattering analyses are very often encountered. A great many techniques have been developed for such purposes. One of these techniques is the Geometrical Theory of Diffraction (GTD) analysis [3] [4] [1]. This is a high frequency technique that applies to analyzing both the near field as well as the far field electromagnetic problems. It should be noted that in the near field region, measurements can easily be performed to verify the accuracy of the GTD analysis. However, in contrast to measured near field results, the GTD solutions can easily be extended to the far field computation without employing any transformations [1].

1.1 Fundamentals of GTD

The GTD analysis is a high frequency approach developed by J.B. Keller and his associates at the Courant Institute of Mathematical Sciences [5] in the late 1950s. Within the asymptotic high frequency solution of Maxwell's Equation, geometrical optics (GO) is the dominant term in the lit region [5]. As such, GO is also the influential term in the GTD solution. The scheme involves the inclusion of diffracted fields which is an extension of GO through a generalization of Fermat's Principle (this principle will be discussed subsequently in this section). In the GTD analysis, diffraction is a local phenomenon, because, it depends only on the nature of the

boundary surface and the incident field in the neighborhood of the point of diffraction. Consequently, the diffracted wave propagates such that: (1) power is conserved in a tube (or strip of rays), and (2) the phase delay along the ray path equals the product of the wave number of the medium and the distance. All these are in fact postulates of Keller's theory, now popularly known as GTD [5].

Nonetheless, a profound difficulty in GTD was the discontinuity at reflection and shadow boundaries [5]. As a result, Uniform GTD (UTD) [5] [7] was developed at the ElectroScience Laboratory in the 1970s. In this theory, the diffracted field compensates for the discontinuity at those boundaries. Hence, the total field for the high frequency is uniformly continuous away from the source. With this technique, high frequency analysis may be performed on objects which are as small as a wavelength. In addition, it allows the partitioning of the entire problem into smaller isolated modules for special analysis, unlike the low frequency Moment Method (MM) which requires that the entire body be accounted for. This is especially useful when determining the source of a particular field contribution so that appropriate measures may be undertaken.

In general, with reference to Figure 1.1, Fermat's Principle applied to GTD is stated as follows [6]:

> *The diffracted rays connecting two points Q and P in the exterior of
> the convex body are those linking Q and P which have stationary (optical)
> lengths among all curves from Q to P having an arc on the body surface.*

In Figure 1.2, the diffraction on a smooth, convex, perfectly conducting surface is illustrated schematically [5]. It should be noted that the radius of curvature of the convex surface is large in terms of wavelength. Region I in the figure is the lit region. This region is associated with the GO incident and reflected ray optical fields. Region III, on the other hand, is the shadow region in which only the surface diffracted rays are of concern. Between these two regions is Region II which contains the shadow boundary that separates the lit and the shadow regions. In fact, this is a

GEODESIC ARC ON
SURFACE FROM Q_1
TO P_1

STRAIGHT LINE TANGENT
TO SURFACE AT Q_1

Q_1

P_1

Q

P

CONVEX SURFACE

STRAIGHT LINE TANGENT
TO SURFACE AT P_1
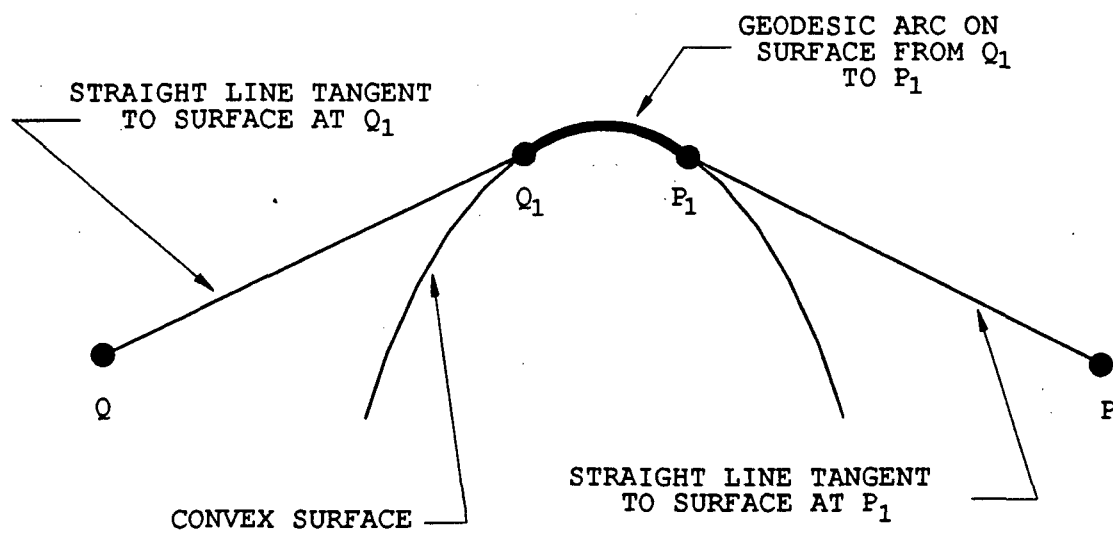
Figure 1.1: A schematic illustrating Fermat's Principle.
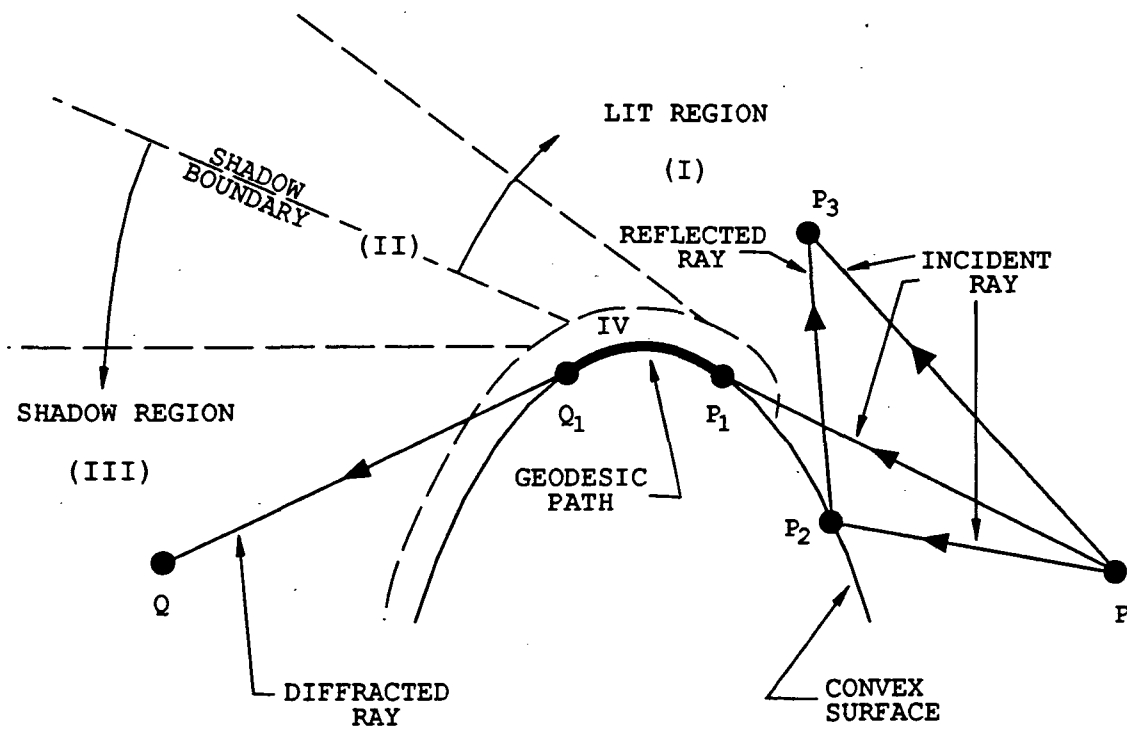
Figure 1.2: Diffraction on a smooth, convex, perfectly conducting surface.

4

transitional region, whereby, with regards to the UTD solution, the ray optical field description is transformed gradually from the GO field in Region I to the surface diffracted field in Region III. On the convex surface, at point P_1, the incident ray launches a surface ray that propagates into the shadow region (Region III) along a geodesic path to point Q_1, as stipulated by Fermat's Principle.

An application of GTD (herewith, the term GTD implies UTD as well) involves the modelling of complicated structures using a combination of simple geometries in which the GTD solution is easily determined. Furthermore, structures very far away from the source location in terms of wavelength or deep into the shadow region may be in some instances neglected. An example of such an application is the Aircraft Code developed for high frequency GTD analysis of airborne antennae.

1.2   The Aircraft Code - NEWAIR3

The Aircraft Code is a computer code written in FORTRAN 77 for high frequency GTD analysis of antennae mounted on aircraft fuselages [1]. This code was developed at ESL and NEWAIR3 is the third version of the original code.

The output solution of NEWAIR3 is in fact computed using the GTD high frequency approach. It is a GTD code capable of near- and far-field analyses. Field contribution from any secondary source, that is, field not directly originating from the primary source which is the antenna itself, may be isolated for separate analysis. Futhermore, it allows the user to determine the individual contributions from various field components such as the direct source radiation, reflection, and diffraction. Each combination of reflections and diffractions may also be considered individually, as described in [1].

For executing NEWAIR3 the aircraft structure must be simulated using a composite ellipsoid and a set of flat, finite polygonal plates, such that the antenna mounted on the aircraft fuselage is positioned on the ellipsoid surface. This implies

that the composite ellipsoid should closely approximate the fuselage surface. The composite ellipsoid in this context is defined as a close-fit composite ellipsoid.

A good fit in the vicinity of the antenna location must be obtained, if for some reasons a good global fit of the entire fuselage cannot be achieved. This is attributed to the fact that, in the high frequency GTD analysis, the fuselage is assumed to be very large in terms of wavelength, and as such, portion of the fuselage that is far away in terms of wavelength has very small influence on the computed solution. An example of a composite ellipsoid is illustrated in Figure 1.3. The definitions of the parameters A_0, B_0, C_0 and D_0 utilized in the figure will be presented in Chapter 2, together with a detailed description of the composite ellipsoid itself.

As far as the plates are concerned, the corners of the plate must be defined in accordance with the Right-hand Rule [1]. With the right-hand thumb pointed towards the lit region, the four other fingers of the right-hand should follow the edges of the plate all around. Hence, the order by which the corners of the plate are input into the code is specified by the order by which the fingers encounter the corners, as illustrated in Figure 1.4. If, in any case, the plate is to be attached onto the composite ellipsoid, the plate corners should then be specified such that the first and the last corners would be the two corners to be attached to the ellipsoid.

Due to the nature of the GTD approach, NEWAIR3 has certain limitations. For the composite ellipsoid, the radii of curvature in its principle planes at the antenna location must be at least a wavelength in extent. As for the plates, the direct distance between any two corners of any plates should be at least a wavelength apart, but in some cases, may be decreased down to only a quarter wavelength [1]. In addition, the antenna should be placed at least a wavelength away from any edges and corners.

In fact, the entire composite ellipsoid and plate information, together with all other essential data which would not be discussed here, are input into NEWAIR3 in the form of an input file, as described in [1].

6
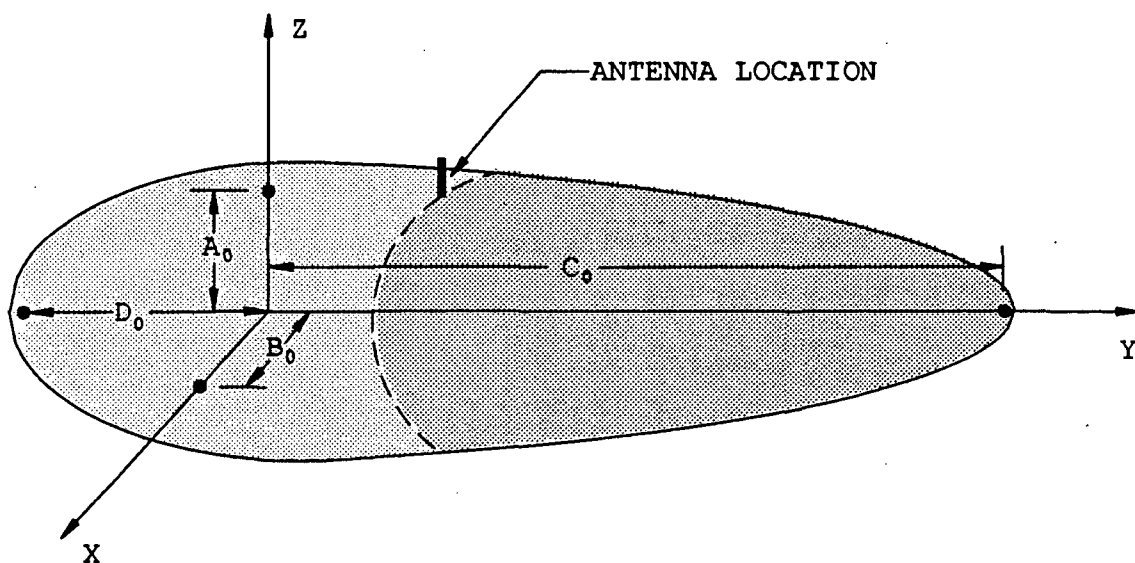
Figure 1.3: An example of a composite ellipsoid for inputting into NEWAIR3.

DIRECTION TOWARDS
THE LIT REGION

1

2

4

3
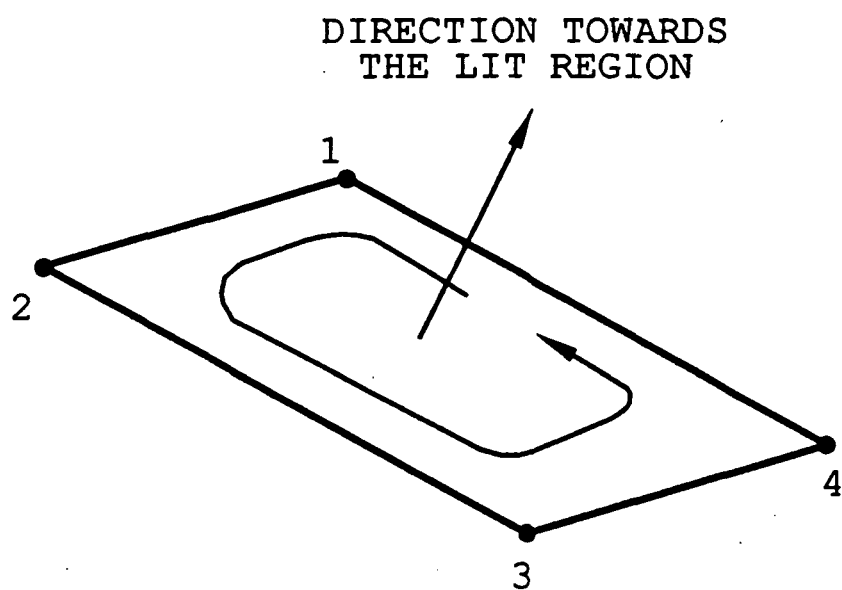
Figure 1.4: An illustration of the use of the Right-hand Rule for defining the corners of a flat polygonal plate. In this figure, the order by which the corners are input into NEWAIR3 is in accordance with the numerical labels of the corners.

1.3 The HARP Code

At ESL, the development of an integrated software package for analyzing the far-field radiation and scattering phenomena of an antenna mounted on a helicopter is currently underway. The code is formally known as the *H*elicopter *A*ntenna *R*adiation *P*rediction (HARP) Code [2]. It will be a computer code that integrates advance computer graphics together with the GTD and the Moment Method (MM) [8] numerical techniques. It will be executed on a Tektronics 4337 3D Graphics Workstation through a user interface driven by an X Windows menu.

Assuming that the cross-sections of the actual helicopter fuselage are symmetrical in terms of its left and right side, only points on the right half portion of the cross-section is input. A form of spline-fitting procedure is then performed on these data points to obtain a smooth and accurate representation of the right half portion of the actual cross-section [2]. Subsequently, the left half of the remaining portion is obtained by reflecting the right half on a centerline PQ, as illustrated in Figure 1.5. The right half portion, together with its reflected image which represents the left half, form a complete cross-section model of the actual fuselage of the helicopter.

For the entire code itself, the XYZ-coordinate system depicted in the Figure 1.5 is utilized, with the y-component increasing towards the tail end of the helicopter. The cross-section illustrated in the figure will now be referred to as the XZ-plane cross-section. The positions of the points on the cross-section are defined in terms of parameters y and T, where y is the y-component of the coordinate system utilized in the code, and T is the normalized arc-length of the cross-section contour. Directly at the top of the fuselage, the value for parameter T is zero, or 1. On the other hand, directly at the bottom of the fuselage, the value for T is 0.5. Once defined, the cross-sections are assembled to create a smooth continuous representation of the entire helicopter fuselage, as illustrated in Figure 1.6 and Figure 1.7. Fins of the helicopter, if any, on the other hand, may be modelled by the flat polygonal plates described in Section 1.2.

9

1.4 GTD in HARP and ELLC

For the high frequency end of the HARP code, the entire helicopter is modelled by a composite ellipsoid and flat plates which were described in Section 1.2, with the condition that the composite ellipsoid fits well the surface of the helicopter fuselage in the vicinity of the antenna location. It is indeed desirable that such modelling be undertaken automatically without any user interaction.

As such, the automated fitting of the composite ellipsoid to the fuselage surface is achieved through the development of the *ELL*ipsoid *C*ode (ELLC), which essentially provides the parameters necessary for constructing the composite ellipsoid. In spite of this, the automation of the plate modelling module, hereby referred to as the PLATES code, is yet to commence. Eventually, nevertheless, the outputs of ELLC and PLATES would be merged into a data file for inputting into NEWAIR3 then employed to perform the near- and far-field GTD analysis for HARP. Figure 1.8 illustrates a simplified flow diagram of HARP, emphasizing on the detailed location of ELLC with respect to other modules. In order to execute ELLC, two types of

10
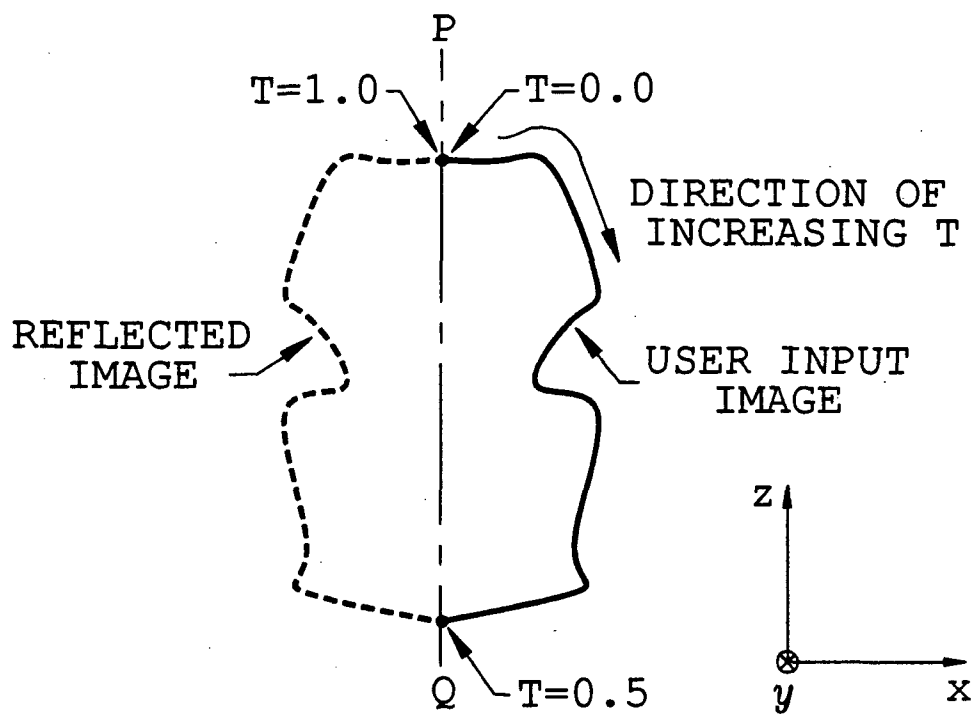
Figure 1.5: An example of a fuselage cross-section of a helicopter input into the HARP Code. Only the right half of the actual cross-section is input, with its reflected image representing the left half of it.
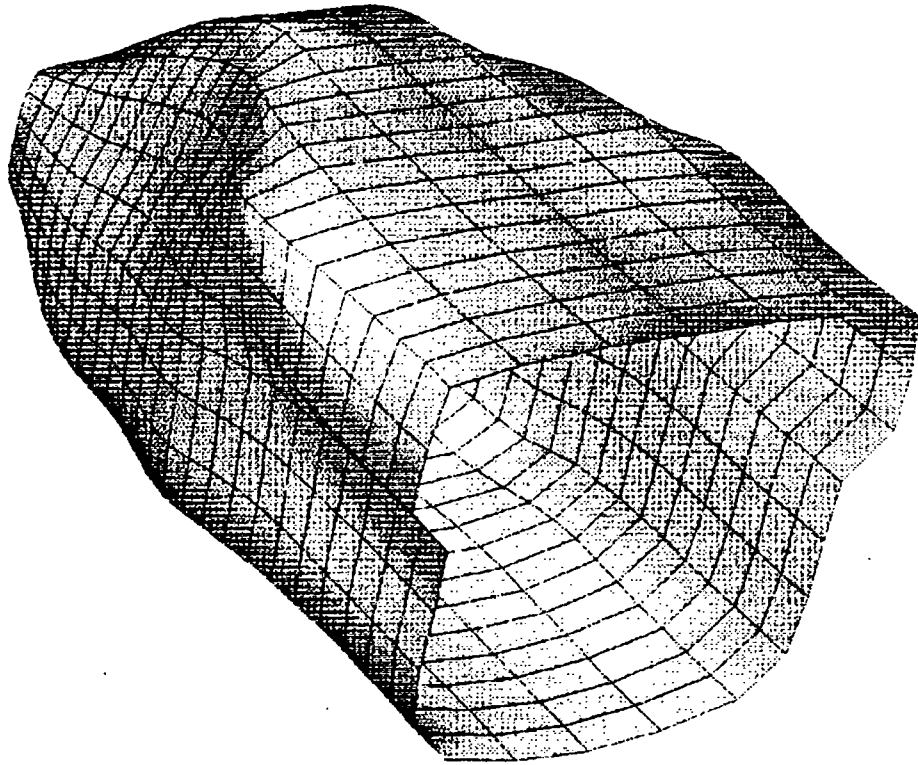
Figure 1.6: Cross-sections are assembled to create a smooth continuous representation of the entire helicopter fuselage.
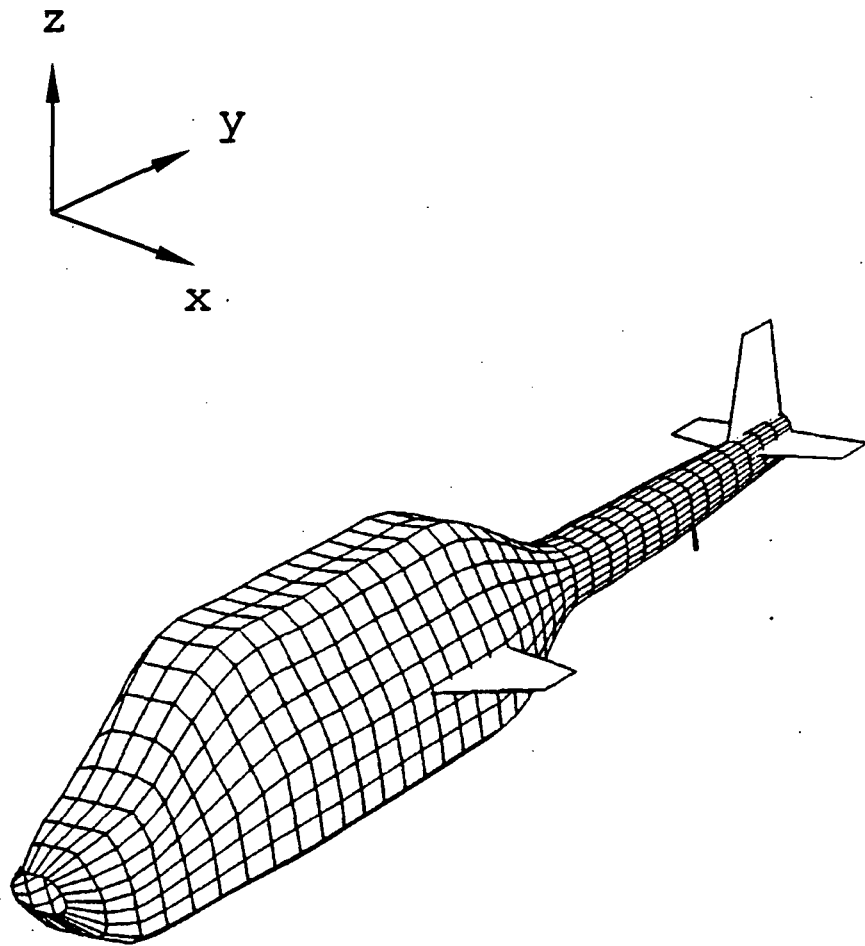
Figure 1.7: A smooth continuous surface representation of a helicopter fuselage.

information from HARP must be provided. These are:

1. the spline-fitted cross-section of the fuselage, and

2. the antenna location, also known as the source point, in terms of parameters y and T.

In ELLC, the actual 3-dimensional problem of fitting a composite ellipsoid to the surface fuselage of the helicopter in the vicinity of the antenna location is divided into two 2-dimensional problems:

1. The problem of fitting an ellipse to the surface of the cross-section in the XZ-plane.

2. The problem of fitting a composite ellipse to the surface of the cross-section in the YR-plane.

Details of these problems will be provided in Chapter 2.

MM ←——————— HARP

ELLC   PLATES

NEWAIR3

↓

OUTPUT
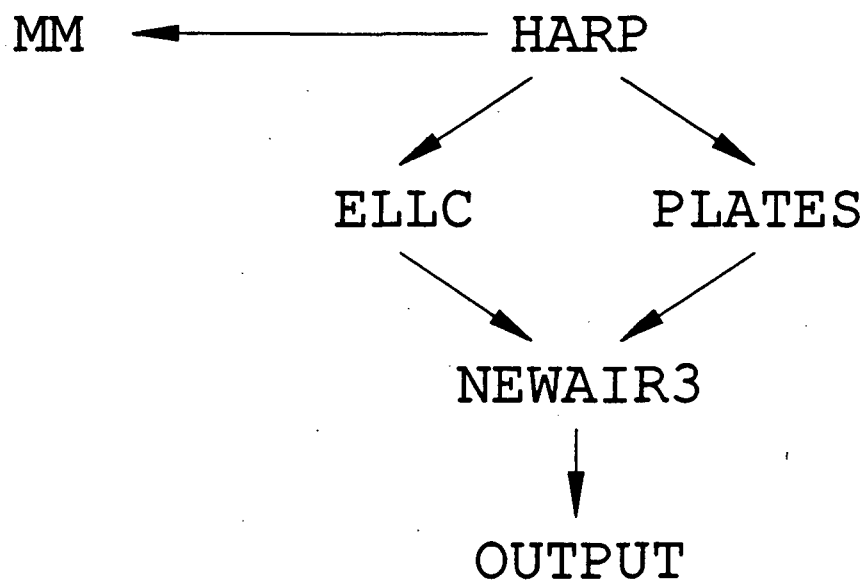
Figure 1.8: A simplified flow diagram of HARP, with special details illustrating the location of ELLC with respect to other modules.

Chapter 2

Theories and Concepts

In Chapter 1, it has been pointed out that the utilization of NEWAIR3 in HARP necessitates that the helicopter fuselage be modelled using a composite ellipsoid and a set of flat, finite polygonal plates. The computer code for automatically generating the parameters for constructing the composite ellipsoid is essentially provided by ELLC. It is important to note that the scheme described in this report to fit the composite ellipsoid to the helicopter fuselage in the vicinity of the antenna location is a preliminary result. Several improvements have been made to the technique discussed here, which will be reported at a later date. This chapter contains the theoretical descriptions of the theories and concepts employed in ELLC. An important point to note is that the whole idea of such a surface modelling is founded on the fact that it depends heavily on the mathematical, as well as the graphical, interpretations of the actual surface and how precise a fit is to be achieved.

2.1 The composite ellipsoid

Prior to the development of ELLC, the parameters of the composite ellipsoid must first be explicitly defined. Therefore, the material on composite ellipsoid presented in [1] will be discussed in this section, but in the terms of notations and conventions utilized in HARP, which would also be utilized in ELLC.

For this application, the composite ellipsoid is actually constructed of two el-

lipsoid sections fused together back to back at the antenna location (X_s, Y_s, Z_s) such that the resulting surface is continuous and smooth at that interface. In other words, the first-order derivative of the surface at the interface must be continuous. 2-dimensional schematic views of the composite ellipsoid construction are illustrated in Figure 2.1 and Figure 2.2. As is depicted in these figures, the center of the composite ellipsoid is assigned the parameters (X_c, Y_c, Z_c). Solid lines are employed to represent sections of the ellipsoid that are utilized for constructing the composite ellipsoid, whereas dashed lines are employed to indicate those that are discarded.

Since the composite ellipsoid is constructed of two individual ellipsoid sections, there are two ellipsoid centers in which one is shifted a value Y_{sh} along the y-axis from the other. Each of these centers is an origin of a coordinate system. Hence, two coordinate systems are employed in the composite ellipsoid construction, with one shifted a value Y_{sh} along the y-axis from the other. The computation of the parameter Y_{sh} will be presented in Section 2.5.

Prime notations will be used to represent parameters referenced to the shifted coordinate system. The term "right ellipsoid" will be used to refer to the ellipsoid whose center is located to the right of the center of the other, which in the figures, is the ellipsoid whose center is shifted a value Y_{sh}. On the other hand, the term "left ellipsoid" will refer to the ellipsoid whose center is located to the left of the center of the other, which is the ellipsoid whose center is unshifted. The unshifted coordinate system is also utilized for dimensioning the composite ellipsoid. Hence, it is a coordinate system associated with the composite ellipsoid, with the origin being the center (X_c, Y_c, Z_c) of the composite ellipsoid itself. For the ease of referencing, the case for which $Y_s \geq Y_c$ is referred to as Case 1, and that for which $Y_s < Y_c$ is referred to as Case 2.

Referring to Figure 2.1, which is the composite ellipsoid schematic for Case 1, the semi-axes of the "left ellipsoid" are A_F, B_F and C_F. As for the "right ellipsoid", the semi-axes are A'_F, B'_F and D'_F. The sections where $y < Y_s$ (that is, the left sections)

17

(a) CASE 1 $(Y_s \geq Y_c)$: SIDE VIEW

(b) CASE 1 $(Y_s \geq Y_c)$: TOP VIEW

Figure 2.1: 2-dimensional schematic views of a composite ellipsoid constructed from two ellipsoids for Case 1, where $Y_s \geq Y_c$. Solid lines represent sections of the ellipsoids utilized for creating the composite ellipsoid. Dashed lines represent sections of the ellipsoids discarded.
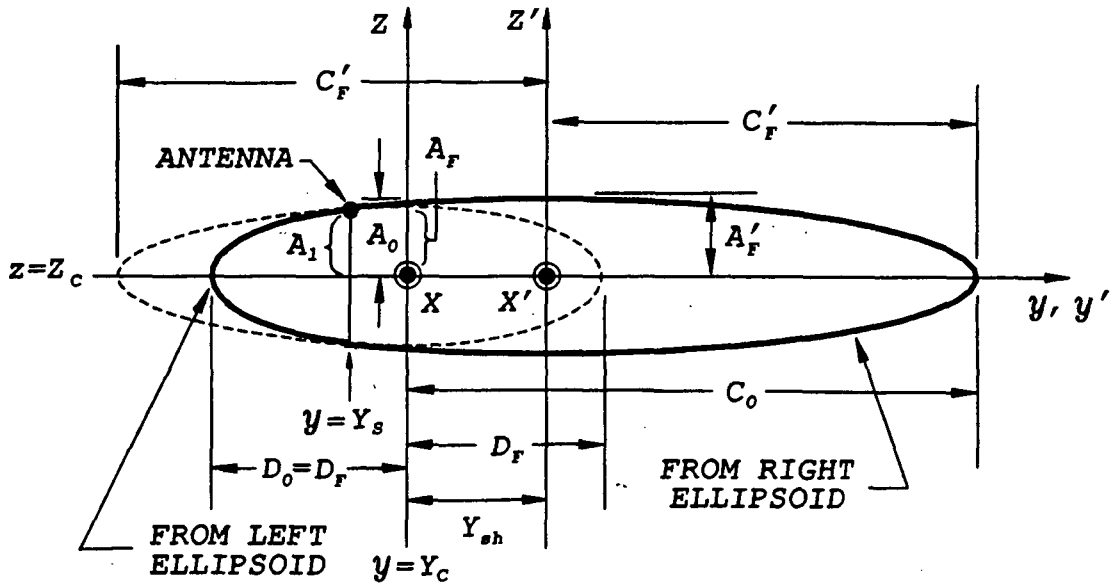
(a) CASE 2 $(Y_s < Y_c)$: SIDE VIEW
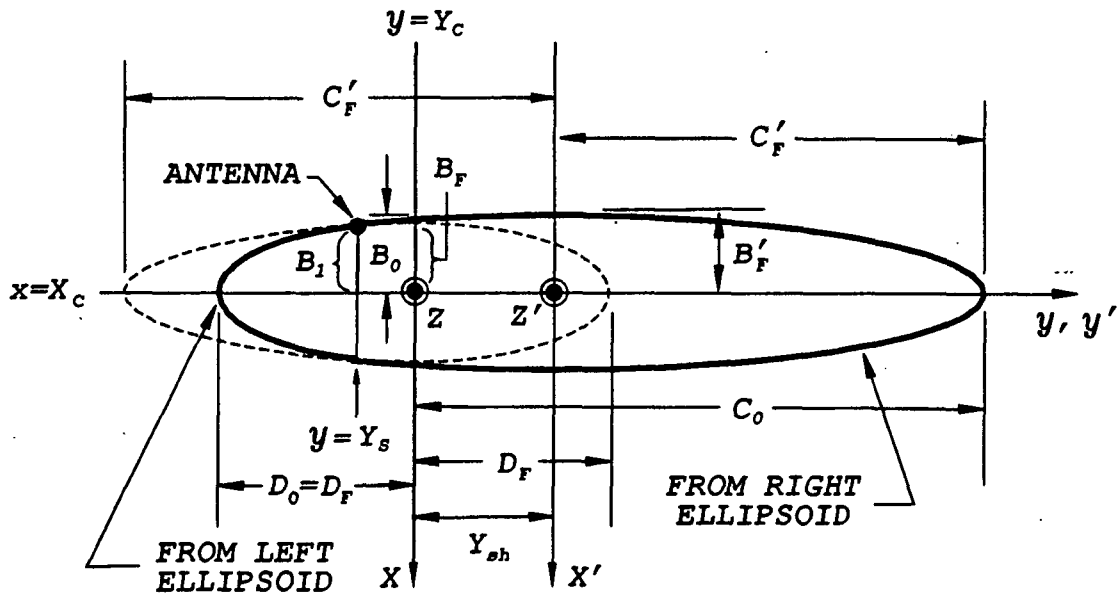
(b) CASE 2 $(Y_s < Y_c)$: TOP VIEW

Figure 2.2: 2-dimensional schematic views of a composite ellipsoid constructed from two ellipsoids for Case 2, where $Y_s < Y_c$. Solid lines represent sections of the ellipsoids utilized for creating the composite ellipsoid. Dashed lines represent sections of the ellipsoids discarded.

of the "right ellipsoid" and the sections where $y \geq Y_s$ (that is, right sections) of the "left ellipsoid" are interfaced together at $y = Y_s$ to form a composite ellipsoid. This is in fact the interface on which the antenna is located. The cross-section of the composite ellipsoid at $y = Y_s$ is located in an XZ-plane at $y = Y_s$. In this plane, the cross-section is an ellipse with semi-minor axis A_1 and semi-major axis B_1. The parameters representing the dimensions of the composite ellipsoid are A_0, B_0, C_0 and D_0. For Case 1, A_0 is the distance from the center of the composite ellipsoid to the point of intersection of the z-axis with the surface of the composite ellipsoid. Similarly, B_0 is the distance from the center of the composite ellipsoid to the point of intersection of the x-axis with the surface of the composite ellipsoid. However, since the right most end of the composite ellipsoid is also the right most end of the "left ellipsoid", the semi-axis C_F of the "left ellipsoid" is also the parameter C_0 of the composite ellipsoid. The parameter D_0, on the other hand, is the distance from the center of the composite ellipsoid to the left most end of the composite ellipsoid. This, in fact, is represented by $D'_F - Y_{sh}$.

As for Case 2, the schematic of the composite ellipsoid is illustrated in Figure 2.2. The semi-axes of the "left ellipsoid" as well as the "right ellipsoid" in this case are assigned the same labels as those for Case 1. For Case 2, the sections where $y < Y_s$ (that is, the left sections) of the "left ellipsoid" and the sections where $y \geq Y_s$ (that is, right sections) of the "right ellipsoid" are interfaced together at $y = Y_s$ to form a composite ellipsoid. Again, this interface is where the antenna is located, and the cross-section of the composite ellipsoid at $y = Y_s$ is contained in an XZ-plane at $y = Y_s$. In this plane, the cross-section is an ellipse with semi-minor axis A_1 and semi-major axis B_1. However, the dimensioning parameters A_0, B_0, C_0 and D_0 of the composite ellipsoid are now represented differently, except for the parameters A_0 and B_0 which are defined similarly as those in Case 1. The parameter C_0 in this case is now the distance from the center of the composite ellipsoid to the right most end of the composite ellipsoid. This is represented by $C'_F + Y_{sh}$. As for the parameter

D_0, it is represented by the semi-axis D_F of the "left ellipsoid", since the left most end of the composite ellipsoid is also the left most end of the "left ellipsoid".

2.2 The approach

At the present moment, the fuselage surface of the helicopter fuselage is provided in the form of on-line computer data files. With such information, the actual contour of the helicopter fuselage is simulated using a form of spline-fitting technique. As a result, the helicopter fuselage is made available in the form of cross-section cuts along the y-axis of the helicopter coordinate system depicted in Figure 1.7 of Chapter 1. In this section, a brief outline of the approach employed in ELLC for generating the composite ellipsoid will be presented.

It should be anticipated that the actual fuselage surface of the helicopter would contain convex surfaces as well as concave ones, the quantity of these being dependent on the particular design of the helicopter. Therefore, a distinct convention is employed to identify such surface types. With reference to Figure 2.3 (a), a surface in the vicinity of a point location A on the helicopter fuselage is defined as convex if the surface in the vicinity of that particular point, that is, the portion of the surface within the dashed circle in the figure, forms a convex arc relative to the unit normal vector $\hat{n}$ of the surface at that point. On the other hand, referring to Figure 2.3 (b), a surface in the vicinity of a point location B on the helicopter fuselage is defined as concave if the surface in the vicinity of that particular point, that is, the portion of the surface within the dashed circle in the figure, forms a concave arc relative to the outward unit normal vector $\hat{n}$ of the surface at that point.

In Section 2.1, it is mentioned that the close-fit composite ellipsoid can be generated by specifying a set of four parameters A_0, B_0, C_0 and D_0, as well as the center (X_c, Y_c, Z_c) of the composite ellipsoid itself. As pointed out in Chapter 1, the task of fitting a composite ellipsoid to the helicopter body has been divided into several steps. First an ellipse is fit to the X-Z cross-section of the body at the antenna
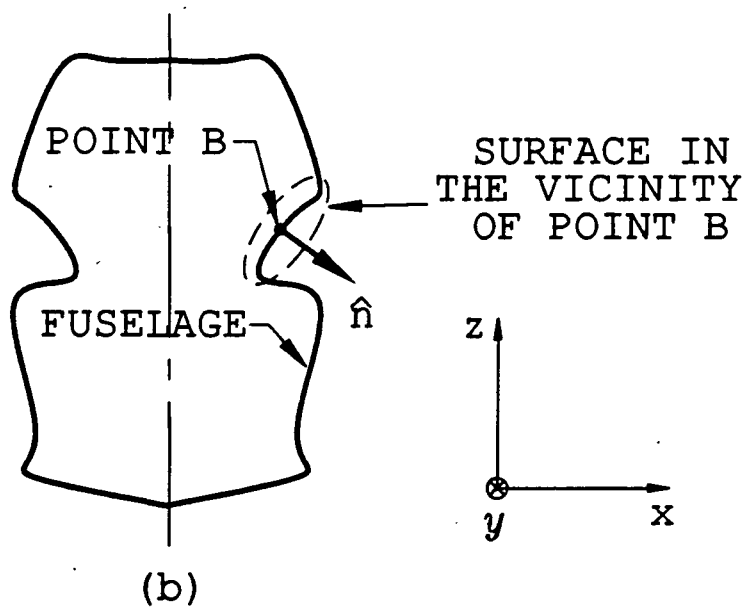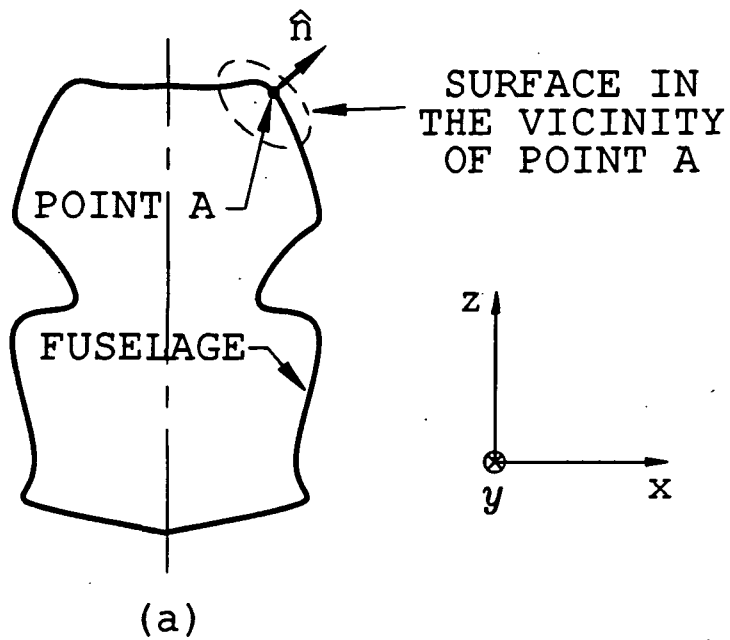
Figure 2.3: (a) A figure of a convex surface in the vicinity of a point A on the fuselage surface, and (b) A figure of a concave surface in the vicinity of a point B on the fuselage surface.

location. Second, a composite ellipse is fit to the Y-R section of the body, also at the antenna location. This Y-R section is a plane containing the antenna location and the center of the X-Z ellipse; this plane is parallel to the Y-axis. Below are described the algorithms which determine the best-fit X-Z ellipse, which generate points on the body in the Y-R plane and an algorithm which determines the best-fit in the Y-R plane.

1. The problem of fitting an ellipse to the surface of the cross-section in the XZ-plane at the antenna location:

   In this problem, the fuselage cross-section in the XZ-plane at $y = Y_s$ is of particular interest. The close-fit ellipse to the surface of the cross-section in the XZ-plane at the antenna location is obtained through the evaluation of the center (X_c, Z_c) of the close-fit ellipse and its semi-minor axis A_1 and semi-major axis B_1. Data points on the cross-section at specific intervals in the proximity of the antenna location are utilized for such purpose. A schematic of the close-fit ellipse is illustrated in Figure 2.4.

   It should be noted that, in certain cases, due to the nature of the data points, numerically accurate solutions could not be obtained. Therefore, for such cases, a form of a perturbation technique is applied to the data points. This procedure shifts some points to a new position such that good numerical approximations can be generated.

2. The problem of fitting a composite ellipse to the surface of the cross-section in the YR-plane at the antenna location:

   Once a close-fit ellipse to the cross-section in the XZ-plane at the antenna location is obtained, a YR-plane can be constructed. Referring to Figure 2.4, an R-axis is created from the extrapolation of the radial line from the center (X_c, Z_c) of the close-fit ellipse to the antenna location on the fuselage surface. The $R = 0$ line, which is orthogonal to the XZ-plane, is defined to coincide
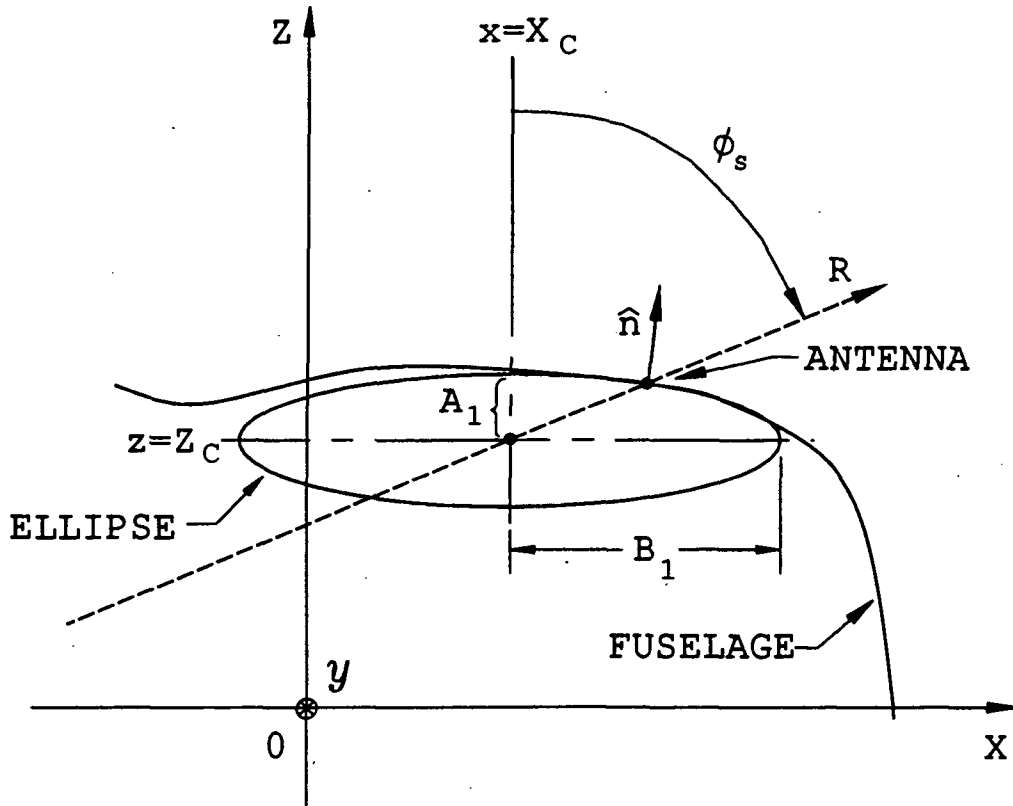
Figure 2.4: A schematic of a close-fit ellipse to the surface of the cross-section in the XZ-plane at the antenna location. The point at (X_c, Z_c) is the center of the close-fit ellipse, and A_1 and B_1 are its semi-minor and semi-major axes, respectively. Vector ñ is the outward unit normal vector of the fuselage surface at the antenna location.

with the horizontal axis of the composite ellipsoid that is orthogonal to the XZ-plane. The direction of increasing R is the direction such that an increase in R always implies an increase in z. The plane containing this R-axis that is orthogonal to the XZ-plane is the YR-plane. Indeed, the YR-plane is inclined at an angle ϕ_s from the minor (vertical) principle plane of the close-fit ellipse.

For obtaining the fuselage cross-section in the YR-plane, the intersection of the fuselage surface with the YR-plane is traced out. This is achieved by obtaining a data point at each specific interval DY to the front and rear of the antenna location in the YR-plane. Since the tail end of the helicopter fuselage is towards the direction of increasing y, the phrase "front of the antenna location" is defined as referring to the portion of the cross-section in the YR-plane immediately to the front of the antenna location in the direction of decreasing y, and the phrase "rear (or back) of the antenna location" as referring to the portion of the cross-section in the YR-plane immediately to the rear of the antenna location in the direction of increasing y. Interpolating these adjacent data points with straight lines, a continuous line modelling the actual surface of the cross-section in the YR-plane in the vicinity of the antenna location is created. This is illustrated in Figure 2.5.

For ELLC, the antenna location is input using the coordinate form (Y_s, T) corresponding to the coordinate (X_s, Y_s, Z_s) of the antenna location. In fact, Y_s is the y-component of the coordinate of the antenna location. It indicates particular cross-section in the XZ-plane on which the antenna is located. T, on the other hand, is the normalized arc-length from $T = 0$ to the antenna location on the XZ-plane cross-section at $y = Y_s$. Details of the parameter T has been presented in Section 1.3. Once the data points in the YR-plane are determined, a close-fit composite ellipse to the surface of the cross-section in the YR-plane at the antenna location is generated through the evaluation of the parameters C_0, D_0, Y_c and Y_{sh}.
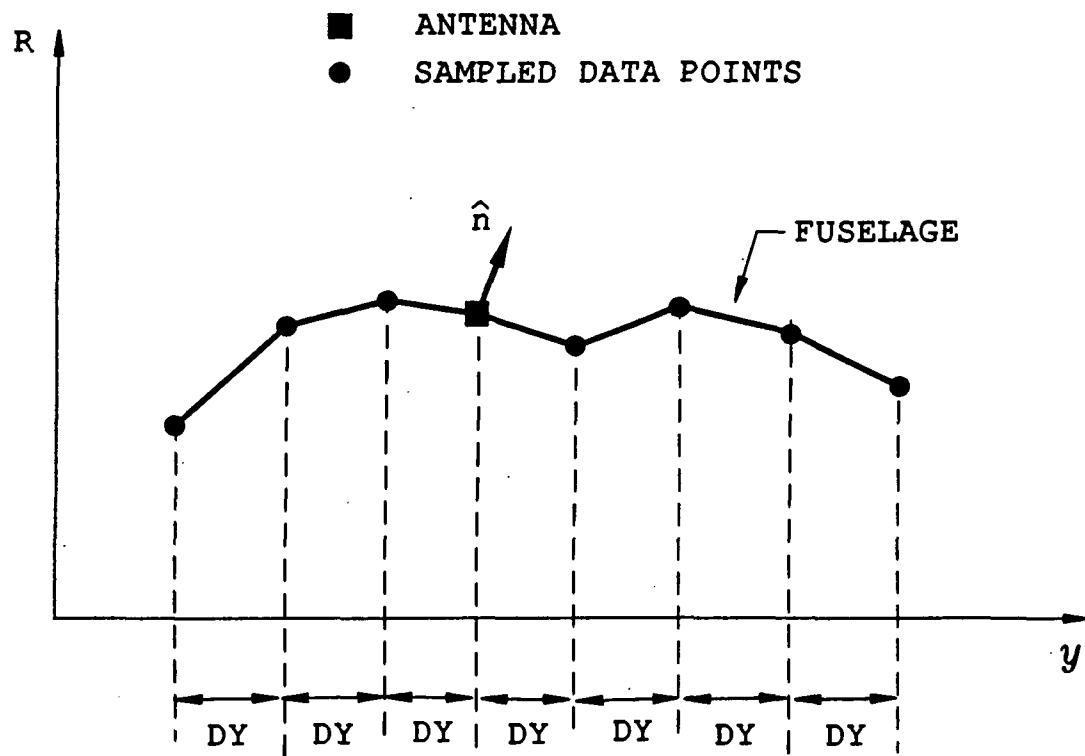
Figure 2.5: A schematic of a portion of the fuselage surface in the YR-plane as formed by the antenna location and the data points determined through the intersection of the fuselage surface with the YR-plane. Note that DY is the sampling distance of the data points in the YR-plane, and ñ is the outward unit normal vector of the surface at the antenna location.

26

The remaining parameters of the composite ellipsoid that is yet to be computed are A_0 and B_0. In fact, these parameters are functions of the parameters A_1, B_1, C_0, D_0, Y_c and Y_{sh}, which have been evaluated. Hence, A_0 and B_0 are easily obtainable.

In the subsequent sections, further details of the fitting of the composite ellipsoid to the helicopter fuselage are discussed and appropriate mathematical analysis presented.

2.3 Determination of best-fit X-Z ellipse

This is the first stage for generating the close-fit composite ellipsoid to the actual surface fuselage of the helicopter. Work on this was accomplished by Klevenow and Scheick utilizing the method of least squares [2] [10].

Seven points are taken on the X-Z section near the antenna; the antenna is at (x_4, z_4). These points are generated using the algorithms described in Reference [2] Chapter 3.

The four parameters B,C,D, and E of the best-fit ellipse, namely

$$x^2 + Bz^2 + Cx + Dz + E = 0 \qquad (2.1)$$

are determined by minimizing

$$\frac{1}{2} \sum_{i=1}^{7} (x_i^2 + Bz_i^2 + Cx_i + Dz_i + E)^2 \qquad (2.2)$$

subject to three constraints. The constraints guarantee that the conic section (2.1) is an ellipse and that this ellipse fits onto the inside of the X-Z cross-section.

The constraints are derived by completing the square on equation (2.1); this results in

$$\frac{(x + \frac{C}{2})^2}{FF} + B \frac{(y + \frac{D}{2B})^2}{FF} = 1. \qquad (2.3)$$

This conic section is an ellipse if

$$B > 0 \qquad (2.4)$$

and

$$FF \equiv \frac{C^2}{4} + \frac{D^2}{4B} - E > 0. \qquad (2.5)$$

One of the problems encountered in fitting an ellipse onto the fuselage was that in many cases the ellipse was located on the outside of the X-Z cross section as depicted in Figure 2.6 Thus, a third constraint which guarantees that the ellipse is inside the X-Z cross-section is obtained by requiring that the angle between the unit outward normal at the antenna location, $\hat{n} = (XN, ZN)$, and the vector $\hat{\rho}$ from the center of the best-fit ellipse, $(\frac{-C}{2}, \frac{-D}{2B})$, to the antenna location be $< \frac{\pi}{2}$ in absolute value, where the vectors $\hat{n}$ and $\hat{\rho}$ are shown in Figure 2.7. This amounts to requiring that

$$DRDN \equiv (XN, ZN) \bullet (x_4 + \frac{C}{2}, z_4 + \frac{D}{2B}) > 0. \qquad (2.6)$$

Here

$$(XN, ZN) = \frac{(z_3 - z_5, x_5 - x_3)}{\sqrt{(z_3 - z_5)^2 + (x_5 - x_3)^2}}. \qquad (2.7)$$

This is an approximation to the unit outward normal since the points (x_i, z_i) are taken clock-wise around the cross-section y=constant. The vector (XN, ZN) is obtained by turning the vector from (x_3, z_3) to (x_5, z_5) through $+\frac{\pi}{2}$ and normalizing it. This forces (XN, ZN) to point outward.

To realize constraints (2.4), (2.5), and (2.6) in the minimization of equation (2.2) penalty functions were used. This function is large and positive when the argument is less than a parameter OFFSET=0.2 and is zero otherwise; see Figure 5.12 in [2]. This penalty function is

$$PEN(x) = \begin{cases} (1 - \frac{x}{OFFSET})^3 & x < OFFSET \\ 0 & otherwise \end{cases} \qquad (2.8)$$

The penalty function is used to prevent the minimization algorithm from iterating to a solution where the arguments of the penalty functions are substantially less than OFFSET.

28

Equation (2.2) is minimized subject to the three given constraints by minimizing

$$\psi(B,C,D,E) \equiv \frac{1}{2}\sum_{i=1}^{7}(x_i^2 + Bz_i^2 + Cx_i + Dz_i + E)^2$$
$$+ \ PEN(B) + PEN(FF) + PEN(DRDN) \qquad (2.9)$$

This is done by finding a zero of

$$F(B,C,D,E) \equiv \nabla\psi(B,C,D,E) \qquad (2.10)$$

by a modified Newton-Raphson method. An algorithm has been developed to solve (2.9) subject to the constraints mentioned above.

First, seven points are taken on the X-Z cross-section near the antenna; the antenna is at (x_4, z_4). A band of half-width DD=0.04 is constructed about the line from (x_1, z_1) to (x_7, z_7). If any of the seven points are outside this band in the direction of $-\hat{n}$ the algorithm is stopped and an error flag is set; no attempt is made to fit an ellipse to a portion of the X-Z cross-section of the body which is not approximately convex when viewed from outside the section.

If one of the second thru sixth points is within this band of width 2DD then the portion of the cross-section near the antenna is assumed to be essentially flat and the points are perturbed. This perturbation is done to avoid trying to solve the ill-posed problem of fitting an ellipse to one side of a straight line. This perturbation is achieved by moving (x_4, z_4) by +DD times $\hat{n}$ and by moving (x_1, z_1) and (x_7, z_7) by −DD times $\hat{n}$. The Newton-Raphson method is then used to find the zero of (2.10).

The starting guess for the method is obtained by calculating B,C,D, and E for a circle with radius r=$\sqrt{(x_1 - x_7)^2 + (z_1 - z_7)^2}$ and center at

$$\begin{pmatrix} X_c \\ Z_c \end{pmatrix} = \begin{pmatrix} x_4 \\ x_4 \end{pmatrix} - r * \hat{n}. \qquad (2.11)$$

Setting

$$W_i = \begin{pmatrix} B_i \\ C_i \\ D_i \\ E_i \end{pmatrix} \qquad (2.12)$$

and

$$h = \begin{pmatrix} \Delta B_i \\ \Delta C_i \\ \Delta D_i \\ \Delta E_i \end{pmatrix} \qquad (2.13)$$

the iteration proceeds as follows.

Solve $F(W_i - h) \approx F(W_i) - \nabla F(W_i)h = \vec{0}$ giving

$$h = (\nabla F(W_i))^{-1} F(W_i). \qquad (2.14)$$

This gives a direction h along which a search can be made looking for a value of $|F(W_{i+1})|^2$ smaller than $|F(W_i)|^2$: this is the line search. This line search amounts to choosing a value of the parameter t such that

$$\phi(t) \leq (1 + 2 * 10^{-4} * t)\phi(0) \qquad (2.15)$$

where $\phi(t) \equiv |F(W_i - t * h)|^2$. The first t of the values $1, \frac{1}{2}, \frac{1}{4}, \frac{1}{8}$, etc. which satisfies equation (2.15) is selected; the next iterate is then taken to be $W_{i+1} = W_i - t * h$. This line search guarantees that $|F|^2$ always decreases at each step of the iteration. See Reference [10] §7.5 Armijo's rule. If $2 * 10^{-4} * t$ is less than the computer double precision epsilon the iteration is stopped and an error flag is set. If $|F(W_i)| \leq 10^{-4}$ the iteration is stopped successfully and the ellipse parameters are calculated. No more than 500 iterations are permitted.

2.4 Generating Points on Y-R Section

Before the task of fitting an ellipse in the Y-R plane can be started, it is necessary to generate data points of the fuselage body on this Y-R plane. This is accomplished

as follows. Given an antenna location (y_{ant}, t_{ant}) this algorithm generates one point which is on the intersection of the plane $y = y_{sol}$ and the Y-R section of the aircraft body; this Y-R section is in a plane parallel to the Y-axis and which contains the antenna location and the center, (x_{ce}, z_{ce}), of the best-fit X-Z ellipse to the antenna position. See Figure 2.8.

This point is found by projecting the plane $y = y_{ant}$ in the direction of the y-axis into the plane $y = y_{sol}$. The algorithm finds a point in this composite plane given by (x_{sol}, z_{sol}) on the body section $y = y_{sol}$ so that the angle θ between the vector from (x_{ce}, z_{ce}) to (x_{ant}, z_{ant}) and the vector from (x_{ce}, z_{ce}) to (x_{sol}, z_{sol}) is zero. See Figure 2.9. Note that given values of y and t the algorithms of Reference [2], Chapter 3, are used to generate the corresponding values of x and z.

This angle θ is a function of t which is the parameter which goes from zero to one as you move clock-wise around any body cross-section y=constant. Finding a $t = t_{sol}$ so that $\theta(t_{sol}) = 0$ gives (x_{sol}, z_{sol}): the desired solution point in the plane $y = y_{sol}$.

The initial guess at t_{sol} is provided by the algorithm user; $t_0 = t_{ant}$ is usually a good starting guess. This initial guess must be as close to t_{sol} as possible.

Next a direction of search for the root of $\theta(t)$ is determined. A direction S is selected so that $|\theta(t_0 + S * \Delta t)| < |\theta(t_0)|$. Here $S = \pm 1$ and $\Delta t = \frac{1}{50}$. It is assumed that θ is decreasing in absolute value in this direction S.

The algorithm next searches for an interval of t in which the root of θ lies. The variable t is increased in steps of Δt in direction S until

$$\theta(t_0 + i * S * \Delta t) * \theta(t_0 + (i+1) * S * \Delta t) < 0. \qquad (2.16)$$

The desired root of θ then is in the interval $(t_0 + i * S * \Delta t, t_0 + (i+1) * S * \Delta t)$ since the sign of θ changes in this interval. If no interval can be found where θ changes sign an error flag is set and the algorithm is stopped. This stop condition can occur if the Y-R plane does not intersect the body cross-section at $y = y_{sol}$.

The root t_{sol} of $\theta = 0$ is found by iteration using a combination of the interval halving method and a secant-like methods. At each step of the iteration the width of the interval containing the zero is decreased. At no time is the new iterate produced by the secant-like method allowed to fall outside the given interval.

Each step of the iteration proceeds as follows. An interval in t, (t_L, t_H), is given in which the root of θ is known to lie: θ is of opposite sign at each end of this interval. A new iterate is obtained by the secant-like method using line search . Two points are taken in the interval: $t_1 = t_L + \frac{t_H - t_L}{4}$ and $t_2 = \frac{t_L + t_H}{2}$. A line is constructed thru $(t_1, \theta(t_1))$ and $(t_2, \theta(t_2))$. A direction of line search is determined by the slope of this secant. The next iterate t_{NEW} is selected by a line search in the direction determined by the secant so that $|\theta(t_{NEW})|^2 < |\theta(t_2)|^2$. If t_{NEW} is outside the interval (t_L, t_H) the midpoint of this interval is taken for t_{NEW}: this is where the interval-halving method is used in this algorithm. If $|\theta(t_{NEW})| < 10^{-5}$ the algorithm stops successfully and returns $t_{sol} = t_{NEW}$. If $|\theta(t_{NEW})|$ is still too large a new interval containing the root is obtained from (t_L, t_{NEW}) and (t_{NEW}, t_H) by checking that the sign of $\theta(t)$ at the end points of the intervals. If the signs of θ are opposite at the ends of the interval this guarantees the root is in the interval. The above iteration is repeated at most 100 times.

2.5   A close-fit in the YR-plane

The scheme described here to fit a composite ellipsoid in the YR-plane is a preliminary result which requires further improvement. The method was developed in such a way that only a minimum number of points along the surface of the helicopter are used. Obviously, to obtain a good fit, it will be necessary to use more points along the helicopter surface. A method has been developed by Scheick and Klevenow which uses more points, however, it will not be described here.

In the YR-plane, a close-fit composite ellipsoid is generated using the parameters
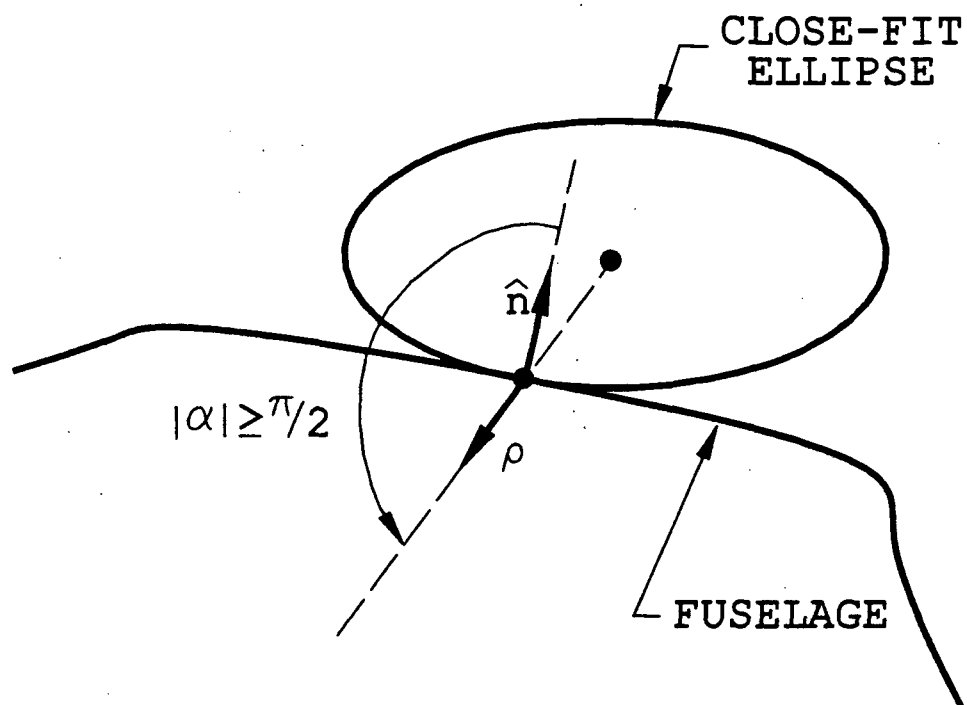
Figure 2.6: A figure of a close-fit ellipse on the undesirable side of the fuselage surface with $| \alpha | \geq \frac{\pi}{2}$.
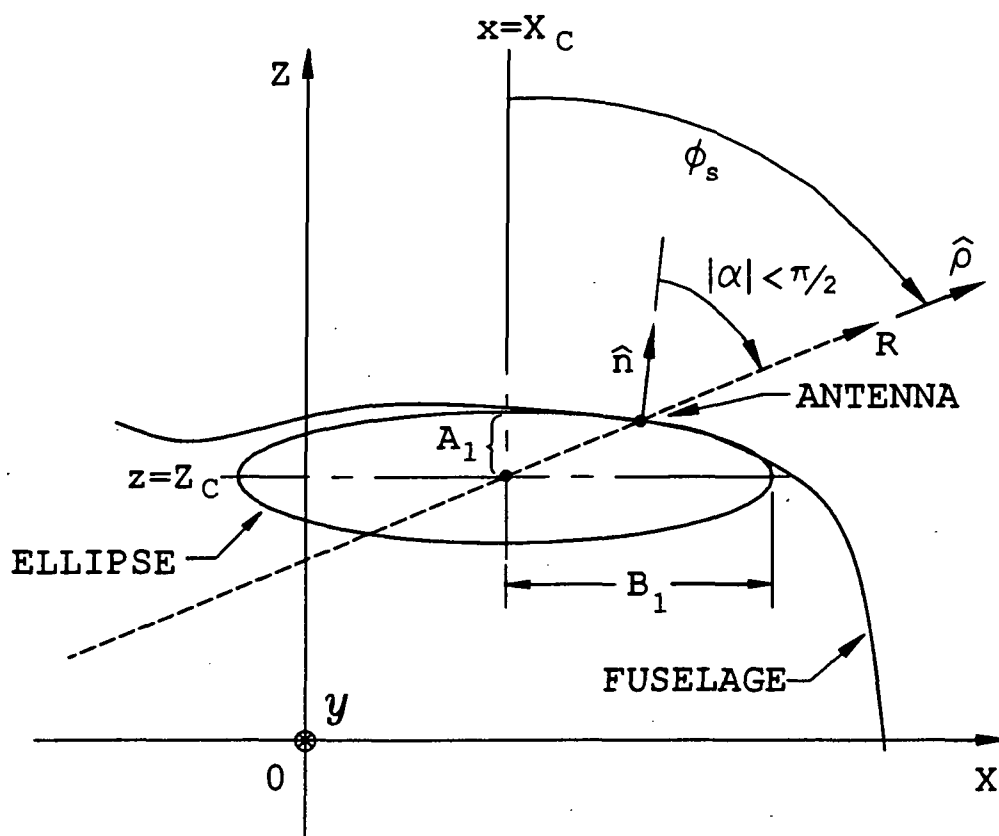
Figure 2.7: A close-fit ellipse in the XZ-plane at $y = Y_s$ with $\mid \alpha \mid < \frac{\pi}{2}$.

Y-R SECTION FOR
GIVEN ANTENNA POSITION

DESIRED
SOLUTION
POINT

ANTENNA (y_{ant}, z_{ant})

CENTER OF
BEST-FIT ELLIPSE
AT ANTENNA (x_{ce}, z_{ce})
IN $y=y_{ant}$ PLANE

SECTION AT
$y=y_{sol}$
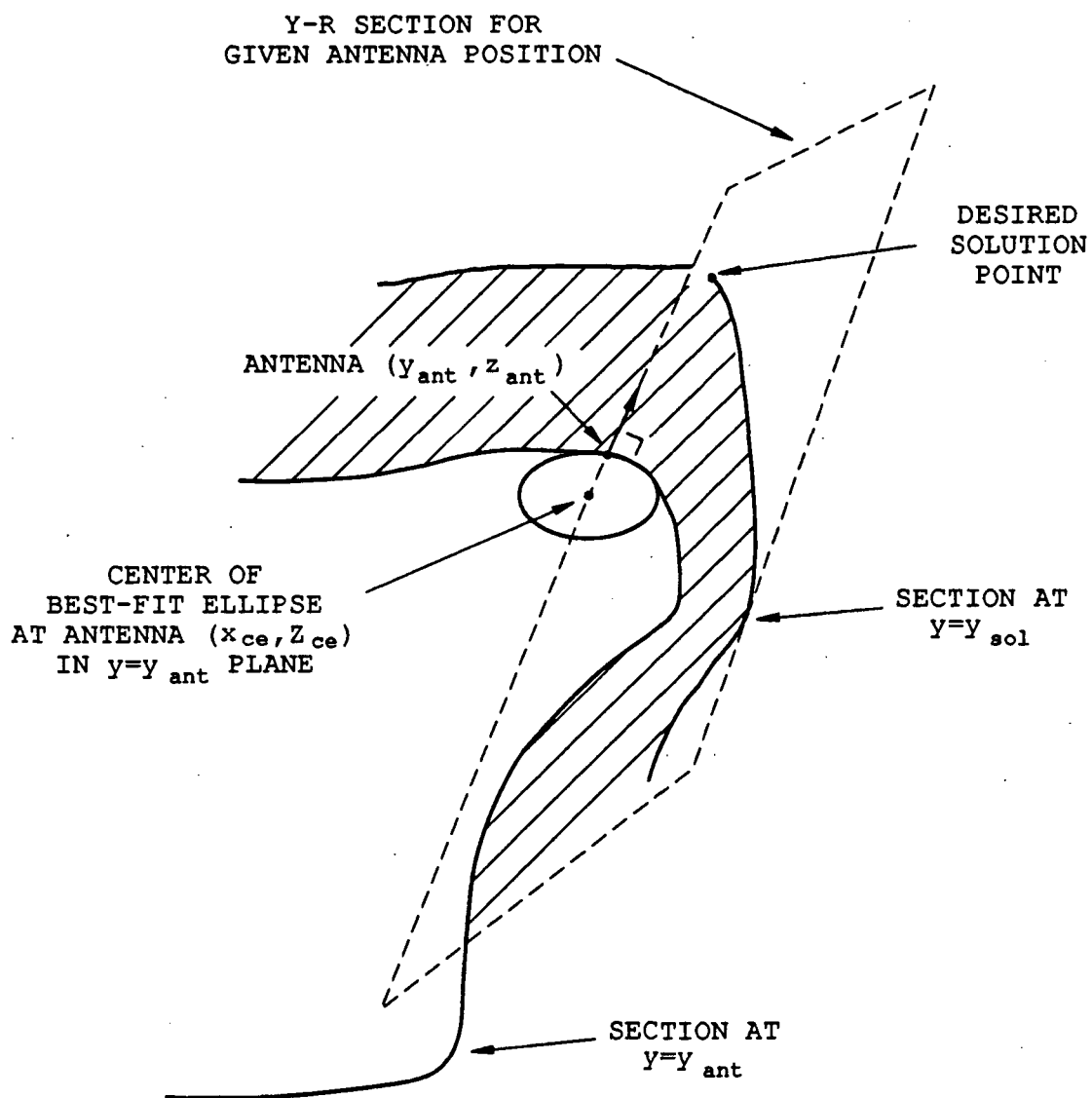
SECTION AT
$y=y_{ant}$

Figure 2.8: Interaction of the Y-R and $Y = Y_{sol}$ planes.
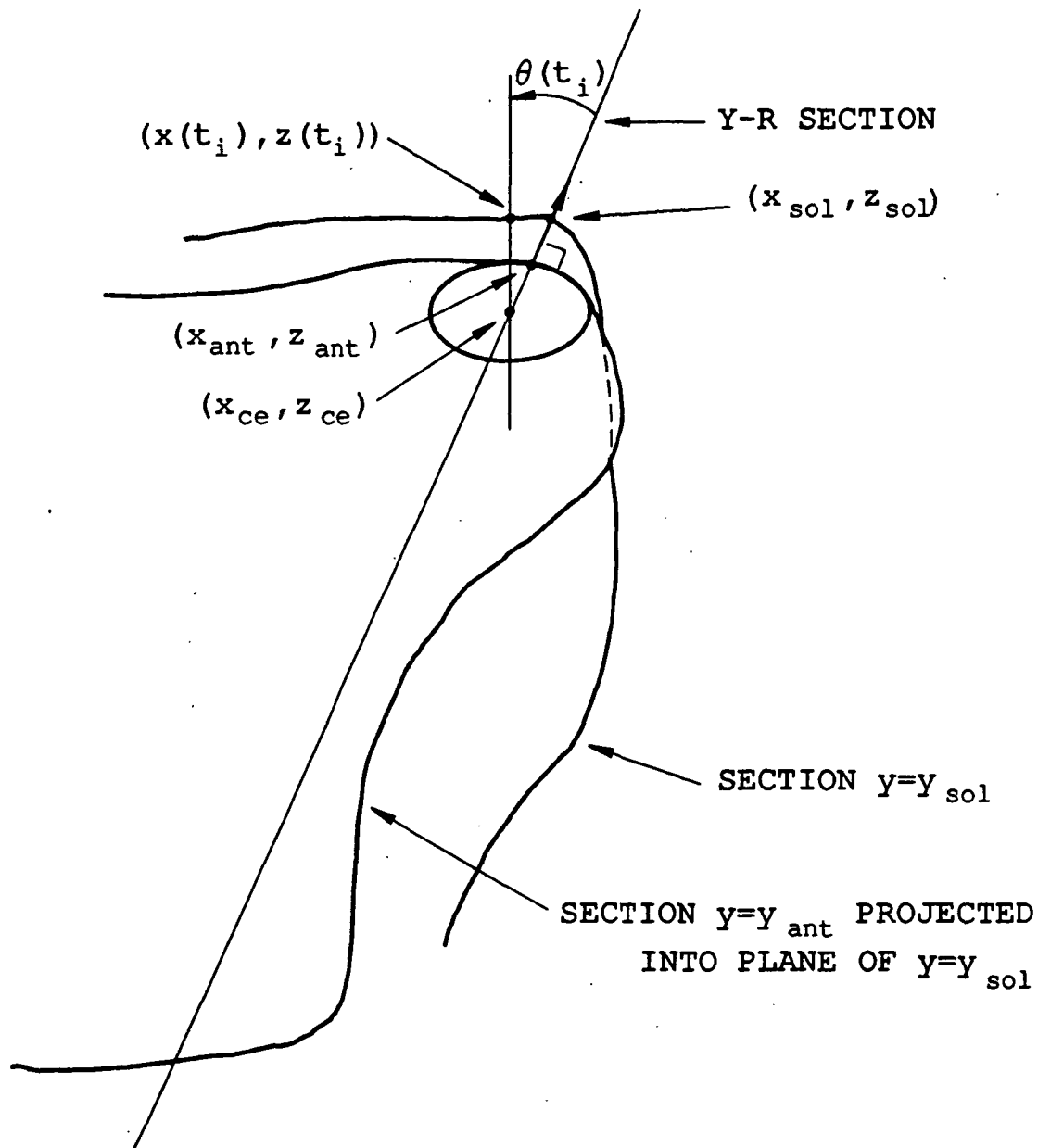
Figure 2.9: Definition of the angle θ which is used to find the point (X_{sol}, Z_{sol}) on the plane $Y = Y_{sol}$.

obtained in the previous sections. If a close-fit solution can not be obtained, some approximations are made to obtain a solution.

For this close-fitting procedure, two essential pairs of equations are utilized. One pair represents the case for which $Y_s \geq Y_c$, which is arbitrarily defined as a Case 1 problem. This pair of equations is For $Y_s \geq Y_c$:

$$f_1 = \frac{\tilde{A}\cos^2 V_{es} + (y - Y_c)^2}{C_0^2} - 1 = 0 \; ; \quad y \geq Y_s \qquad (2.17)$$

where

$$\tilde{A} = \frac{[(x - X_c)\sin\phi_s' + (z - Z_c)\cos\phi_s']^2}{(X_s - X_c)^2 + (Z_s - Z_c)^2}$$

$$\cos^2 V_{cs} = \frac{C_0^2 - (Y_s - Y_c)^2}{C_0^2}$$

$$\sin\phi_s' = \frac{X_s - X_c}{\sqrt{(X_s - X_c)^2 + (Z_s - Z_c)^2}}$$

$$\cos\phi_s' = \frac{Z_s - Z_c}{\sqrt{(X_s - X_c)^2 + (Z_s - Z_c)^2}}$$

$$C_0 > 0$$

and

$$f_2 = \tilde{A}\cos^2 V_{es}' + \frac{(y - Y_c - Y_{sh})^2}{(D_0 + Y_{sh})^2} - 1 = 0 \; ; \quad y \leq Y_s \qquad (2.18)$$

where

$$\cos^2 V_{es}' = \frac{[C_0\cos V_{es} + \tan V_{es}(D_0 + (Y_s - Y_c))]^2 - \tan^2 V_{es}(D_0 + (Y_s - Y_c))^2}{[C_0\cos V_{es} + \tan V_{es}(D_0 + (Y_s - Y_c))]^2}$$

$$Y_{sh} = \frac{(Y_s - Y_c) - D_0\sin V_{es}'}{1 + \sin V_{es}'}$$

However, (2.17) is simplified by rewriting it as follows

$$f_1 = a\,C_0^2 + b\,Y_c^2 + c\,Y_c + d = 0 \qquad (2.19)$$

where

$$a = \tilde{A} - 1$$
$$b = 1 - \tilde{A} = -a$$
$$c = 2\left(\tilde{A}Y_s - y\right)$$
$$d = y^2 - \tilde{A}Y_s^2$$

It should be pointed out that the expression in the middle of (2.19) is a variation of the equation representing a quadratic surface. The general form for representing a quadratic surface is $a\,x^2 + b\,y^2 + c\,x + d\,y + e = 0$ [2]. Since (2.19) is now a function of two variables C_0 and Y_c, two equations are required to solve for the solutions simultaneously. In other words, this system of equations requires the use of two data points to form the two equations. These are actually two surface points in the YR-plane on the fuselage to the rear of the antenna location. Therefore, by using the subscript 1 to represent parameters evaluated using the first data point to the rear of the antenna location and the subscript 2 to represent parameters evaluated using the second data point to the rear of the antenna location, the following system of equations with constraints are obtained:

$$f_{1_1} = a_1 C_0^2 + b_1 Y_c^2 + c_1 Y_c + d_1 = 0 \qquad (2.20)$$

$$f_{1_2} = a_2 C_0^2 + b_2 Y_c^2 + c_2 Y_c + d_2 = 0 \qquad (2.21)$$

subject to

$$Y_s - Y_c \geq 0 \qquad (2.22)$$

$$C_0 > 0 \qquad (2.23)$$

$$C_0, Y_c \in \mathcal{R} \qquad (2.24)$$

where

$$a_1 = \tilde{A}_1 - 1 \qquad (2.25)$$

$$b_1 = 1 - \tilde{A}_1 = -a_1 \qquad (2.26)$$

38

$$c_1 = 2\left(\tilde{A}_1 Y_s - y_1\right) \tag{2.27}$$

$$d_1 = y_1^2 - \tilde{A}_1 Y_s^2 \tag{2.28}$$

$$\tilde{A}_1 = \frac{[(x_1 - X_c)\sin\phi_s' + (z_1 - Z_c)\cos\phi_s']^2}{(X_s - X_c)^2 + (Z_s - Z_c)^2} \tag{2.29}$$

$$a_2 = \tilde{A}_2 - 1 \tag{2.30}$$

$$b_2 = 1 - \tilde{A}_2 = -a_2 \tag{2.31}$$

$$c_2 = 2\left(\tilde{A}_2 Y_s - y_2\right) \tag{2.32}$$

$$d_2 = y_2^2 - \tilde{A}_2 Y_s^2 \tag{2.33}$$

$$\tilde{A}_2 = \frac{[(x_2 - X_c)\sin\phi_s' + (z_2 - Z_c)\cos\phi_s']^2}{(X_s - X_c)^2 + (Z_s - Z_c)^2} \tag{2.34}$$

and $\mathcal{R}$ is a set of real numbers. The inequality constraints in (2.22) through (2.24) are known as functional constraints. The system of equations (2.20) and (2.21) are solved simultaneously without the constraints, and by eliminating C_0, the equation

$$\left(b_2 - \frac{a_2}{a_1}b_1\right)Y_c^2 + \left(c_2 - \frac{a_2}{a_1}c_1\right)Y_c + \left(d_2 - \frac{a_2}{a_1}d_1\right) = 0 \tag{2.35}$$

is obtained. Note that the coefficient expression of the first term in (2.35) is in fact zero, since the terms in the expression cancels each other out. As a result, (2.35) is reduced to a linear equation. With further algebraic manipulation, the solutions produced are

$$Y_c = -\left(\frac{d_2 - \frac{a_2}{a_1}d_1}{c_2 - \frac{a_2}{a_1}c_1}\right) \tag{2.36}$$

and

$$C_0 = \pm\sqrt{Y_c^2 - \frac{c_1}{a_1}Y_c - \frac{d_1}{a_1}} \tag{2.37}$$

Since C_0 and Y_c are real, and C_0 must be positive, (2.37), is rewritten as

$$C_0 = \sqrt{Y_c^2 - \frac{c_1}{a_1}Y_c - \frac{d_1}{a_1}} \tag{2.38}$$

It should be pointed out that this approach of mathematical derivation provides only one of the few possible sets of solution to the system of equations of (2.20) and (2.21). For a system of equations that have a solution set, the solution set

can be feasible, that is, it satisfies all of the functional constraints, or it can be infeasible, that is, it does not satisfy all of the functional constraints [10]. Thus, (2.36) and (2.38) is only one of the solution sets that may, or may not, satisfy all of the constraints (2.22) through (2.24), that is, the solution set may, or may not, be feasible. However, there exists one other possible solution for Y_c which could be approximated without much difficulty, if

$$| y_i - Y_s | \gg | Y_s - Y_c |$$

or

$$| y_i - Y_s | \ll | Y_s - Y_c |$$

for $i = 1, 2$, where $i = 1$ and $i = 2$ would represent the first and second data points, respectively, to the front of the antenna location. In fact, in (2.17), Y_c appears at two places in the expression for f_1, one in the equation defining the term $\cos^2 V_{es}$, and the other in the term $(y - Y_c)^2$.

For this approximation, consider the expression $(Y_s - Y_c)^2$ in the numerator of the equation defining the term $\cos^2 V_{es}$ in (2.17). Assuming that the value for this expression is η, the equation

$$(Y_s - Y_c)^2 = \eta, \quad \eta \geq 0 \qquad (2.39)$$

is thus created. There are indeed two possible values of Y_c that satisfy (2.39), namely

$$Y_c^* = Y_s - \sqrt{\eta} \qquad (2.40)$$

and

$$Y_c^{\natural} = Y_s + \sqrt{\eta} \qquad (2.41)$$

As for the term $(y - Y_c)^2$, it is represented as

$$\varepsilon(Y_c) = (y - Y_c)^2 \qquad (2.42)$$

40

Thus, for $Y_c = Y_c^*$ and $Y_c = Y_c^\sharp$, (2.42) becomes

$$\varepsilon(Y_c^*) = \varepsilon^* = (y - Y_c^*)^2 = (y - Y_s + \sqrt{\eta})^2 \tag{2.43}$$

and

$$\varepsilon(Y_c^\sharp) = \varepsilon^\sharp = (y - Y_c^\sharp)^2 = (y - Y_s - \sqrt{\eta})^2 \tag{2.44}$$

respectively. Therefore, for the condition

$$|y_i - Y_s| \gg |\sqrt{\eta}| = |Y_s - Y_c^*| = |Y_s - Y_c^\sharp|, \quad \text{for i=1,2}; \tag{2.45}$$

or

$$|y_i - Y_s| \ll |\sqrt{\eta}| = |Y_s - Y_c^*| = |Y_s - Y_c^\sharp|, \quad \text{for i=1,2}; \tag{2.46}$$

ε is such that $\varepsilon^* \approx \varepsilon^\sharp$. This implies that the change in ε would be negligibly small when the Y_c value was switched from Y_c^* to $Y_c^\sharp$, or vice-versa, if condition (2.45), or (2.46), was satisfied. The switching of such specific values from Y_c^* to $Y_c^\sharp$, or vice-versa, may be regarded as a reflection of $Y_c = Y_c^*$, or of $Y_c = Y_c^\sharp$, respectively, on the reflection plane Y_s to its corresponding image $Y_c = Y_c^\sharp$, or of $Y_c = Y_c^*$, respectively. Indeed, this approximation approach could be utilized if the solution for Y_c in (2.36) did not satisfy constraint (2.22), provided that the condition

$$|y_i - Y_s| \gg |Y_s - Y_c|$$

or

$$|y_i - Y_s| \ll |Y_s - Y_c|$$

for $i = 1, 2$ is met. Note that for Case 1, where $Y_s \geq Y_c$, (2.40) would approximate the feasible solution if the Y_c value computed in (2.36) is equal to that computed in (2.41).

In addition, Y_s must be within the range

$$Y_c \leq Y_s < (Y_c + C_0)$$

41

so that it is located on the rear section of the composite ellipse. This can be conspicuously observed from (2.17), whereby the numerator of the expression for $\cos^2 V_{es}$ must be positive. Hence, a further set of functional constraints arising from these are produced:

$$Y_c^2 - \frac{c_1}{a_1} Y_c - \frac{d_1}{a_1} > 0 \qquad (2.47)$$

$$C_0^2 - (Y_s - Y_c)^2 > 0 \qquad (2.48)$$

Indeed, (2.47) is the expression for the argument in the square-root function of (2.38), whereas (2.48) is the expression in the numerator for defining $\cos^2 V_{es}$ in (2.17).

In fact, no solution to the original equations (2.20) and (2.21) were found, the inequality constraints (2.47) and (2.48) would have to be satisfied in order to produce a composite ellipse in the YR-plane, given the solutions obtained for the XZ-plane, the first-order derivative of the fuselage surface at the antenna location, and the first data point to the rear of the antenna location. This could be achieved by algebraically eliminating C_0 in (2.48) and rewriting the set of functional constraints (2.48) and (2.47) as

$$Y_c^2 - \frac{c_1}{a_1} Y_c - \frac{d_1}{a_1} > 0 \qquad (2.49)$$

$$\left(2Y_s - \frac{c_1}{a_1}\right) Y_c - \frac{d_1}{a_1} - Y_s^2 > 0 \qquad (2.50)$$

from which Y_c could be solved simultaneously. As a result, the locus of the composite ellipse would pass through the first data point since there would be a dependency on the first data point, and that C_0 would be derived from (2.47) given Y_c as determined previously.

On the other hand, (2.18) is a function of a single variable D_0. It is thus wise to solve it numerically using a root-finding method. Therefore, in order to obtain a reasonably good value for D_0, two data points are utilized, instead of one. These two data points would be points on the actual fuselage surface to the front of the antenna location. Restating these, and representing the parameters evaluated using

42

the first data point to the front (that is, $i = 1$) as subscript 1 and those evaluated using the second data point to the front (that is, $i = 2$) as subscript 2, the problem from (2.18) becomes:

$$f_{2_i} = \tilde{A}_i \cos^2 V'_{cs_i} + \frac{(y_i - Y_c - Y_{sh_i})^2}{(D_{0_i} + Y_{sh_i})^2} - 1 = 0 \; ; \; \text{i=1,2} \qquad (2.51)$$

With this, D_0 would be the average value of the real roots D'_{0_1} and D'_{0_2}.

On the other hand, the other pair of equations represents the case for which $Y_s < Y_c$, and is arbitrarily defined as a Case 2 problem. These equations are

For $Y_s < Y_c$:

$$f_1 = \frac{\tilde{A} \cos^2 V_{es} + (y - Y_c)^2}{D_0^2} - 1 = 0 \; ; \; y \leq Y_s \qquad (2.52)$$

where

$$\tilde{A} = \frac{[(x - X_c)\sin \phi'_s + (z - Z_c)\cos \phi'_s]^2}{(X_s - X_c)^2 + (Z_s - Z_c)^2}$$

$$\cos^2 V_{es} = \frac{D_0^2 - (Y_s - Y_c)^2}{D_0^2}$$

$$\sin \phi'_s = \frac{X_s - X_c}{\sqrt{(X_s - X_c)^2 + (Z_s - Z_c)^2}}$$

$$\cos \phi'_s = \frac{Z_s - Z_c}{\sqrt{(X_s - X_c)^2 + (Z_s - Z_c)^2}}$$

$$D_0 > 0$$

and

$$f_2 = \tilde{A} \cos^2 V'_{es} + \frac{(y - Y_c - Y_{sh})^2}{(C_0 + Y_{sh})^2} - 1 = 0 \; ; \; y \geq Y_s \qquad (2.53)$$

where

$$\cos^2 V'_{es} = \frac{[D_0 \cos V_{es} - \tan V_{es}(C_0 - (Y_s - Y_c))]^2 - \tan^2 V_{es}(C_0 - (Y_s - Y_c))^2}{[D_0 \cos V_{es} - \tan V_{es}(C_0 - (Y_s - Y_c))]^2}$$

$$Y_{sh} = \frac{(Y_s - Y_c) - C_0 \sin V'_{es}}{1 - \sin V'_{es}}$$

Note that in (2.52), instead of C_0, the parameter is substituted with D_0, and in (2.53), instead of D_0, the parameter is replaced with C_0. Just as before, (2.52)

43

is reduced to a system of two equations represented by two data points which are selected off the actual surface of the fuselage in the YR-plane to the front of the antenna location and are subjected to a set of functional constraints. This system of constrained equations are

$$f_{1_1} = a_1 D_0^2 + b_1 Y_c^2 + c_1 Y_c + d_1 = 0 \tag{2.54}$$

$$f_{1_2} = a_2 D_0^2 + b_2 Y_c^2 + c_2 Y_c + d_2 = 0 \tag{2.55}$$

subject to

$$Y_s - Y_c < 0 \tag{2.56}$$

$$D_0 > 0 \tag{2.57}$$

$$D_0, Y_c \in \mathcal{R} \tag{2.58}$$

where

$$a_1 = \tilde{A}_1 - 1 \tag{2.59}$$

$$b_1 = 1 - \tilde{A}_1 = -a_1 \tag{2.60}$$

$$c_1 = 2\left(\tilde{A}_1 Y_s - y_1\right) \tag{2.61}$$

$$d_1 = y_1^2 - \tilde{A}_1 Y_s^2 \tag{2.62}$$

$$\tilde{A}_1 = \frac{[(x_1 - X_c)\sin\phi_s' + (z_1 - Z_c)\cos\phi_s']^2}{(X_s - X_c)^2 + (Z_s - Z_c)^2} \tag{2.63}$$

$$a_2 = \tilde{A}_2 - 1 \tag{2.64}$$

$$b_2 = 1 - \tilde{A}_2 = -a_2 \tag{2.65}$$

$$c_2 = 2\left(\tilde{A}_2 Y_s - y_2\right) \tag{2.66}$$

$$d_2 = y_2^2 - \tilde{A}_2 Y_s^2 \tag{2.67}$$

$$\tilde{A}_2 = \frac{[(x_2 - X_c)\sin\phi_s' + (z_2 - Z_c)\cos\phi_s']^2}{(X_s - X_c)^2 + (Z_s - Z_c)^2} \tag{2.68}$$

and $\mathcal{R}$ is a set of real numbers. From (2.54) and (2.55), Y_c and D_0 are then solved simultaneously to obtain

$$Y_c = -\left(\frac{d_2 - \frac{a_2}{a_1}d_1}{c_2 - \frac{a_2}{a_1}c_1}\right) \tag{2.69}$$

44

and

$$D_0 = \sqrt{Y_c^2 - \frac{c_1}{a_1}Y_c - \frac{d_1}{a_1}} \qquad (2.70)$$

Again, as in Case 1, the reflection approximation equations of (2.40) and (2.41) could be applied in this case, if the solution for Y_c in (2.69) did not satisfy constraint (2.56), provided that the condition

$$| y_i - Y_s | \gg | Y_s - Y_c |$$

or

$$| y_i - Y_s | \ll | Y_s - Y_c |$$

for $i = 1,2$, where $i = 1$ and $i = 2$ would represent the first and second data points, respectively, to the rear of the antenna location, occurred. Therefore, for the Case 2 problem, where $Y_s < Y_c$, (2.41) would approximate the feasible solution if the Y_c value evaluated in (2.69) is equal to that evaluated in (2.40).

Proceeding on, algebraically eliminating D_0, similar to (2.49) and (2.50), the functional constraints for this case are

$$Y_c^2 - \frac{c_1}{a_1}Y_c - \frac{d_1}{a_1} > 0 \qquad (2.71)$$

$$\left(2Y_s - \frac{c_1}{a_1}\right)Y_c - \frac{d_1}{a_1} - Y_s^2 > 0 \qquad (2.72)$$

If, however, no solution to (2.54) and (2.55) was obtained, then the constraints (2.72) and (2.71) would be utilized. That is, Y_c and D_0 could be solved simultaneously from (2.72) and (2.71). It should be observed that (2.59) through (2.68), (2.69), (2.72) and (2.71) are the same expressions as those for Case 1.

As for (2.53), the same root-finding method employed in Case 1 is applied in this case. In other words, the expression for this case is

$$f_{2_i} = \tilde{A}_i \cos^2 V'_{es_i} + \frac{(y_i - Y_c - Y_{sh_i})^2}{(C_{0_i} - Y_{sh_i})^2} - 1 = 0 \; ; \; i=1,2 \qquad (2.73)$$

Thus, C_0 is the average value of the real roots C'_{0_1} and C'_{0_2}.

As for the data points to be employed in obtaining the parameters for constructing the composite ellipse, two data points on the actual fuselage to front, and two on the actual fuselage to rear, of the antenna location in the YR-plane is sampled at a specific interval DY as illustrated in Figure 2.10. For a Case 1 problem, the two selected data points to the rear would be utilized in (2.20) through (2.27), and the other two to the front would be utilized in (2.51). Contrarily, for a Case 2 problem, the two selected data points to the front would be utilized in (2.54) through (2.58), and the other two to the rear would be utilized in (2.73). If, however, at least one of the selected data points was located over on the other side of the $R = 0$ line instead of on the same side as where the antenna location is, that is, in the $R < 0$ region if the antenna location is in the $R > 0$ region, or vice-versa, caution must be taken. The case for which the antenna location is in the $R > 0$ region, but with one of the data points in the $R < 0$ region, is depicted in Figure 2.11. Since, as mentioned in Section 2.2, the $R = 0$ line coincides with the axis of the composite ellipsoid that is orthogonal to the XZ-plane, the $R = 0$ line also coincides with the axis of the composite ellipse in the YR-plane, which is in fact a YR-plane cross-section of the composite ellipsoid. Thus, the composite ellipse must be symmetrical along the $R = 0$ line.

By referring to Figure 2.11 (a) as an example, the locus of the composite ellipse may be conformed to pass very closely by, if not directly, the antenna location and the data points located on the same $R > 0$ region as where the antenna location is, but not the data point below the $R = 0$ line. This is attributed to the symmetrical property of the composite ellipse along the $R = 0$ line, as is conspicuous in the figure. As a result, the point below the $R = 0$ line cannot be applied to (2.21) for Case 1, or (2.21) for Case 2, to produce an accurate solution. Therefore, the data points to be utilized must be selected from the portion of the cross-section surface that is located on the same side of the $R = 0$ line as where the antenna location is.
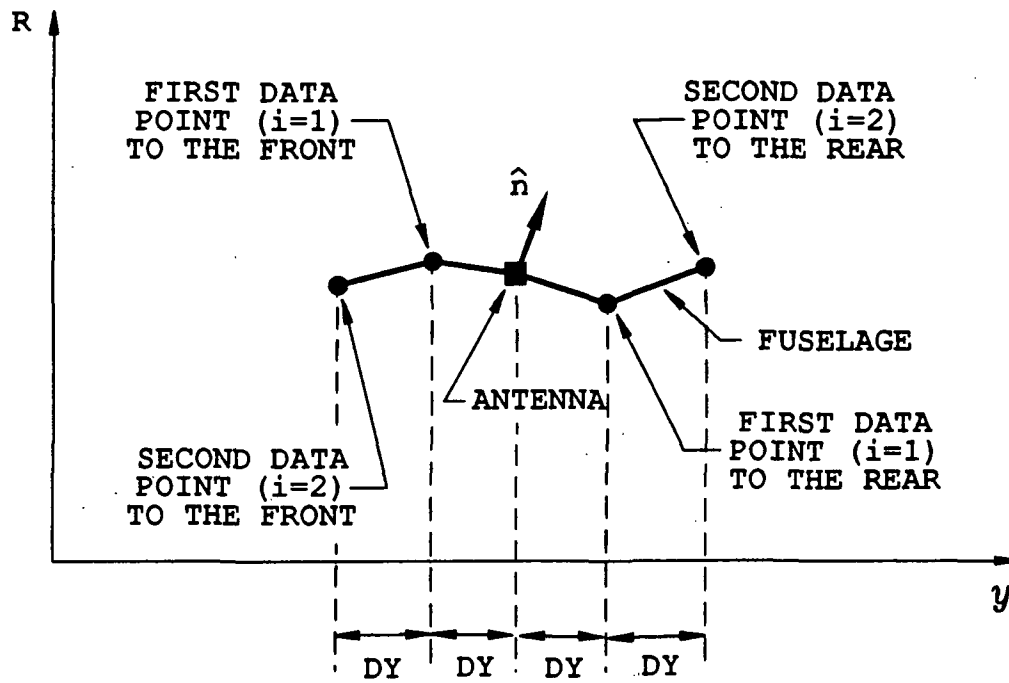
Figure 2.10: Antenna location with four data points approximating the the surface of the cross-section in the YR-plane in the vicinity of the antenna location. DY is the sampling interval from one data point to the other, and $\hat{n}$ is the outward unit normal vector of the surface at the antenna location.

47
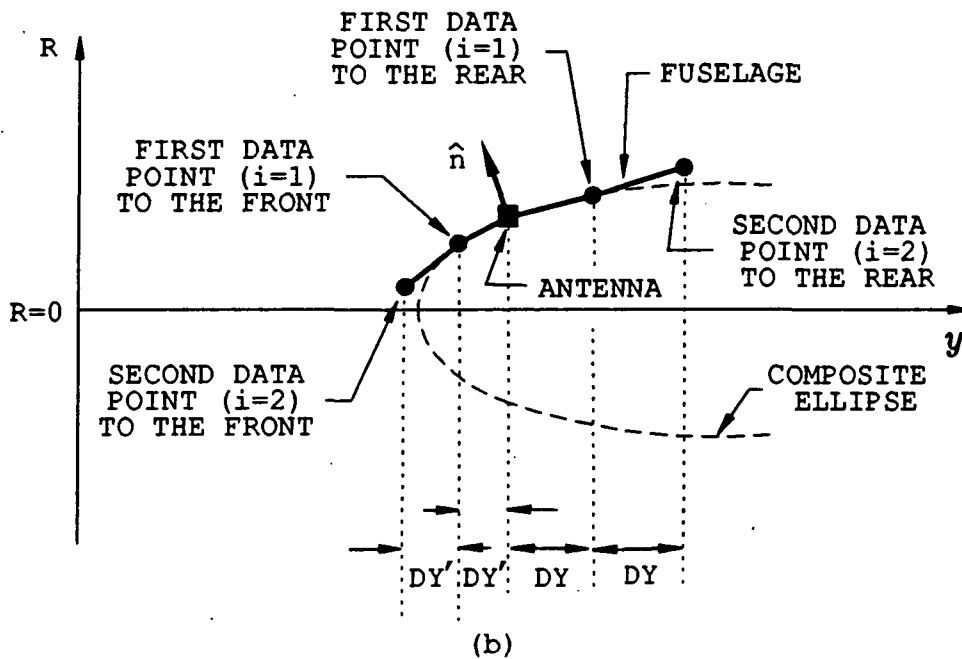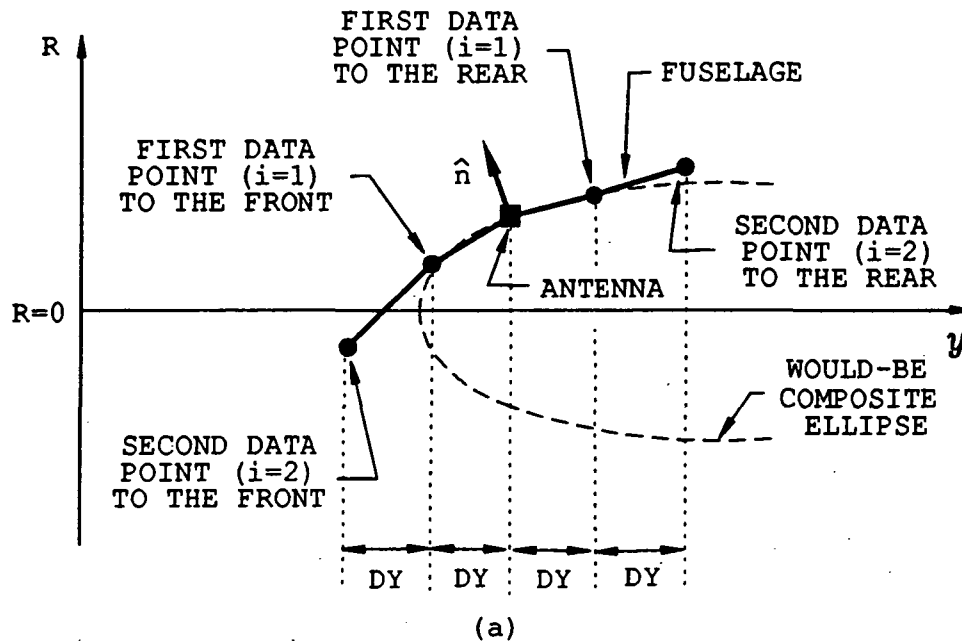
Figure 2.11: (a) An example of the YR-plane surface for the case where the antenna location is in the $R > 0$ region, but with a data point in the $R < 0$ region, and (b) Each interval DY to the front of the antenna location is reduced to DY' so that a composite ellipse may be fitted to the surface formed by the data points.

To execute this, the sampling interval DY must be reduced. In fact, this reduced DY is DY' in Figure 2.11 (b).

In order to mathematically determine if the antenna is located on the top half of the composite ellipsoid, or the bottom half of it, the angle parameter ϕ_s in Figure 2.7 is evaluated. This is an angle of inclination of the YR-plane from the YZ-plane. If $\phi_s \leq 90^\circ$, then the antenna would be considered to be on the top half of the composite ellipsoid. On the other hand, if $\phi_s > 90^\circ$, then the antenna would be considered to be on the bottom half of the composite ellipsoid.

Once the location of the antenna is determined in the context of top or bottom half of the composite ellipsoid, the problem can be easily identified as a Case 1 problem or a Case 2 problem. This is achieved by determining the first-order derivative of the surface at the antenna location. For the antenna located on the top half of the composite ellipsoid, the problem would be a Case 1 problem if the first-order derivative of the fuselage surface at the antenna location was less than or equal to -0.01; and the problem would be a Case 2 problem if the first-order derivative of the fuselage surface at the antenna location was greater than 0.01. On the contrary, for the antenna located on the bottom half of the composite ellipsoid, the problem would be a Case 1 problem if the first-order derivative of the fuselage surface at the antenna location was greater then or equal to 0.01; and the problem would be a Case 2 problem if the first-order derivative of the fuselage surface at the antenna location was less than -0.01. Note that the value 0.01 is utilized instead of zero so that values within the neighbourhood of zero are considered as zeros. As a graphical illustration, these are summarized in Figure 2.12 and Figure 2.13. Indeed, such antenna location information is also especially important when initializing the parameters of NEWAIR3 [1].

49
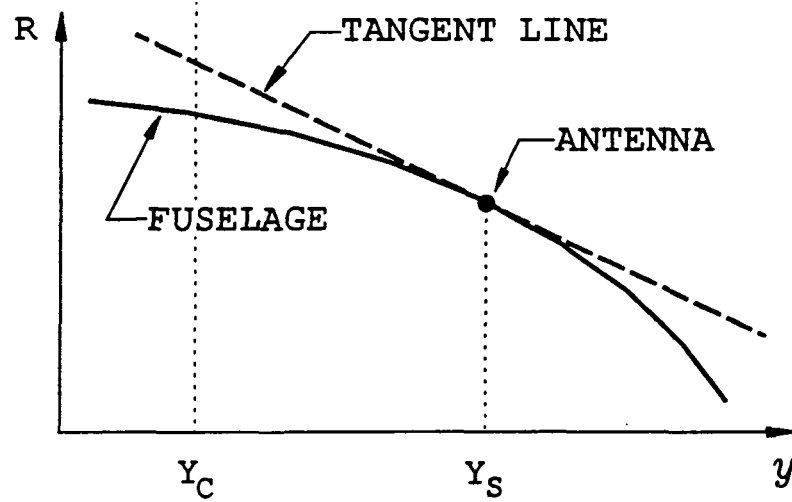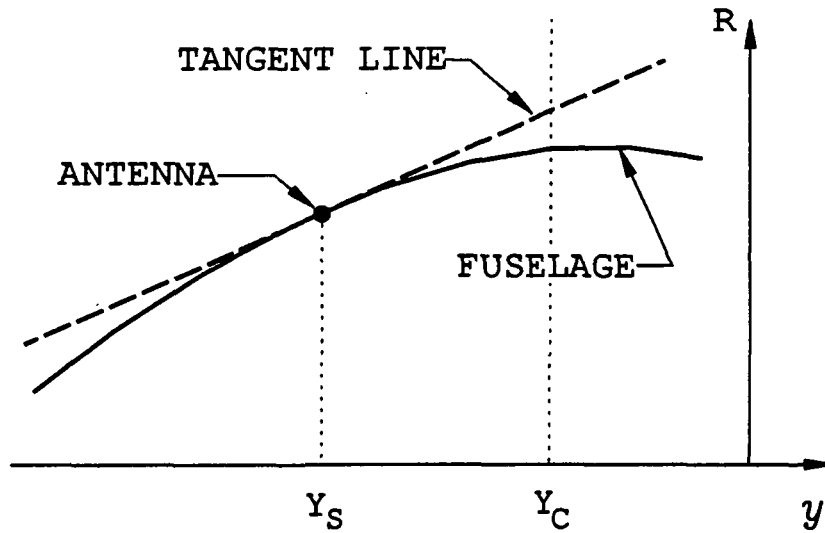
(a)   CASE 1 ($Y_S \geq Y_C$)

(b)   CASE 2 ($Y_S < Y_C$)

Figure 2.12: Schematics of the fuselage cross-section in the YR-plane for the antenna location on the top half of the close-fit composite ellipsoid: a) for Case 1 ($Y_s \geq Y_c$): The first-order derivative of the surface is less than or equal to -0.01, and b) for Case 2 ($Y_s < Y_c$): The first-order derivative of the surface is greater than 0.01.
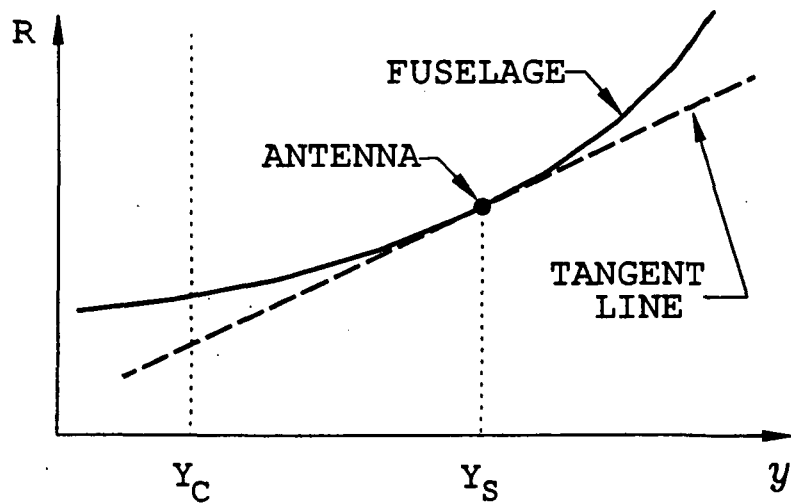
(a) CASE 1 $(Y_S \geq Y_C)$
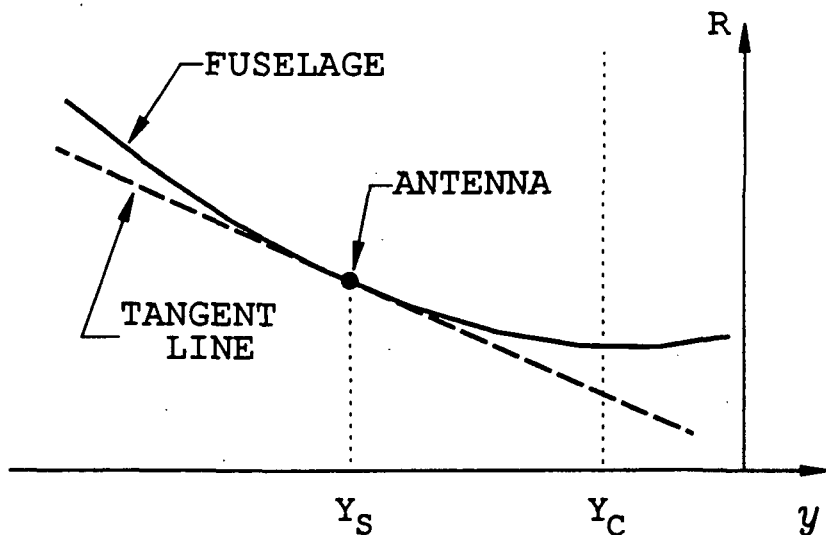
(b) CASE 2 $(Y_S < Y_C)$

Figure 2.13: Schematics of the fuselage cross-section in the YR-plane for the antenna location on the bottom half of the close-fit composite ellipsoid: (a) for Case 1 $(Y_s \geq Y_c)$: The first-order derivative of the surface is greater than or equal to 0.01, and (b) for Case 2 $(Y_s < Y_c)$: The first-order derivative of the surface is less than -0.01.

2.6 Perturbation of Data Points

It should be noted that the approximation technique discussed above does no always produce numerically a good approximation of a close-fit composite ellipsoid. Therefore, some form of perturbation technique must be performed, so as to distort the data points such that a good numerical approximation is obtainable. This is especially true if the actual surface of the fuselage is entirely planar, or just very slightly concave, within the vicinity of the antenna location. For such a surface, a perfectly fitting model of a composite ellipsoid is ill-posed.

2.6.1 Perturbation in the XZ-plane

In this section, the perturbation of the data points in the XZ-plane, developed by Klevenow and Scheick, is discussed briefly.

Such a perturbation is performed when a close-fit ellipse at the antenna location in the XZ-plane is difficult to calculate due to the actual surface at the antenna location being essentially planar. In the XZ-plane, this is an almost straight line in the vicinity of the antenna location.

For the purpose of presenting this perturbation concept, the general xy-coordinate system is employed, instead of the coordinate system of the XZ-plane. Assuming that the data points, together with the antenna location are, (x_i, y_i), $i = 1, ..., N$, where N is an odd number (the antenna location is now regarded as a point in the middle of the array of N points), a straight line is constructed between the two end points (x_1, y_1) and (x_N, y_N). This straight line is described by the the normal equation

$$f_n(x_i, y_i) = A x_i + B y_i + C \qquad (2.74)$$

Hence, by adding a parallel line, Line 1, at a distance DD away from the normal line on one side, and another, Line 2, at the same distance DD on the other side, a linear band of width $2 \times DD$ is created, as illustrated in Figure 2.14. For the

outward normal direction $\hat{n}$ shown the figure, Line 1 is a linear line described by

$$f_n(x_i, y_i) = A\, x_i + B\, y_i + C = DD \qquad (2.75)$$

and Line 2, also a linear line, by

$$f_n(x_i, y_i) = A\, x_i + B\, y_i + C = -DD \qquad (2.76)$$

The points (x_i, y_i), $i = 1, ..., N$, are considered as forming a concave arc when viewed from outside of the cross-section if any one of them lies in the $f_n(x_i, y_i) < -DD$ region depicted in the figure, that is, below Line 2 in the figure. In such a case, no attempt is made to fit an ellipse to the cross-section. Mathematically, these points would produce $f_n(x_i, y_i) < DD$, as described by (2.74). If, however, all of the points were in the $f_n(x_i, y_i) > -DD$ region, that is, above Line 2 in the figure, then the points are considered either as forming a convex arc, or as forming an almost straight line to which a close-fit is not explicitly defined. Mathematically, this corresponds to the points producing $f_n(x_i, y_i) > -DD$, as described by (2.74).

In order to determine as to which of these cases actually occur if all of the points are located in the $f_n(x_i, y_i) > -DD$ region, that is, above Line 2 in the figure, the positions of these points with respect to Line 1 would then be considered. For this evaluation, the points would be regarded as forming an almost straight line if any one of them were in the $f_n(x_i, y_i) < DD$ region, that is, below Line 1 in the figure. When this occurs, it is assumed that the points are located within the band depicted in the figure. Points in this configuration are perturbed. Otherwise, the arc to which they form would be regarded as convex.

2.6.2 Perturbation in the YR-plane

Perturbation of data points in the YR-plane is performed if no close-fit composite ellipsoid at the antenna location in the YR-plane is found. The perturbation process in this plane is, however, different from that in the XZ-plane. For this case, the
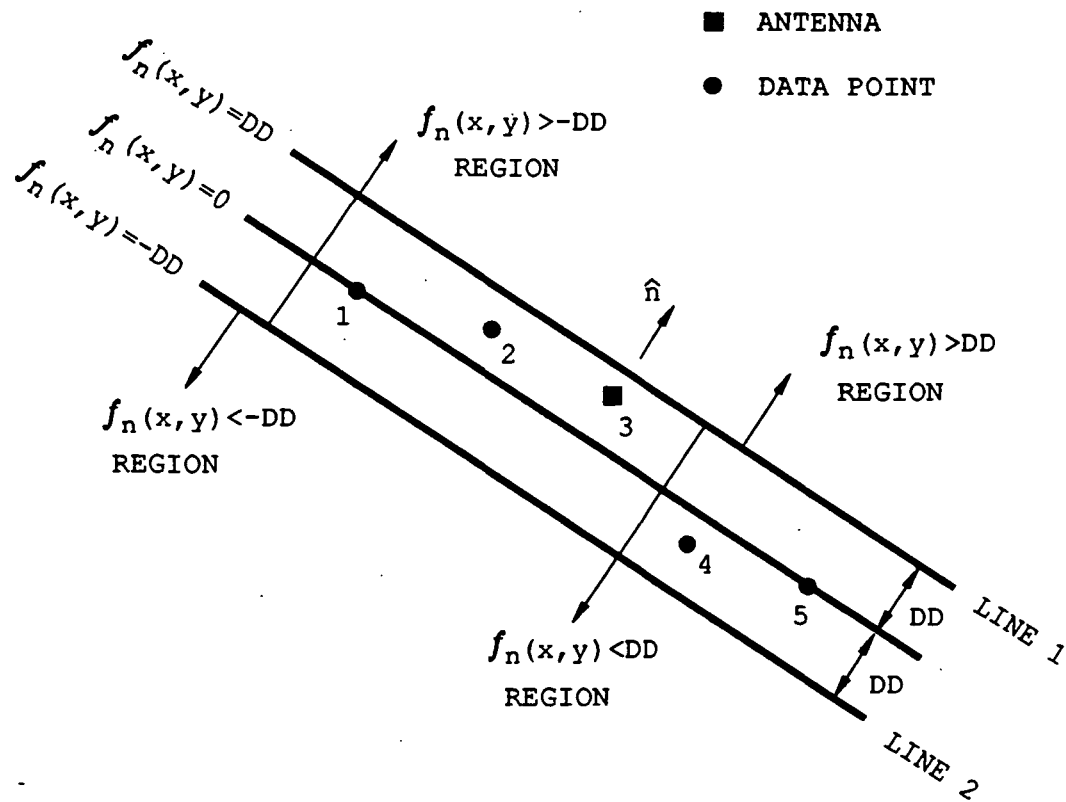
Figure 2.14: A generalized schematic illustrating the perturbation in the XZ-plane at $y = Y_s$. The numerical labels indicate the i-th. point in the figure.

first-order derivative m_1 of the actual fuselage surface at the antenna location is first obtained. A unit direction vector $\hat{d}$ perpendicular to the line m_1 is given by

$$\hat{d} = \pm \frac{1}{\sqrt{1 + m_2^2}} \begin{pmatrix} 1 \\ m_2 \end{pmatrix} \qquad (2.77)$$

where $m_2 = -\frac{1}{m_1}$, "$+$" signs are for $m_1 > 0$, and "$-$" signs are for $m_1 < 0$. The case where $m_1 = 0$ is ignored. With this, any of the data points (y, R) selected can be shifted, or perturbed, to a new position (y', R') along vector $\hat{d}$, as provided by

$$(y', R') = (y^*, R^*) \pm \alpha \hat{d}^\mathsf{T} = \left(y^* \pm \alpha \frac{1}{\sqrt{1 + m_2^2}}, R^* \pm \alpha \frac{m_2}{\sqrt{1 + m_2^2}} \right) \; ; \; \alpha > 0$$

$$(2.78)$$

where

$$\begin{aligned} y^* &= \frac{m_2 y - m_1 y_s - R + R_s}{m_2 - m_1} \\ R^* &= m_1 (y^* - y_s) + R_s \end{aligned}$$

with "$+$" signs for $m_1 > 0$, and "$-$" signs for $m_1 < 0$. In fact, (y^*, R^*) is the intersection point of lines m_1 and m_2. This is illustrated by Figure 2.15 for the perturbation of a single data point.

Therefore, employing (2.78) to the first selected data point (that is, $i = 1$), the expression becomes

$$(y_1', R_1') = (y_1^*, R_1^*) \pm \alpha_1 \hat{d}_1^\mathsf{T} = \left(y_1^* \pm \alpha_1 \frac{1}{\sqrt{1 + m_2^2}}, R_1^* \pm \alpha_1 \frac{m_2}{\sqrt{1 + m_2^2}} \right) \; ; \; \alpha_1 > 0$$

$$(2.79)$$

where

$$\begin{aligned} y_1^* &= \frac{m_2 y_1 - m_1 y_s - R_1 + R_s}{m_2 - m_1} \\ R_1^* &= m_1 (y_1^* - y_s) + R_s \end{aligned}$$

with $m_2 = -\frac{1}{m_1}$, "$+$" signs for $m_1 > 0$, and "$-$" signs for $m_1 < 0$. For this case, (y^*, R^*) is as described previously. With such a perturbation process, there is always

55
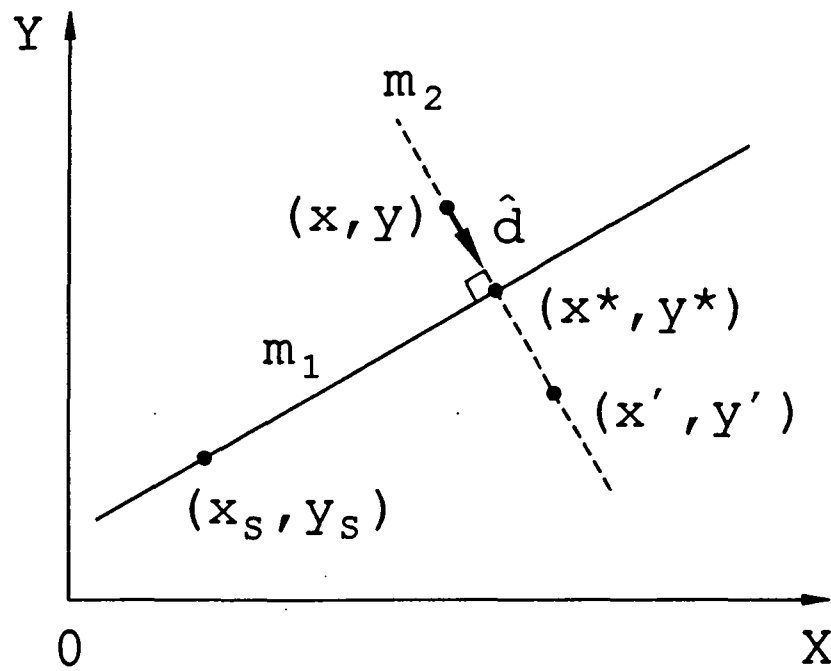
Figure 2.15: A generalized geometrical description of the perturbation equation (2.78).

a possibility that the arc formed by the perturbed data points is concave. So, in order to decrease but not entirely eliminate such a likelihood, the second data point (that is, $i = 2$) is perturbed using the first-order derivative m_1' of a line extrapolated from the midpoint between the first and the second data points to the antenna location, instead of using the first-order derivative m_1 at the antenna location itself. Thus, for the second selected data point (that is, $i = 2$), the expression becomes

$$(y_2', R_2') = (y_2^*, R_2^*) \pm \alpha_2 \, \hat{\mathbf{d}}_2^{\mathsf{T}} = \left(y_2^* \pm \alpha_2 \frac{1}{\sqrt{1 + m_2^2}} \, , \, R_2^* \pm \alpha_2 \frac{m_2}{\sqrt{1 + m_2^2}} \right) \; ; \; \alpha_2 > 0 \tag{2.80}$$

where

$$\begin{aligned} y_2^* &= \frac{m_2' \, y_2 - m_1' \, y_s - R_2 + R_s}{m_2' - m_1'} \\ R_2^* &= m_1' \, (y_2^* - y_s) + R_s \end{aligned}$$

with $m_2' = -\frac{1}{m_1'}$, "+" signs for $m_1' > 0$, and "−" signs for $m_1' < 0$. Nonetheless, (y^*, R^*) for this case is the intersection point of lines m_1' and m_2' instead.

Indeed, this is an idea of shifting points downwards along vector $\hat{\mathbf{d}}$, but in the direction opposite to that of the outward normal of the fuselage which is assumed to be pointing directly upwards. As such, the points are always located below the first-order derivative line m_1. This ensures a convexity in the infinitesimal neighbourhood of the antenna location. It should be noted that any point located above m_1 will cause ELLC to fail.

Particularly, this concept can be applied to discern sets of points forming concave arcs. For data points to the front of the antenna location, the condition

$$\pm m_1' \leq \pm m_1 \tag{2.81}$$

where + signs are for representing antenna locations on the top half of the composite ellipsoid, and − signs for representing antenna locations on the bottom half of the composite ellipsoid, indicates concavity. Such a concavity may only be slight, or it

may be rather severe. Nonetheless, the condition

$$\pm \left(m'_1 \pm \sigma \right) \leq \pm m_1 \qquad (2.82)$$

with $\sigma > 0$ as a sensitivity parameter, is utilized to identify a concavity that is above a certain tolerance.

For data points to the rear of the antenna location, on the other hand, the condition

$$\pm m'_1 \geq \pm m_1 \qquad (2.83)$$

where, again, $+$ signs are for representing antenna locations on the top half of the composite ellipsoid, and $-$ signs for representing antenna locations on the bottom half of the composite ellipsoid, is employed to identify concavity, instead. Specifically, for implementing a condition that accepts a specified tolerance level of slight concavity, the condition

$$\pm \left(m'_1 \mp \sigma \right) \geq \pm m_1 \qquad (2.84)$$

with $\sigma > 0$ as a sensitivity parameter, is utilized instead.

2.7 Computation of parameters A_0 and B_0

As mentioned in Section 2.2, the final parameters that are yet to be determined are the parameters A_0 and B_0. In fact, these parameters are easily computed by geometrical analysis of the entire composite ellipsoid itself using the parameters A_1, B_1, C_0, D_0 and Y_c, which were determined in the preceeding sections. The equations for A_0 and B_0, hence, are, respectively,

$$A_0 = \frac{\cos V'_{es}}{\cos V_{es}} \frac{\left(D_0 + Y_{sh} \right) A_1}{\sqrt{\left(D_0 + Y_{sh} \right)^2 - \left(\left(Y_s - Y_c \right) - Y_{sh} \right)^2}} \qquad (2.85)$$

and

$$B_0 = \frac{\cos V'_{es}}{\cos V_{es}} \frac{\left(D_0 + Y_{sh} \right) B_1}{\sqrt{\left(D_0 + Y_{sh} \right)^2 - \left(\left(Y_s - Y_c \right) - Y_{sh} \right)^2}} \qquad (2.86)$$

58

for $Y_s \geq Y_c$ (Case 1 problem), or

$$A_0 = \frac{\cos V'_{es}}{\cos V_{es}} \frac{(C_0 - Y_{sh}) A_1}{\sqrt{(C_0 - Y_{sh})^2 - ((Y_c - Y_s) + Y_{sh})^2}} \qquad (2.87)$$

and

$$B_0 = \frac{\cos V'_{es}}{\cos V_{es}} \frac{(C_0 - Y_{sh}) B_1}{\sqrt{(C_0 - Y_{sh})^2 - ((Y_c - Y_s) + Y_{sh})^2}} \qquad (2.88)$$

for $Y_s < Y_c$ (Case 2 problem). The expressions for $\cos V_{es}$, as well as $\cos V'_{es}$ and Y_{sh}, for the Case 1 problem are as stated in (2.17), and (2.18), respectively. On the other hand, those for the Case 2 problem are as stated in (2.52), and (2.53), respectively.

Chapter 3

The Algorithms

This chapter provides a concise description of the major algorithms employed in ELLC, the FORTRAN code that generates the close-fit composite ellipsoid for inputting into NEWAIR3C as part of the HARP code. Basically, ELLC consists of a number of subroutines that are called independently at various stages of the code. It should be noted that, at the present moment, the entire contour data of the helicopter fuselage is already provided in the form of data files from which ELLC is able to access.

3.1 Subroutine ELLC

This is the main subroutine that executes a number of other subroutines to be described subsequently. It integrates these subroutines into a compact subroutine that outputs the final solutions A_0, B_0, C_0, D_0 and Y_{sh}, necessary for constructing the close-fit composite ellipsoid, as well as the stop-run parameter STATSTOP. The inputs that are necessary for this subroutine are the coordinate location of the antenna on the helicopter fuselage surface and the data files containing the coordinates of the points that form the fuselage cross section itself. In fact, the antenna location on the helicopter fuselage is specified in the (Y_s, T) format described in Section 2.2. A flow-chart of ELLC is illustrated in Figure 3.1 through Figure 3.4. Note that

subroutines INARSEC, YENDS, POINT, ELLXZ and PNTTHY were developed by Scheick and Klevenow [?], and details of these are not to be discussed in this report.

This subroutine commences by initializing the various variables to be utilized in subsequent routines, which determine the points on a particular cross section of the helicopter fuselage, through the subroutine INARSEC. Then subroutine YENDS is called upon to determine the positions of the nose and the tail ends of the helicopter fuselage. To determine the rectangular coordinate of the antenna location, subroutine POINT is executed. Following this, subroutine ELLXZ is utilized to generate a close-fit ellipse to the points on the fuselage surface in the XZ-plane in the vicinity of the antenna location. This XZ-plane is in fact the cross section at the antenna location where $y = Y_s$. Among the parameters produced by ELLXZ are the semi-axes A_1 and B_1 of the close-fit ellipse, as well as the center of the ellipse itself which consists of the x- and z-components, X_c and Z_c, of center of the close-fit composite ellipsoid. If, however, no acceptable solution was found, ELLC would halt with an appropriate error message. Once completed, the rectangular coordinates of the antenna location (X_s, Y_s, Z_s) are transformed into YR-coordinates (R_s, Y_s, ϕ_s), where ϕ_s is the angle of the YR-plane (in which the antenna is also located) from the z-axis.

At spacing DY1 from each other, the YR-coordinates of the points behind the antenna location in the YR-plane are generated via subroutine PNTTHY until the actual surface of the helicopter fuselage in the YR-plane ceases, or until a point in the YR-plane cannot be determined precisely, that is, the stop-run condition ISTOP of subroutine PNTTHY is nonzero. With regards to the latter condition, for the antenna located too close to an end point of the fuselage, ELLC would produce a STATSTOP of value 13, indicating that the necessary data points on the fuselage surface were indeterminate, and finally halts with an appropriate error message. However, prior to encountering this condition, STATSTOP = 7 and the spacing DY1 is adjusted such that a minimum number of two points are generated behind the the antenna location. Also, the spacing DY1 may be reduced so that the none of the
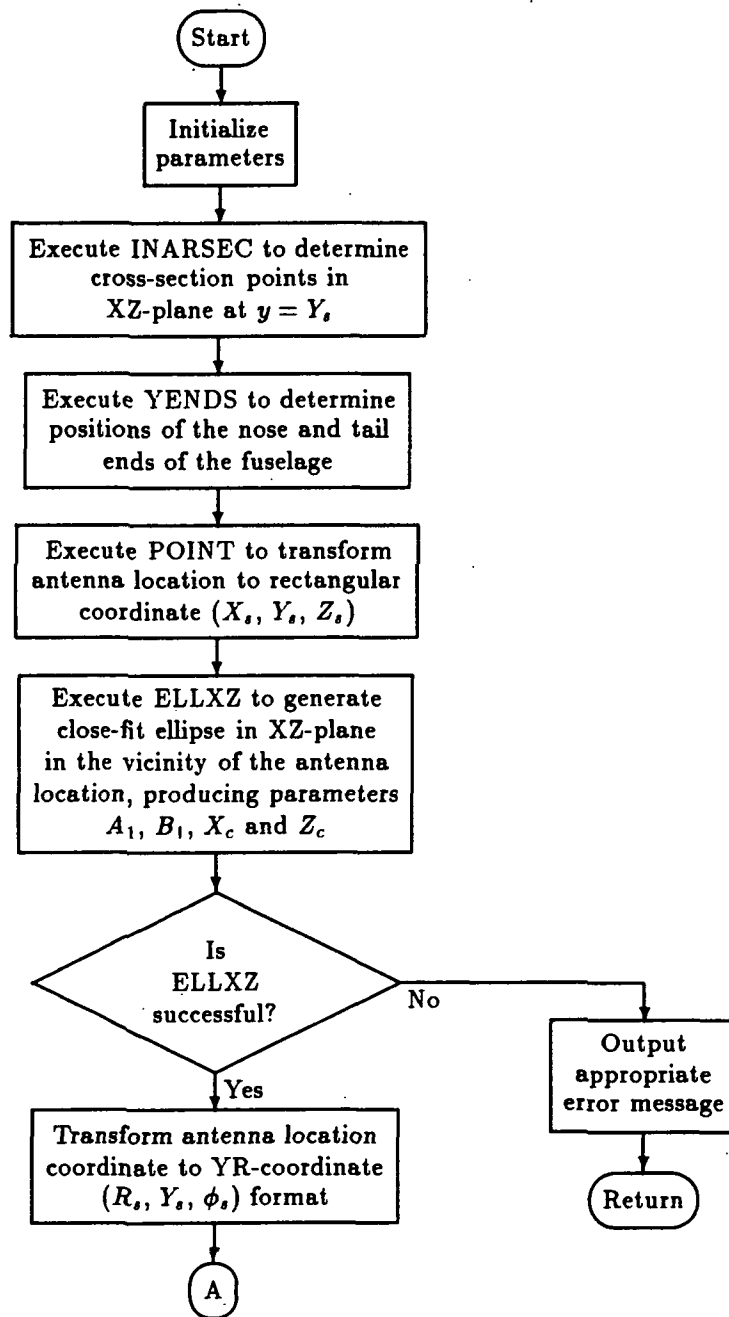
Figure 3.1: A simplified flow-chart for subroutine ELLC.

62
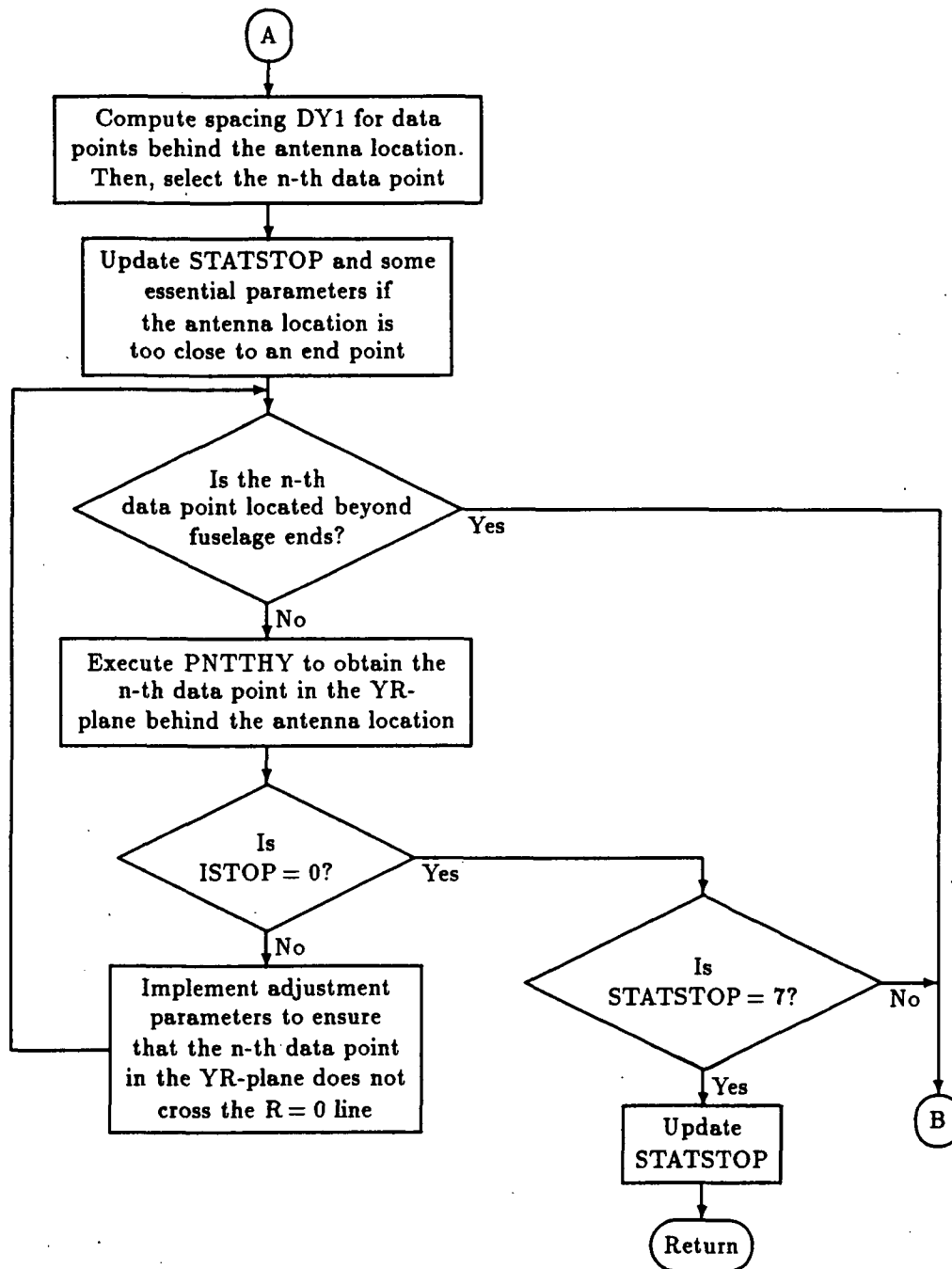
Figure 3.2: Continuation from Figure 3.1.

B

Compute spacing DY2 for data points
in front of the antenna location.
Then, select the m-th data point

Update STATSTOP and some
essential parameters if
the antenna location is
too close to an end point

Is the m-th
data point located beyond
fuselage ends?

Yes

No

Execute PNTTHY to obtain
the m-th data point in
the YR-plane in front of
the antenna location

Is
ISTOP = 0?

Yes

No

Implement adjustment
parameters to ensure
that the m-th data point
in the YR-plane does not
cross the R = 0 line

Is
STATSTOP = 7?

No

Yes

Update
STATSTOP

C

Return

Figure 3.3: Continuation from Figure 3.2.

C

Set indicator TOP to
logical TRUE for $|\phi_s| \leq 90^o$
and to logical FALSE for
$|\phi_s| > 90^o$

Execute ELLYR to generate
close-fit composite ellipse in
the YR-plane in the vicinity
of the antenna location,
producing parameters C_0, D_0,
Y_c, $CVES$, $CVESP$ and Y_{sh}.

Is
STATSTOP = 6?　　Yes

No

Are data
points in the YR-plane
convex in the improper
direction?　　Yes

Output
appropriate
error message

No

Compute parameters
A_0 and B_0

Return

Figure 3.4: Continuation from Figure 3.3.

65

two selected data points to the rear of the antenna location crosses over the $R = 0$ line of the YR-plane.

At spacing DY2 from each other, the YR-coordinates of the points in front of the antenna location in the YR-plane are generated until similar conditions as those for spacing DY1 occur. Again, a STATSTOP value of 13 would be generated and ELLC would halt with an appropriate error message if a point in the YR-plane could not be determined accurately. The very same adjustments for the spacing DY1 apply as well for spacing DY2.

Next, the routine determines the orientation of the antenna location with respect to the ellipsoid body: That is, if the antenna was located on the top half of the ellipsoid, the logical indicator TOP would be assigned logical TRUE, and if at the bottom half of it, indicator TOP would be assigned logical FALSE. This is performed to enable subroutine ELLYR to ascertain if the problem is of Case 1 or Case 2. With this information, subroutine ELLYR is then executed to produce the parameters C_0 and D_0, and the y-component Y_c of the center of the entire composite ellipse, as well as the stop-run condition STATSTOP that may occur in ELLYR. If the parameter STATSTOP was 6, indicating that the spacings DY1 and DY2 were changed to beyond the acceptable tolerance whereby the difference algorithm in subroutine ELLYR would provide accurate computations, ELLC would halt with an appropriate error message. For STATSTOP values of 7, 14, 15, 16 and 17, a warning message, indicating that the antenna was too close to an end point of the helicopter fuselage, would be output. For a STATSTOP value of 8, however, a warning message would be produced to indicate that the number of iterations in subroutine ELLYR had exceeded the maximum iterations allowed, and that the selected data points on the fuselage surface were perturbed to maximum tolerance. If, indeed, the surface in the vicinity of the antenna location was determined to be concave by subroutine PTURB in subroutine ELLYR, ELLC would halt with an appropriate error message as well.

Subsequently, the parameters A_0 and B_0 of the close-fit composite ellipsoid are computed by employing (2.85) and (2.86),respectively, for a Case 1 problem, or (2.87) and (2.88), respectively, for a Case 2 problem. Hence, the final results, A_0, B_0, C_0, D_0, Y_{sh}, X_c, Y_c and Z_c, as well as the stop-run parameter STATSTOP, are output.

3.2 Subroutine ELLYR

This is a subroutine that generates a close-fit composite ellipse in the YR-plane, given the parameters X_c and Z_c evaluated by subroutine ELLXZ. That is, it generates the composite ellipsoid parameters C_0 and D_0, as well as the y-component Y_c of the center of the composite ellipsoid. The final output parameters of this subroutine are C_0, D_0, Y_c, CVES, CVESP, Y_{sh}, and several logical variables essential to the main subroutine ELLC. Figure 3.5 through Figure 3.10 illustrates the general outline of the algorithm.

The subroutine begins by first defining and assigning the necessary parameters utilized in this routine. Within this part of the subroutine, decision statements dependent on the stop-run parameter STATSTOP are utilized to initialize several logical variables that will be employed to update values to the parameter STAT-STOP. Then the iteration counter is initiated. As long as the iteration count is not exceeded, the routine continues to initiate yet another parameter, the logical variable ZAEQZS, to logical FALSE. This logical parameter is a $Y_c = Y_s$ condition indicator. Note that this parameter is always initialized to logical FALSE at each iteration count. Following this, the first-order derivative GRADS at the antenna location is computed using an appropriate difference algorithm [11] in which the denominator h is assigned a constant of value 1.8 for point spacings of not greater than 1.9 and not less than 1.3. The 3-pointforward difference algorithm is utilized when spacing DY2 is less than 1.3 or greater than 1.9, and $1.3 \leq DY1 \leq 1.9$; whereas, the 3-point backward difference is utilized when spacing DY1 is less than 1.3 or greater

Figure 3.5: A simplified flow-chart for subroutine ELLYR.

A

Is this a
Case 1 problem? — **No**

↓ **Yes**

Execute SOLVR
to obtain C_0 and Y_c

Is
ZAEQZS=TRUE,
and SOLVR
fails? — **Yes** → **E**

↓ **No**

Update STATSTOP
if necessary

Search for the
first zero-crossing
of function f_2

Generate an initial
guess for RTSAFE
(This is the midpoint
between limits of
the bracketing range)

Obtain real roots
of function f_2
by executing RTSAFE
for $i = 1, 2$

D

Figure 3.6: Continuation from Figure 3.5.

69

Figure 3.7: Continuation from Figure 3.6.

Figure 3.8: Continuation from Figure 3.7.
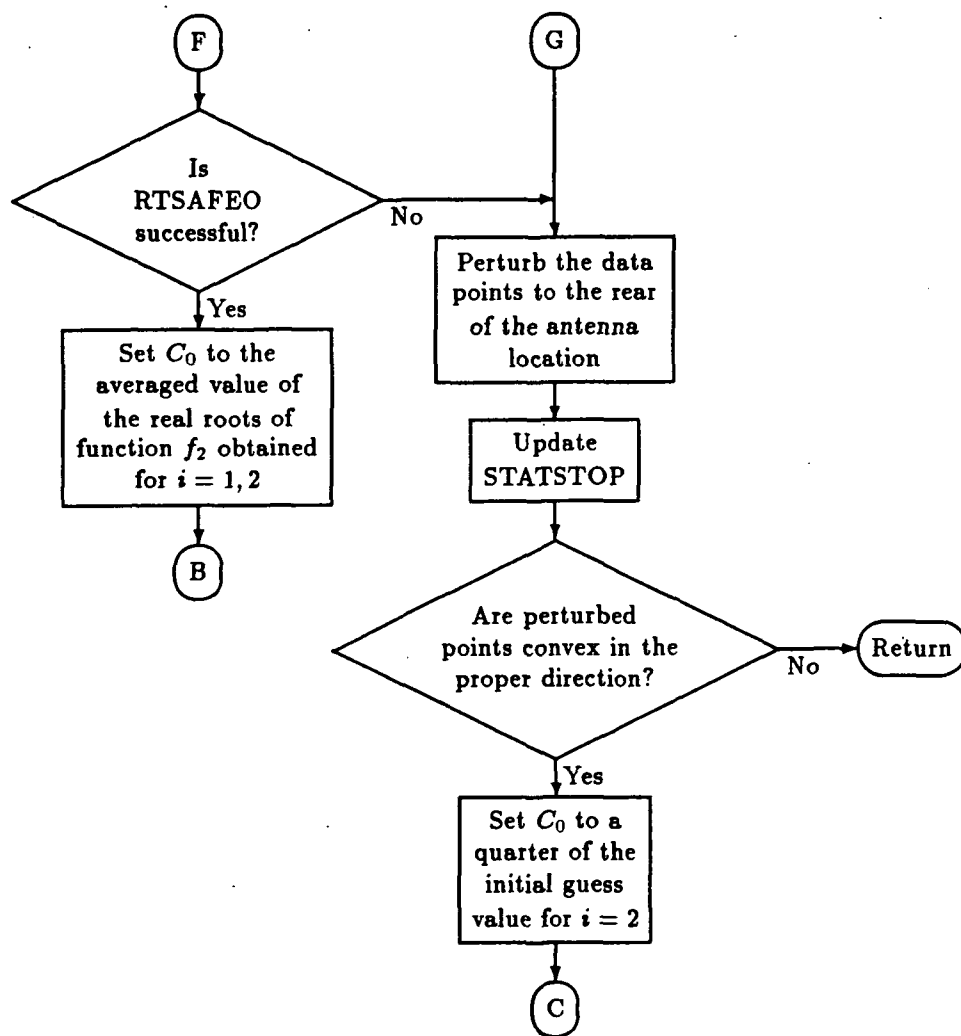
Figure 3.9: Continuation from Figure 3.8.
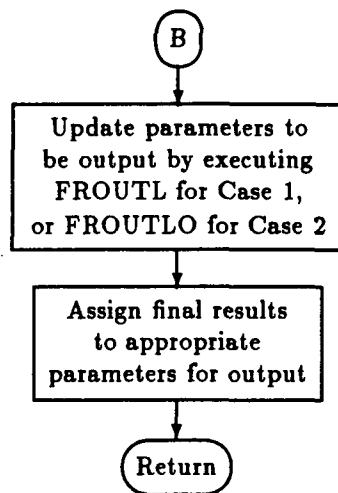
Figure 3.10: Continuation from Figure 3.9.

than 1.9, and $1.3 \leq DY2 \leq 1.9$. The 2-point central difference, on the other hand, is utilized when the values of both DY1 and DY2 are not within these specified domains. A decision is then made to ascertain the problem type at hand: that is, being as a Case 1 problem ($Y_s \geq Y_c$), or a Case 2 problem ($Y_s < Y_c$). When $-0.01 \leq GRADS \leq 0.01$, or $GRADS < -0.01$ and the antenna is located on the top half of the composite ellipsoid, or $GRADS > 0.01$ and the antenna is located on the bottom half of the composite ellipsoid, the problem is assumed as a Case 1 problem. On the other hand, however, when $GRADS > 0.01$ and the antenna is located on the top half of the composite ellipsoid, or $GRADS < -0.01$ and the antenna is located on the bottom half of the composite ellipsoid, the problem is regarded as a Case 2 problem.

For a Case 1 problem, the algorithm proceeds on to the module for the Case 1 problem. The first portion of the module is module SOLVR in which the composite ellipsoid parameter C_0 and the y-component Y_c of the center of the composite ellipsoid are determined. Only if ZAEQZS was assigned to logical TRUE, and C_0 and Y_c could not be determined by module SOLVR, would the algorithm then proceed on to module SOLVRO. Proceeding onwards, the updating procedure for the stop-run parameter STATSTOP is performed, and then module RTSAFE is executed. This module actually determines the composite ellipsoid parameter D_0 which is the averaged values of the real roots of (2.51) for $i = 1, 2$ (that is, for the first and second data points). If, however, module RTSAFE failed, subroutine PTURB would then be executed to perturb the data points in front of the antenna location, an appropriate updating of parameter STATSTOP would be performed, and parameter D_0 would be set to a factor of 0.25 of its initial guess value for $i = 2$ (for the second data point), after which the algorithm control would be returned to the counter incrementing section at the top of the algorithm. Otherwise, the real roots of (2.51) for $i = 1, 2$ would be averaged and assigned as an ultimate solution to parameter D_0.

However, if the problem is determined to be a Case 2 problem, the module for the Case 1 problem would be omitted and the module for the Case 2 problem would be executed. The module for the Case 2 problem is, in fact, very similar to the module for the Case 1 problem described previously. In this module, the composite ellipsoid parameter D_0, instead of C_0, and the y-component Y_c of the center of the composite ellipsoid is determined by module SOLVRO. If logical variable ZAEQZS was assigned to logical TRUE, and no solution was obtained by module SOLVRO, subroutine PTURB, which is at the bottom of this module, would then be executed to perturb, this time, the data points behind the antenna location. Otherwise, the parameter STATSTOP would be updated and module RTSAFEO would be executed. In module RTSAFEO, instead of the parameter D_0, the parameter C_0 would be determined. Again, if module RTSAFEO failed, subroutine PTURB would be executed to perturb the data points behind the antenna location, an appropriate updating of parameter STATSTOP would be performed, and parameter C_0 would be set to a factor of 0.25 of its initial guess value for $i = 1, 2$, after which the algorithm control would be returned to the counter incrementing section at the top of the algorithm. If otherwise, the real roots of (2.73) for $i = 1, 2$ would be averaged and assigned as a final solution to C_0.

If the control was returned to the counter incrementing section at the top of the algorithm, the entire procedure described previously would be repeated until reasonable solutions were obtained, or the maximum iteration counts exceeded. At the end of the entire algorithm execution, appropriate assignments of solutions to the output variables of this algorithm are performed. The control is then returned to the main program ELLC. It should be noted that subroutine ELLYR is able to detect slight concavity through subroutine PTURB, which will be presented subsequently.

3.3 Subroutines SOLVR and SOLVRO

These subroutines are executed by the subroutine. Essentially, the subroutine SOLVR is similar to its twin, the subroutine SOLVRO. These subroutines are the only routines to be called upon to directly provide the first set of parameter solutions to the subroutine ELLYR, given the parameters X_c and Y_c determined by subroutine ELLXZ. Solutions generated from these subroutines would be guaranteed, if GRADS was not assumed as approximately zero.

The subroutine SOLVR is utilized when a Case 1 problem is identified. This routine determines the composite ellipsoid parameter C_0 and the y-component Y_c of the center of the composite ellipsoid for a Case 1 problem. For a Case 2 problem, the subroutine SOLVRO is utilized instead. Here, the composite ellipsoid parameter D_0 and the y-component Y_c of the center of the composite ellipsoid is determined. Initialization of the necessary parameters are first performed, some of which could be passed into subsequent routines in ELLC. Then the variables a_i, b_i, c_i and d_i for $i = 1, 2$ are assigned their respective functions, as specified in (2.20) for subroutine SOLVR, or in (2.54) for subroutine SOLVRO. Finally, subroutine SRRO is executed to provide the respective solutions. Note that the logical indicator ZAEQZS, defined in Section 3.2, serves as one of the input parameters to subroutine SRRO.

Subroutines SOLVR and SOLVRO are guaranteed to return their respectively solutions, except when the logical parameter ZAEQZS is assigned to logical TRUE, and, $Y_s < Y_c$ for subroutine SOLVR or $Y_s \geq Y_c$ for subroutine SOLVRO. This is attributed to the fact that subroutine SRRO always returns a solution, feasible or infeasible. Indeed, this matter is further discussed in Section 3.4.

3.4 Subroutine SRRO

This subroutine contains the essential algorithm for determining the first set of solutions generated by subroutine ELLYR via subroutines SOLVR and SOLVRO. A

logical parameter REFLECT is also output to indicate if the reflecting procedure, to be discussed later in this section, is utilized. An important input parameter to this subroutine is the logical indicator ZAEQZS defined in Section 3.2. The effects of this logical indicator in this subroutine will be discussed eventually in this section. Figure 3.11 through Figure 3.14 illustrates the flow-chart of this subroutine.

The core of this algorithm begins with a decision module: Should $Y_c = Y_s$ condition be utilized? If yes, then Y_c would be assigned the value of Y_s, which is the value of the y-component of the antenna coordinate. Otherwise, the exact value of the parameter Y_c would be computed using (2.36) for a Case 1 problem, or (2.69) for a Case 2 problem. Next, if condition (2.22) for Case 1 or condition (2.56) for Case 2 was not satisfied, then Y_c would be obtained by reflecting Y_c on Y_s so that Y_c falls onto the appropriate feasible side of Y_s by applying (2.39) for Case 1 or (2.41) for Case 2. The logical parameter REFLECT would then be assigned to logical TRUE, which would otherwise be assigned to logical FALSE by default. Proceeding on, there is also a check to ensure that the square-root argument DUMSQRT in (2.38) for Case 1, or (2.70) for Case 2, is positive, so as to ensure a real solution. If, however, DUMSQRT is less than or equal to 10^{-6}, an adjustment procedure would be performed so as to force DUMSQRT into the feasible region.

Briefly, the adjustment procedure is as follows. If DUMSQRT was less than or equal to 10^{-6}, the type of roots (2.49) possesses would be determined. For such a parabolic function, only three possible root types exist: (a) 2 distinct real roots, referred simply as Type 1, (b) 2 equal real roots, which is equivalent to a single value of real root, referred simply as Type 2, and (c) a pair of conjugate roots, referred simply as Type 3. If the roots are real, that is, if they are of Type 1 or Type 2, then the roots are evaluated. Of the two roots obtained, the root which is nearest to Y_s for ZAEQZS=TRUE, or to the exact mathematical solution for ZAEQZS=FALSE, would be selected and assigned to a dummy variable ZA2. The linear function (2.50) for Case 1, or (2.72) for Case 2, is evaluated at $Y_c = $ ZA2. If the
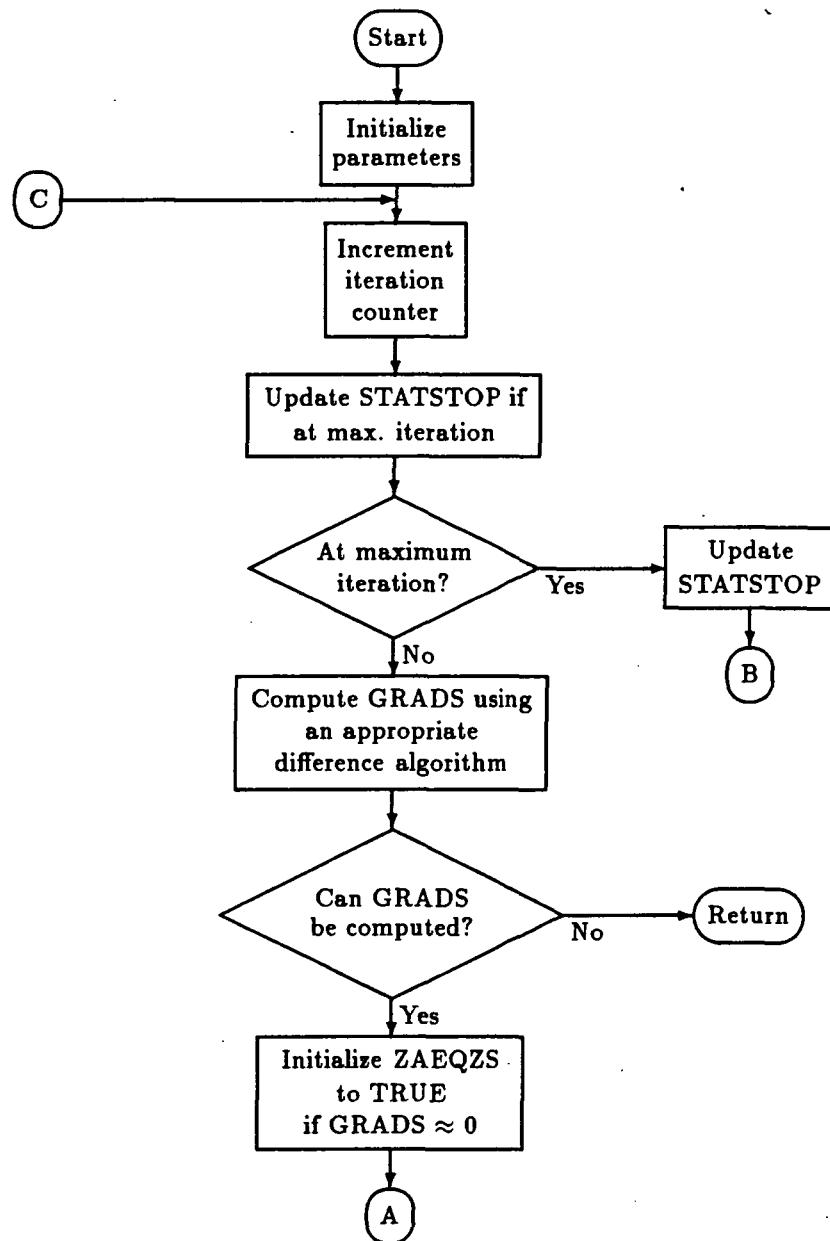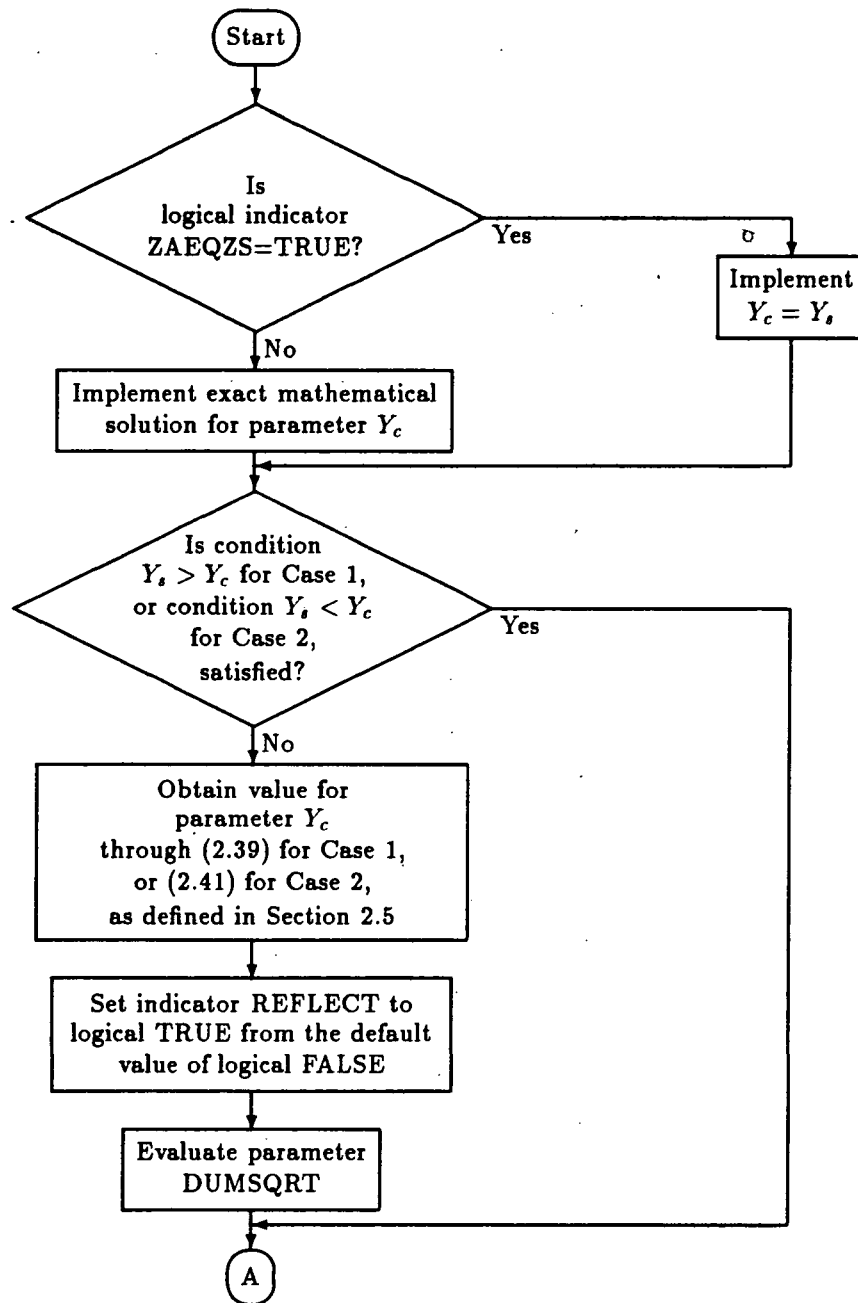
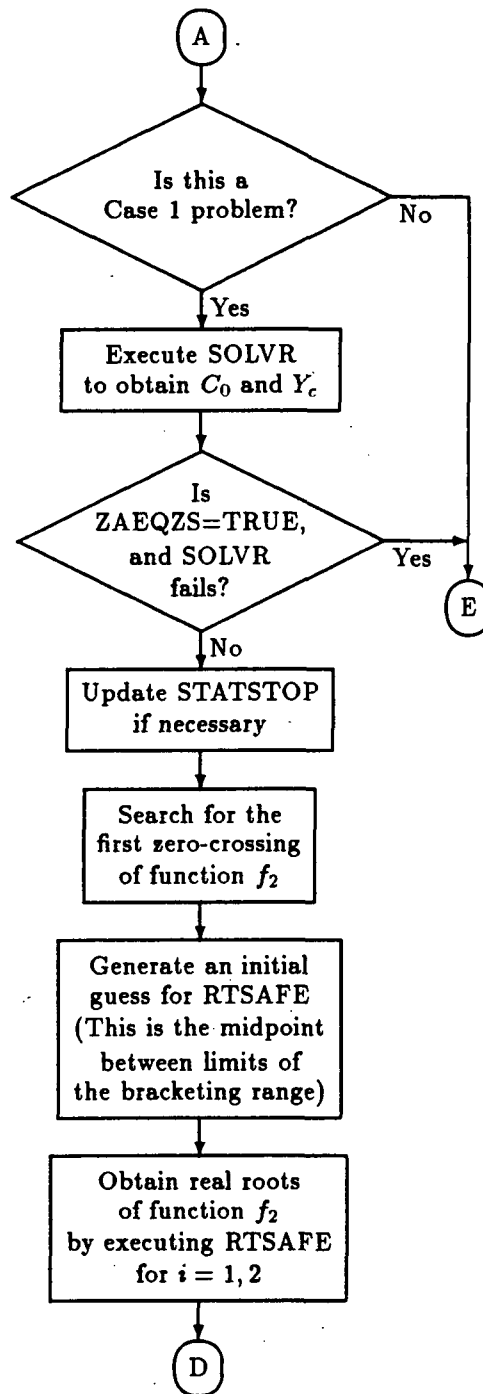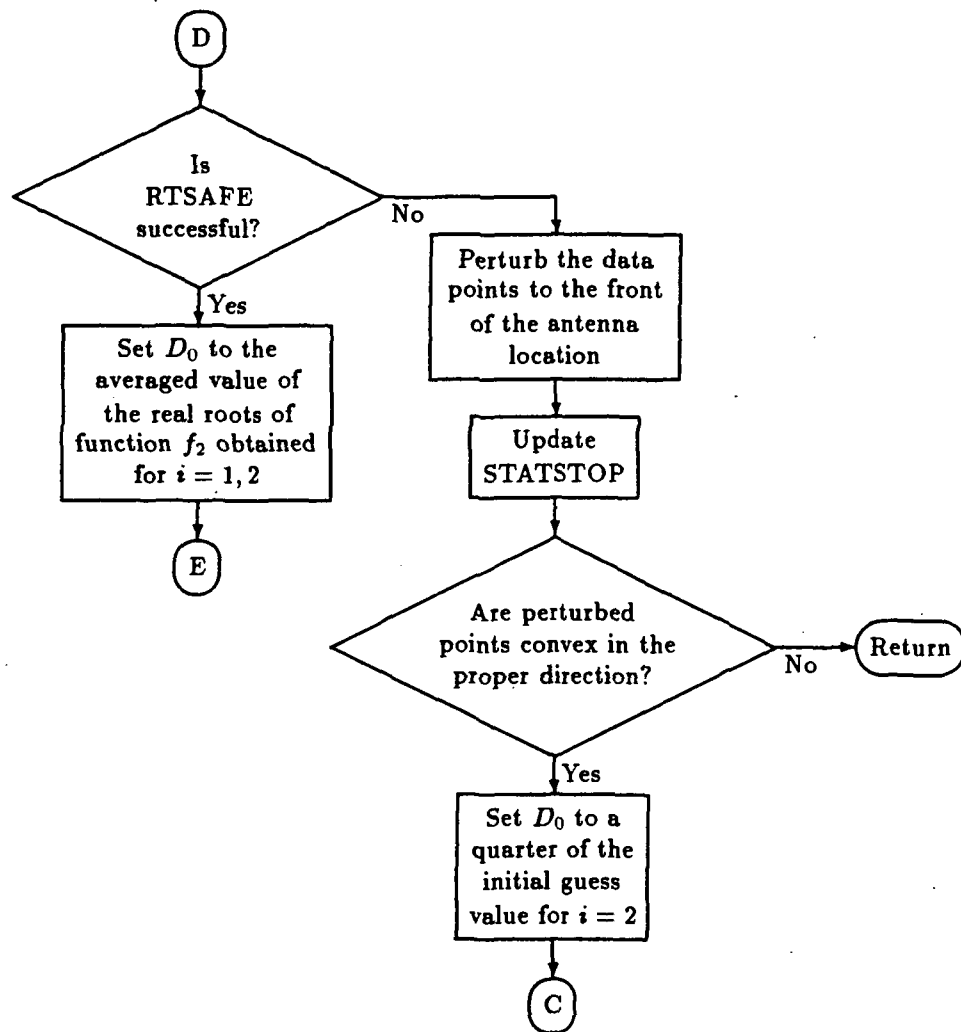Figure 3.11: A simplified flow-chart for subroutine SRRO.
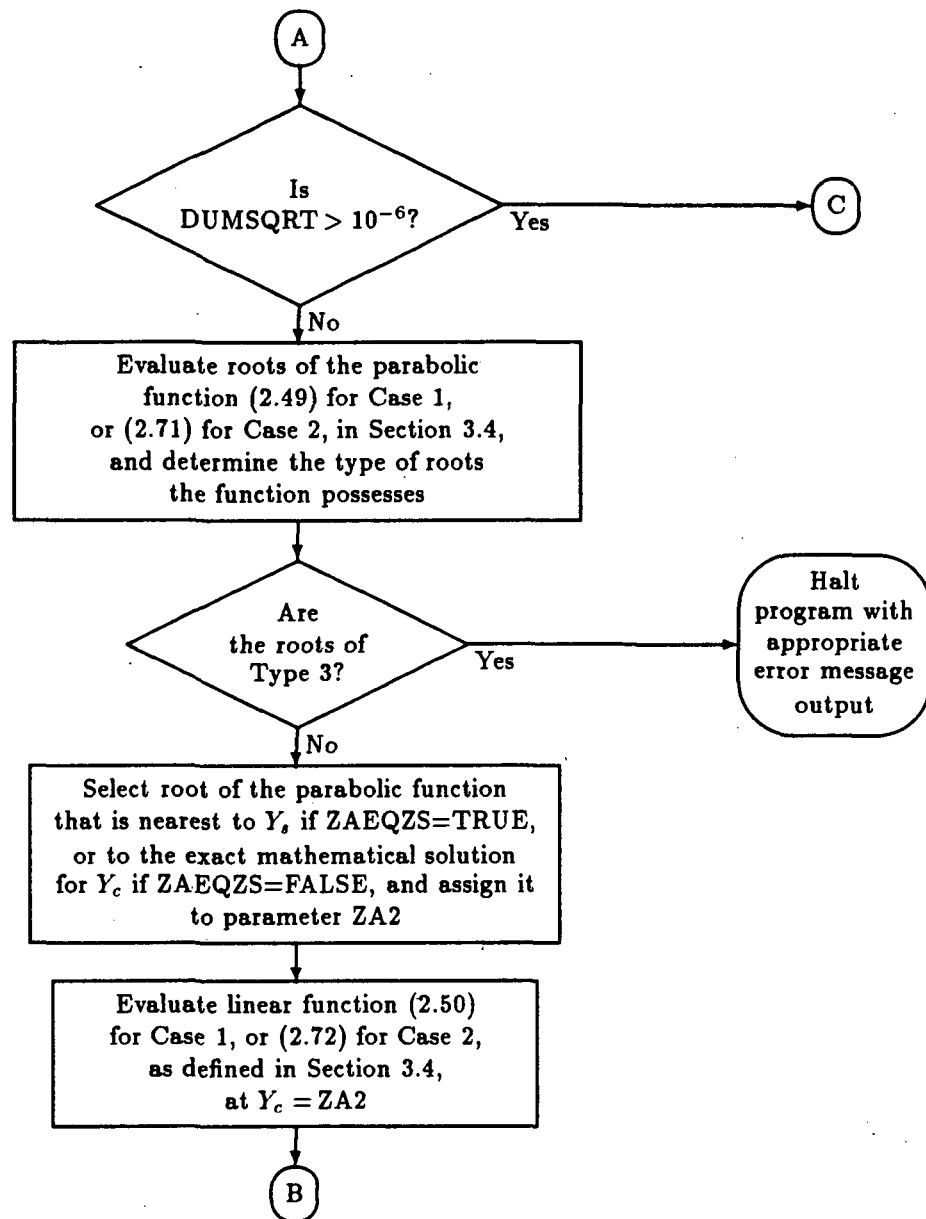
Figure 3.12: Continuation from Figure 3.11.
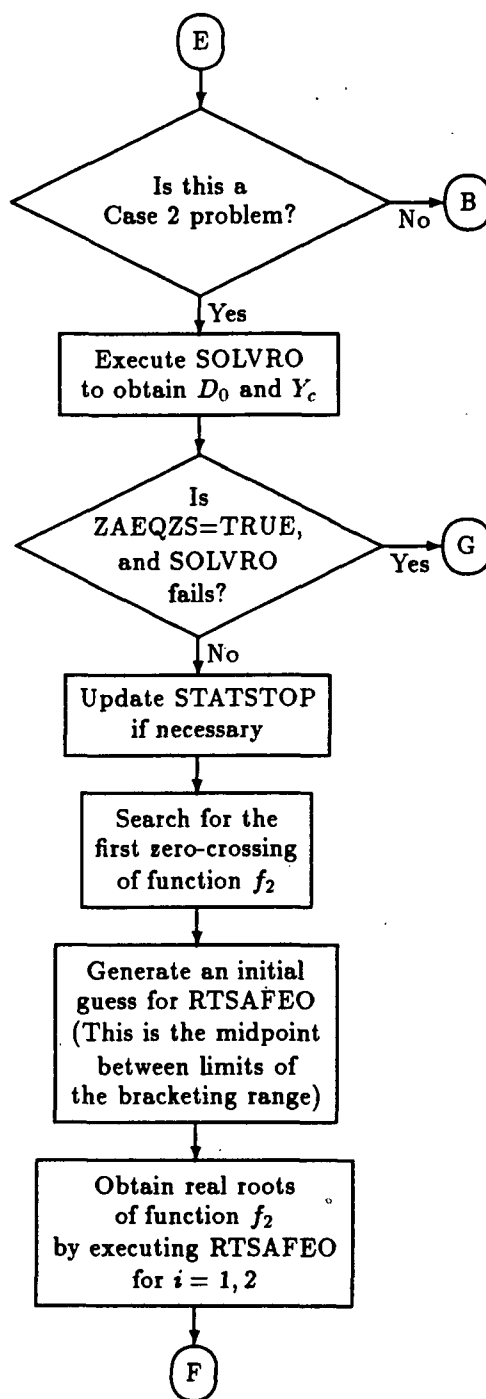
79
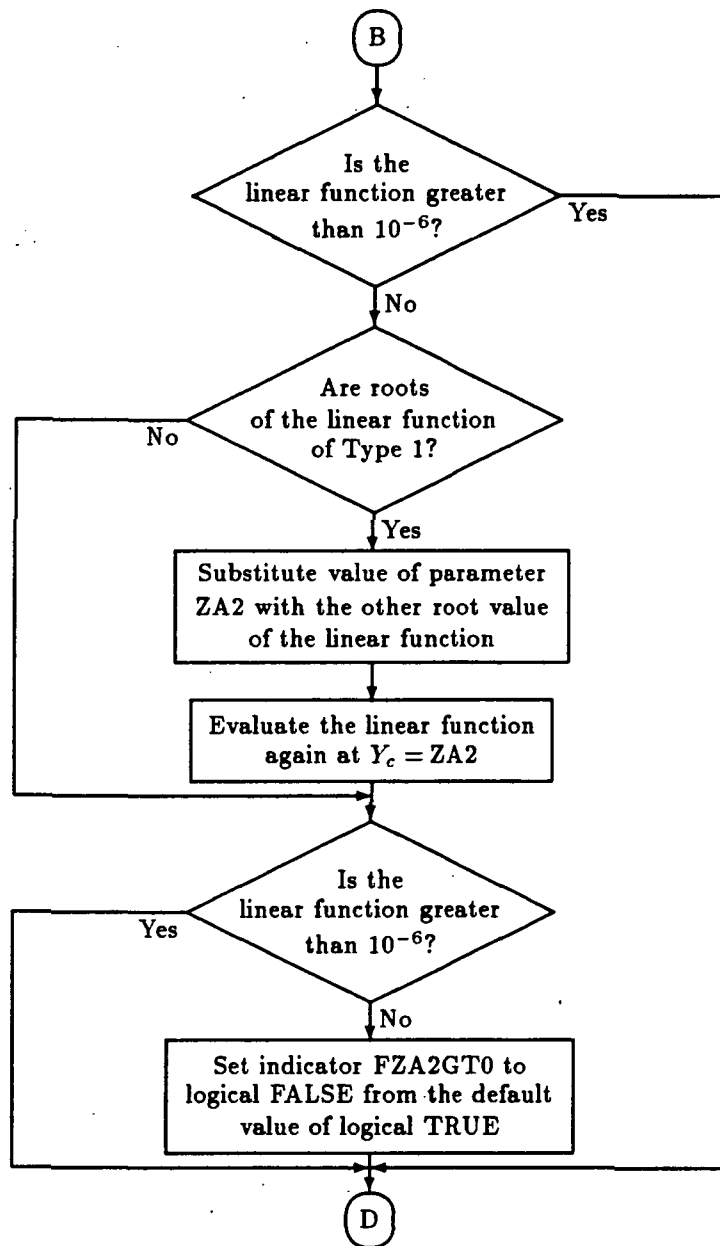
Figure 3.13: Continuation from Figure 3.12.
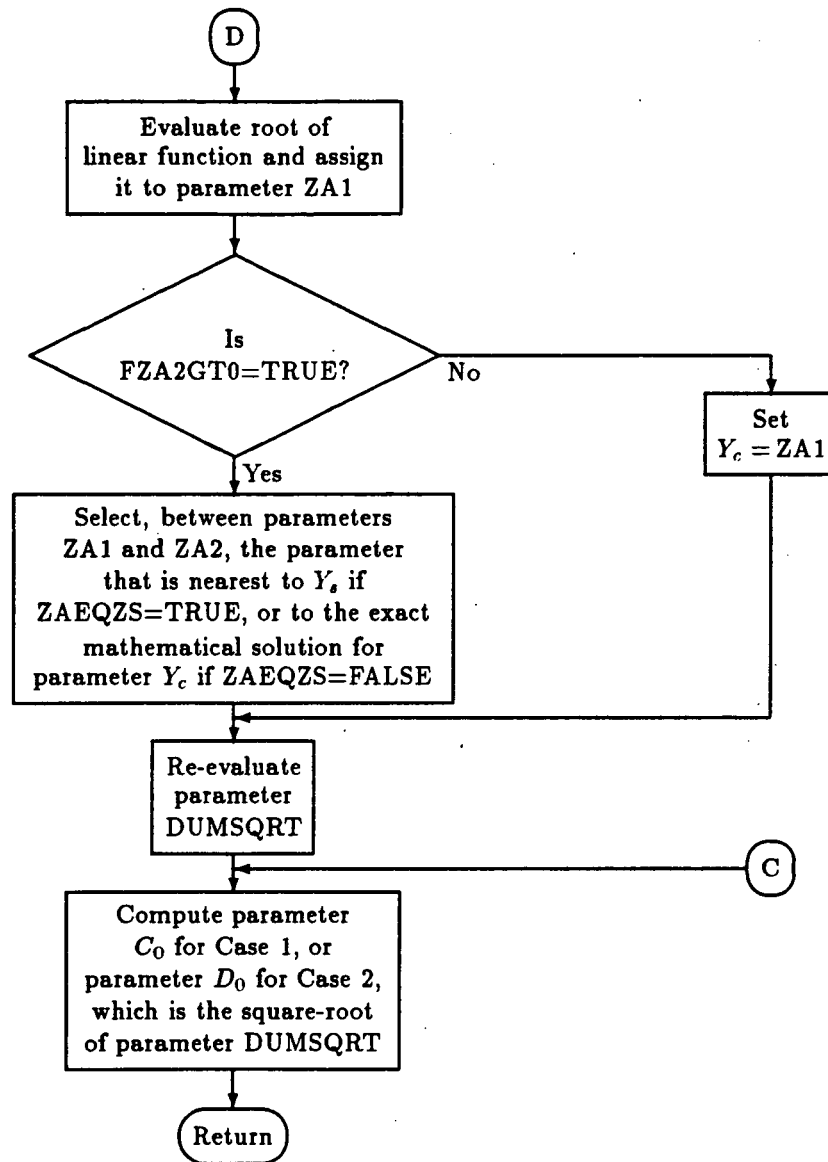
Figure 3.14: Continuation from Figure 3.13.

linear function was found to be less than or equal to 10^{-6}, then if a Type 1 condition is at hand, ZA2 would be assigned the other root value. The linear function would then be re-evaluated again at $Y_c = ZA2$. At this stage, if the linear function is found to be less than or equal to 10^{-6} again, regardless of the root type being as Type 1 or Type 2, an indicator flag FZA2GT0 would be set, from the default logical TRUE, to logical FALSE, indicating that (2.50) or (2.72) was not greater than 10^{-6}. Now, the algorithm proceeds on to evaluate the root of (2.50) or (2.72). If FZA2GT0 was not assigned to logical FALSE, that is, still assigned to logical TRUE, the roots ZA1 and ZA2 of both the parabolic and linear functions, respectively, would be considered for being selected as the root nearest to Y_s for ZAEQZS=TRUE, or to the exact mathematical solution for ZAEQZS=FALSE. Selection would be performed, and thus, Y_c would be obtained. Otherwise, by default, the root ZA1 of the linear function would be selected, and hence, Y_c would be assigned the value ZA1.

Subsequently, DUMSQRT is re-evaluated again so as to assign a proper value to it. It is now, by certainty, greater than 10^{-6}. Parameter C_0, for a Case 1 problem, or parameter D_0, for a Case 2 problem, is then computed by evaluating the square-root of DUMSQRT, which is in fact (2.38) for a Case 1 problem or (2.70) for a Case 2 problem. These parameters, together with the logical parameter REFLECT discussed earlier in this section, form the output parameters of this routine.

3.5 Modules RTSAFE and RTSAFEO, functions RTSAFE and RTSAFEO, subroutines FROUTL and FROUTLO, subroutines AROUTL and AROUTLO

3.5.1 Modules RTSAFE and RTSAFEO

Modules RTSAFE and RTSAFEO are modules in the subroutine ELLYR that determine the composite ellipsoid parameter D_0 via (2.51) for a Case 1 problem, or C_0 (2.73) for a Case 2 problem. Included within each of these modules are function

RTSAFE or RTSAFEO, respectively, subroutine FROUTL or FROUTLO, respectively, and subroutine AROUTL or AROUTLO, respectively. Module RTSAFE is utilized when Case 1 is identified, and module RTSAFEO is utilized when Case 2 is identified instead. The simplified flow-charts for these modules are illustrated in Figure 3.15 through Figure 3.20.

The parameter D_0 for Case 1, or C_0 for Case 2, is determined in two stages: First, through the establishing of a crude bracketing range of the zero-crossing of function f_2 by searching downward from $D_0, C_0 = 200$ to $D_0, C_0 = -200$ at 2 units interval so that D_0, or C_0 is of the largest root within the range. This is to deter the selection of a negative root, if provided the choices of a positive and a negative roots, as the positive root solution is ideologically more proper. Second, through the function RTSAFE for Case 1, or RTSAFEO for Case 2, to significantly refine the solution obtained. Each of these modules consists of two DO loops. The first DO loop varies the parameter i of (2.18) for a Case 1 problem, or (2.53) for a Case 2 problem, from 1 through 2 so that the very same algorithm is administered for both $i = 1$ and $i = 2$. As for the other loop, it enables a downward sweeping of parameter D_0 for Case 1, or C_0 for Case 2, from 200 to -200 at -2 units increments so that the first stage of the root-finding process could be executed. As a matter of fact, the second DO loop is actually nested within the first. In addition, for each of these modules, there are two IF statements responsible for deciding when to execute function RTSAFE for Case 1, or function RTSAFEO for Case 2, and another IF statement for deciding if subroutine PTURB should be executed at all.

Within the first DO loop, the second DO loop constitutes the initial segment of the first. In fact, the second loop actually forms the outer shell of the first stage of the root-finding algorithm. The occurrence of a zero crossing point for a particular value of i of (2.18) for Case 1, or (2.53) for Case 2, is determined to within a certain range bracket, by searching downward from 200 to -200 through the execution of the second DO loop. Assuming that $X1 < D1 < X2$ for Case 1,
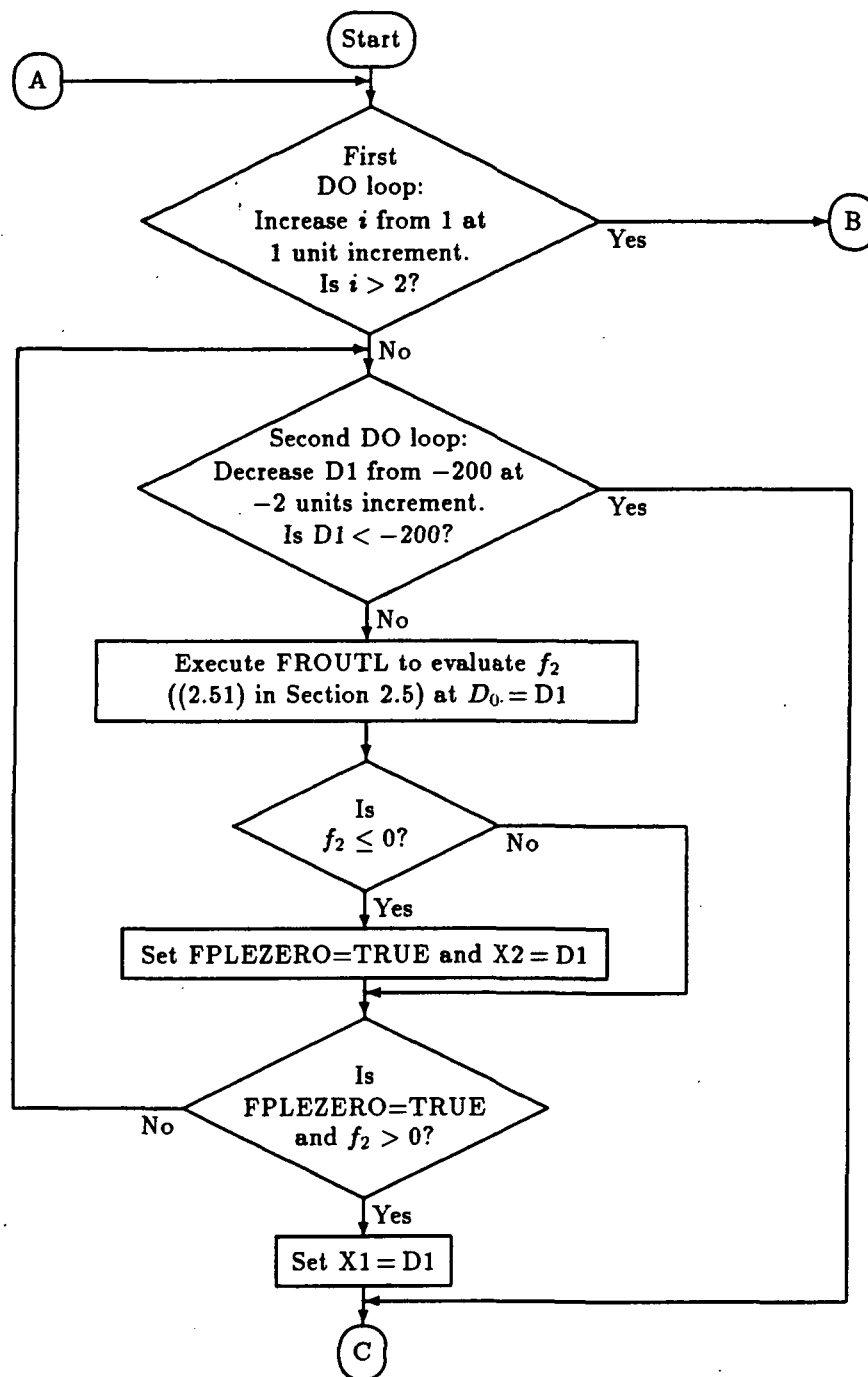
Figure 3.15: A simplified flow-chart for subroutine RTSAFE.

C

Obtain midpoint value
between X1 and X2,
and utilize this as
the initial guess for
passing into function
RTSAFE

Is
$i = 1$? → No

↓ Yes

Execute function RTSAFE
for $i = 1$ to obtain a
real root of f_2 for $i = 1$,
with indicator STATRT1
output as well

Is $i = 1$ and
STATRT1 $\neq 2$? → No

↓ Yes

Execute function RTSAFE
for $i = 2$ to obtain a
real root of f_2 for $i = 2$,
with indicator STATRT2
output as well

A   B

D
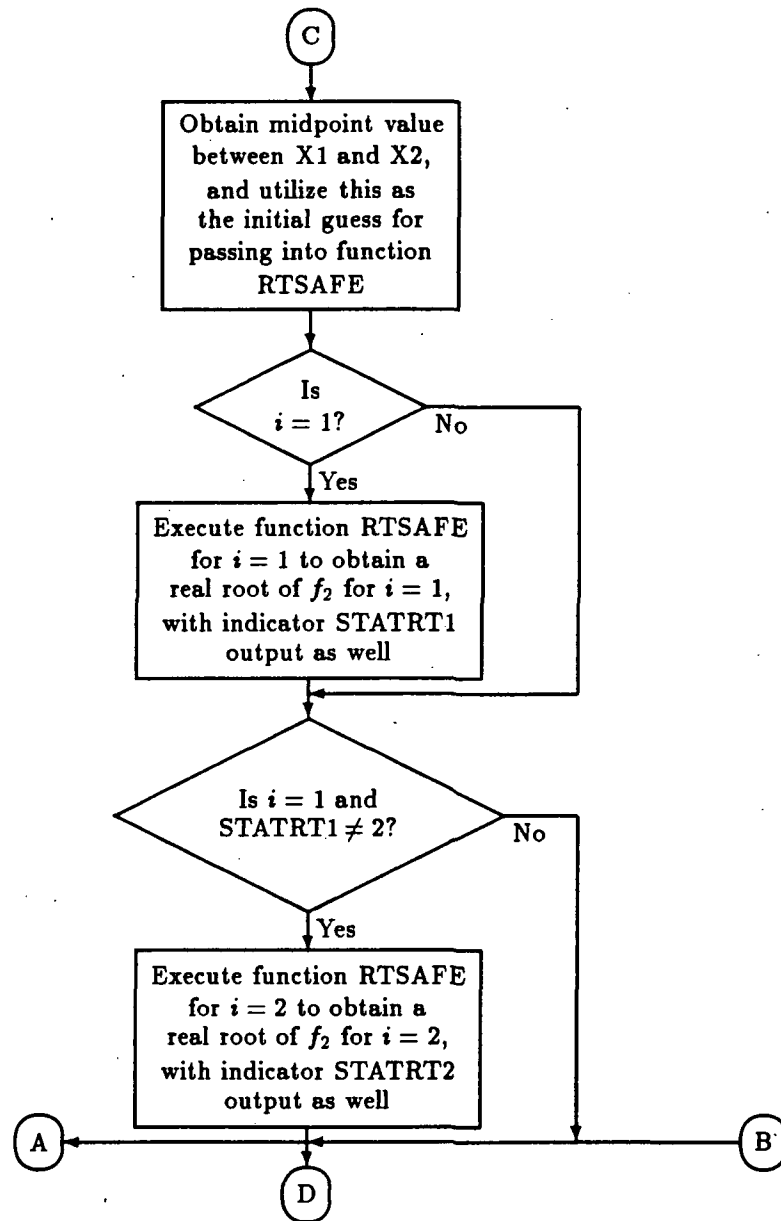
Figure 3.16: Continuation from Figure 3.15.
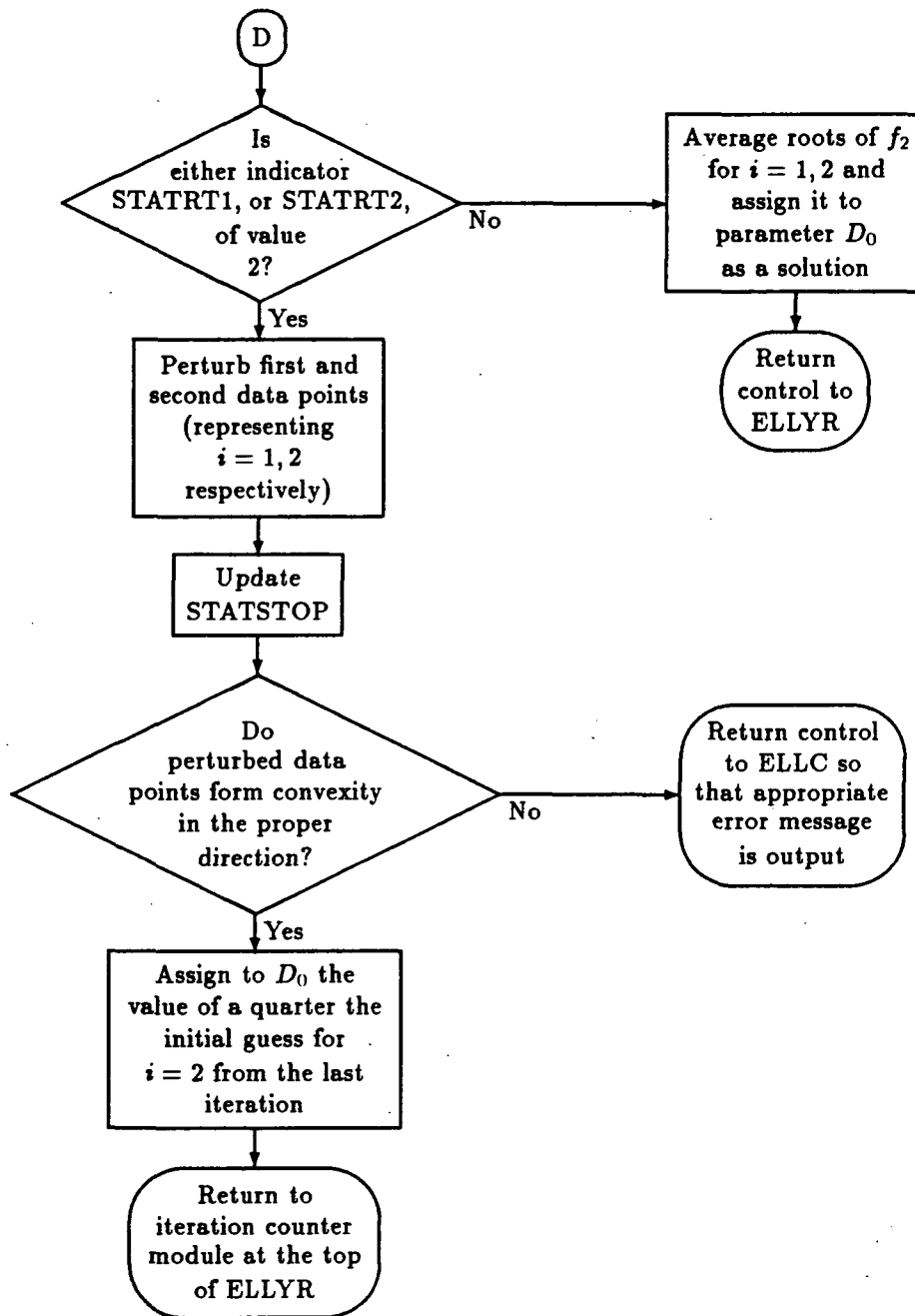
Figure 3.17: Continuation from Figure 3.16.
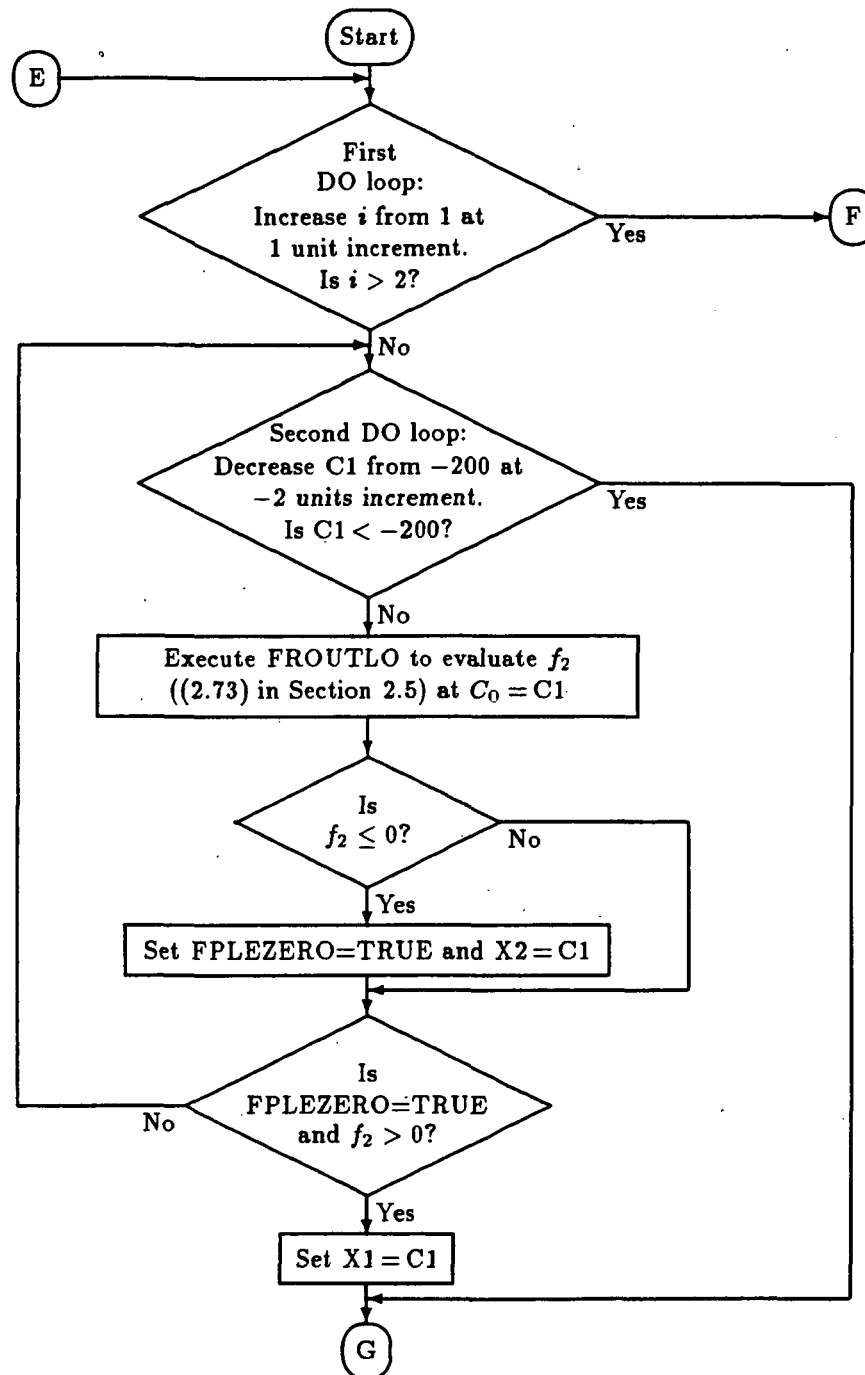
Figure 3.18: A simplified flow-chart for subroutine RTSAFEO.
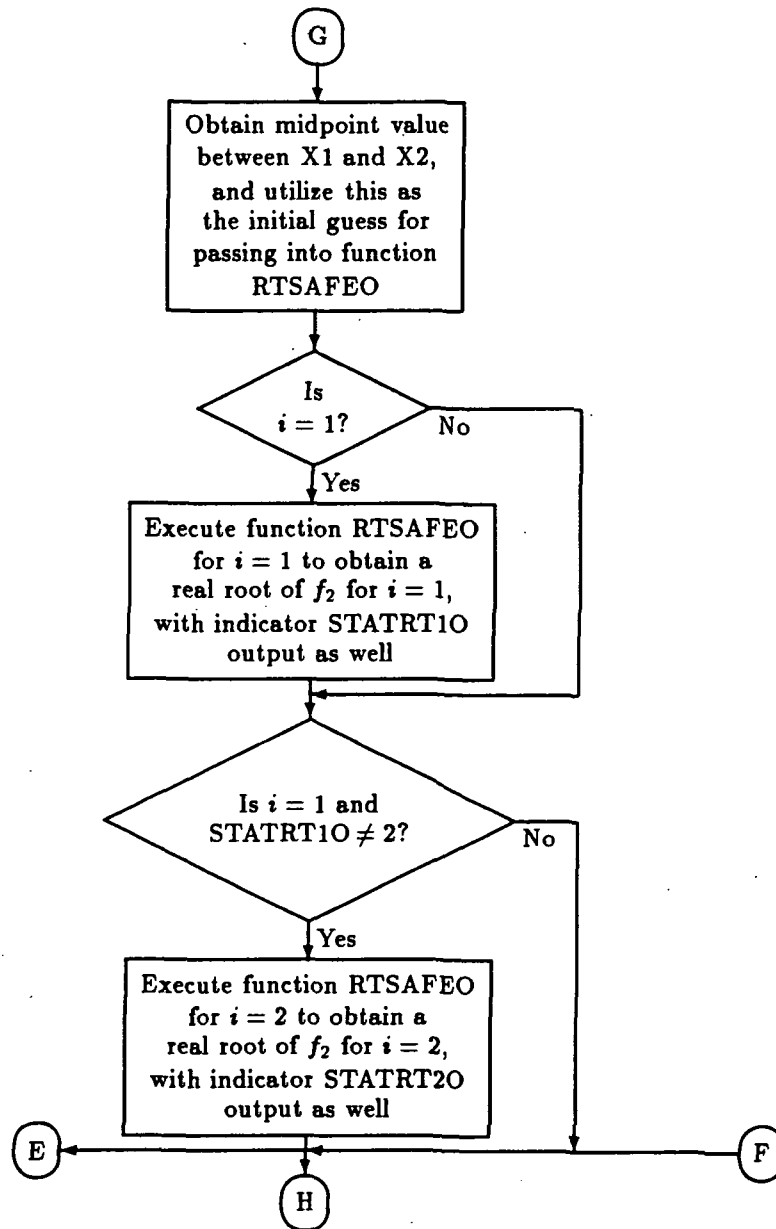
Figure 3.19: Continuation from Figure 3.18.

H

Is either indicator STATRT1O, or STATRT2O, of value 2?

No → Average roots of f_2 for $i = 1, 2$ and assign it to parameter C_0 as a solution

Return control to ELLYR

Yes

Perturb first and second data points (representing $i = 1, 2$ respectively)

Update STATSTOP

Do perturbed data points form convexity in the proper direction?

No → Return control to ELLC so that appropriate error message is output

Yes

Assign to C_0 the value of a quarter the initial guess for $i = 2$ from the last iteration

Return to iteration counter module at the top of ELLYR

Figure 3.20: Continuation from Figure 3.19.

or $X1 < C1 < X2$ for Case 2, is the bracketing range obtained, a zero-crossing at a particular point within the bracketing range would be recognized if $f_2(X1) < 0$ and $f_2(X2) > 0$, or vice-versa. Indeed, the module always selects the very first zero-crossing encountered for evaluation. This is in fact the bracketing range that specifically contains one of the real roots of f_2. The midpoint value of this bracketing range is actually the initial guess value that is to be utilized in function RTSAFE for Case 1, or function RTSAFEO for Case 2. Through these functions, the specific value of the real root in the bracketing range is precisely determined. In addition to this, the indicators STATRT1 and STATRT2 for function RTSAFE, or STATRT1O and STATRT2O for function RTSAFEO, are generated henceforth to arbitrate certain decision statements, as illustrated in the figures. If, however, the first stage of the root-finding algorithm were to fail, the initial guess to function RTSAFE, or function RTSAFEO, could assume any real value. Nonetheless, due to the structure of the algorithm itself, the initial guess would be assigned the value -100 for $f_2 < 0$, or the value zero for $f_2 > 0$.

Once completed, the roots thus obtained for $i = 1, 2$ areaveraged to produce the solution for D_0 if Case 1 is in question, or C_0 if Case 2 is at hand instead. If, however, no acceptable solution was generated, that is, if one of the STATRT indicators for a particular case is of value 2, then subroutine PTURB would be executed to perturb the data points in front of the antenna location for a Case 1 problem, or the data points behind the antenna location for a Case 2 problem. The parameter STATSTOP would then be updated to 10 or 15. The former value would indicate that the perturbed data points are concave. The latter, however, would represent a STATSTOP condition of 7, but the solutions are of STATSTOP $= 10$ type. If the perturbed data points are concave, the statement RETURN would be executed, and the control pointer would exit subroutine ELLYR and return to ELLC. Otherwise, control would be returned to the iteration counter module at the top of subroutine ELLYR for initializing the next iteration.

90

3.5.2   Functions RTSAFE and RTSAFEO

Function RTSAFE determines a real root of (2.51) for a Case 1 problem, and its twin, function RTSAFEO determines a real root of (2.73) for a Case 2 problem. These functions are in fact modified versions of the routine provided in [9], which is in essence, a root solving routine that outputs a real-valued root solution. This routine utilizes the Newton-Raphson and bisection methods of root finding for a 1-D nonlinear function.

Functions RTSAFE and RTSAFEO are modified so as to be able to perform the appropriate range bracketing procedure required by the original version. In fact, these procedures are appended at the beginning algorithm of these functions. Additionally, the calling statements of subroutine FROUTL, or FROUTLO, (representing expression (2.51), or (2.73), respectively), and subroutine AROUTL, or AROUTLO, respectively, (representing its first order derivative), are also included, as required by the original version itself. An indicator STATRT for function RTSAFE, or STATRTO for function RTSAFEO, would be flagged to a value of 1 to indicate that the function does not cross the zero line within maximum iterations, and to a value of 2 to indicate that the function does not cross the zero line within maximum iterations and bracketing range. The default value of 0 for STATRT or STATRTO indicates that a real root solution is obtained prior to maximum iterations or bracketing range.

The range bracketing procedure for functions RTSAFE or RTSAFEO is described as follows. After initializing the parameters necessary for the function concerned, the iteration counter is initialized from 0 to 1. If the iteration count was exceeded, parameter STATRT for Case 1, or STATRTO for Case 2, would be set to 1 and the range increment parameter doubled. The iteration counter would then be re-initialized to zero again. If, however, the new range increment parameter exceeds a specified maximum value of 20, the function would then assume the upper limit of the current bracketing range, and parameter STATRT for Case 1, or STATRTO for Case 2, would be assigned a value of 2, after which statement RETURN would be

executed to return the control to the calling routine. Otherwise, the new limits of the bracketing range would be computed, and (2.51) for Case 1, or (2.73) for Case 2, would be evaluated at the range limits.

If the entire bracketing range was indeed above or below the zero line, the limits would be extended in an attempt to include the zero line within the bracketing range. The algorithm control would then be returned to the iteration counter at the beginning of the algorithm for the next iteration. Nevertheless, it should be noted that, if (2.51) for Case 1, or (2.73) for Case 2, was evaluated at any one of the limits within the tolerance $\pm 10^{-6}$, then the function routine would be assigned to that particular limit value.

3.5.3 Subroutines FROUTL and FROUTLO

Subroutines FROUTL and FROUTLO represent the f_2 functions in (2.51) for the Case 1 problem, and (2.73) for the Case 2 problem, respectively. A required input is the independent variable D_0 for Case 1, or C_0 for Case 2. Other inputs necessary for each of these routines are the parameters essential for evaluating f_2 which have been computed by subroutines SOLVR or SOLVRO prior to the execution of FROUTL or FROUTLO, respectively.

In order to eliminate a possible numerical error which could result in the parameter $\sin V'_{es}$ in f_2 being slightly larger than or equal to 1, or slightly lesser than or equal to -1, IF statements would be utilized to default the value of $\sin V'_{es}$ to 0.999, or -0.999, respectively, if such events ever occurred. Another restriction implemented is the minimum value tolerance of the denominator parameter DENOM = $D_0 + Y_{sh}$ for Case 1, or DENOM = $C_0 - Y_{sh}$ for Case 2. DENOM would be assigned a value of 10^{-6} if its computed value was between -10^{-6} and 10^{-6}. This is implemented to deter a possible occurrence of a division-by-zero error.

3.5.4 Subroutines AROUTL and AROUTLO

Subroutines AROUTL and AROUTLO are subroutines for evaluating the first order derivatives of (2.51) for a Case 1 problem, and (2.73) for a Case 2 problem, respectively. The method of computation employed in each of these subroutines is the method of 4-point central difference [11]. The denominator h in this algorithm is assigned to a constant value of 0.008 for point spacings of not greater than 1.9 and not less than 1.3. Indeed, this algorithm contain CALL statements to subroutines FROUTL and FROUTLO for the former and latter cases, respectively.

3.6 Subroutine PTURB

Subroutine PTURB is a subroutine that executes subroutine CONVEX which actually performs the perturbation process on a given set of data points. In addition, it can identify the set of data points that forms a concavity that exceeds the tolerance specified. With regards to the data points input into the routine, subroutine PTURB assumes that there are two pairs of points flanking the antenna location, a pair on the front and another behind the antenna location. Among the inputs to this subroutine are the parameters ϕ_s and GRADS which have been defined in subroutine ELLYR, as presented in Section 3.2. In fact, these are input parameters essential to subroutine CONVEX.

Following the initialization of some necessary parameters, subroutine CONVEX is executed to perturb the data points downwards along vector $\hat{d}$ defined in (2.77), but in the direction opposite to that of the outward normal of the fuselage which is assumed to be pointing directly upwards. In fact, these data points are perturbed such that they are always located below the tangent line m_l. It should be noted that the perturbation process would be performed only if the original (unperturbed) data points were convex Otherwise, the statement RETURN would be executed to

93

return the algorithm control to module RTSAFE for a Case 1 problem, or module RTSAFEO for a Case 2 problem, in subroutine ELLYR.

Subsequently, the incremented incremental variable DEL, of which its initial value is set externally in subroutine ELLYR, is incremented for future use in the iteration counter module in subroutine ELLYR itself. As outputs, subroutine PTURB returns the appropriate perturbed data points, the incremental variable DEL, and the logical parameter CONCAVE which indicates that the data points form a concavity if its value is logical TRUE, or that the data points form a convexity if its value is logical FALSE.

3.7 Subroutine CONVEX

Subroutine CONVEX is a subroutine that is executed by the parent subroutine PTURB. It computes the perturbed coordinates of the data points in the vicinity of the antenna location provided. If the set of data points were convex, the perturbation process would be performed and a new set of coordinates would be generated. Among the inputs into this subroutine are the parameters ϕ_s and GRADS, which were defined in subroutines ELLC (Section 3.1) and ELLYR (Section 3.2), respectively. A simplified flow-chart of this subroutine is illustrated in Figure 3.21 through Figure 3.23.

The routine commences by initializing some essential parameters. It then acknowledges the position of the antenna location with respect to the composite ellipsoid body: If the antenna was located at the top half of the close-fit composite ellipsoid, that is, $\phi_s \leq 90^\circ$, the sign coefficient parameter SIGN is initialized to 1. At the bottom half of it, that is, $\phi_s > 90^\circ$, parameter SIGN is initialized to -1. The midpoint between the two points to the front of the antenna location is then determined. By extrapolating a line from this midpoint to the antenna location, the first-order derivative MAGVL of the extrapolation line is computed.

94
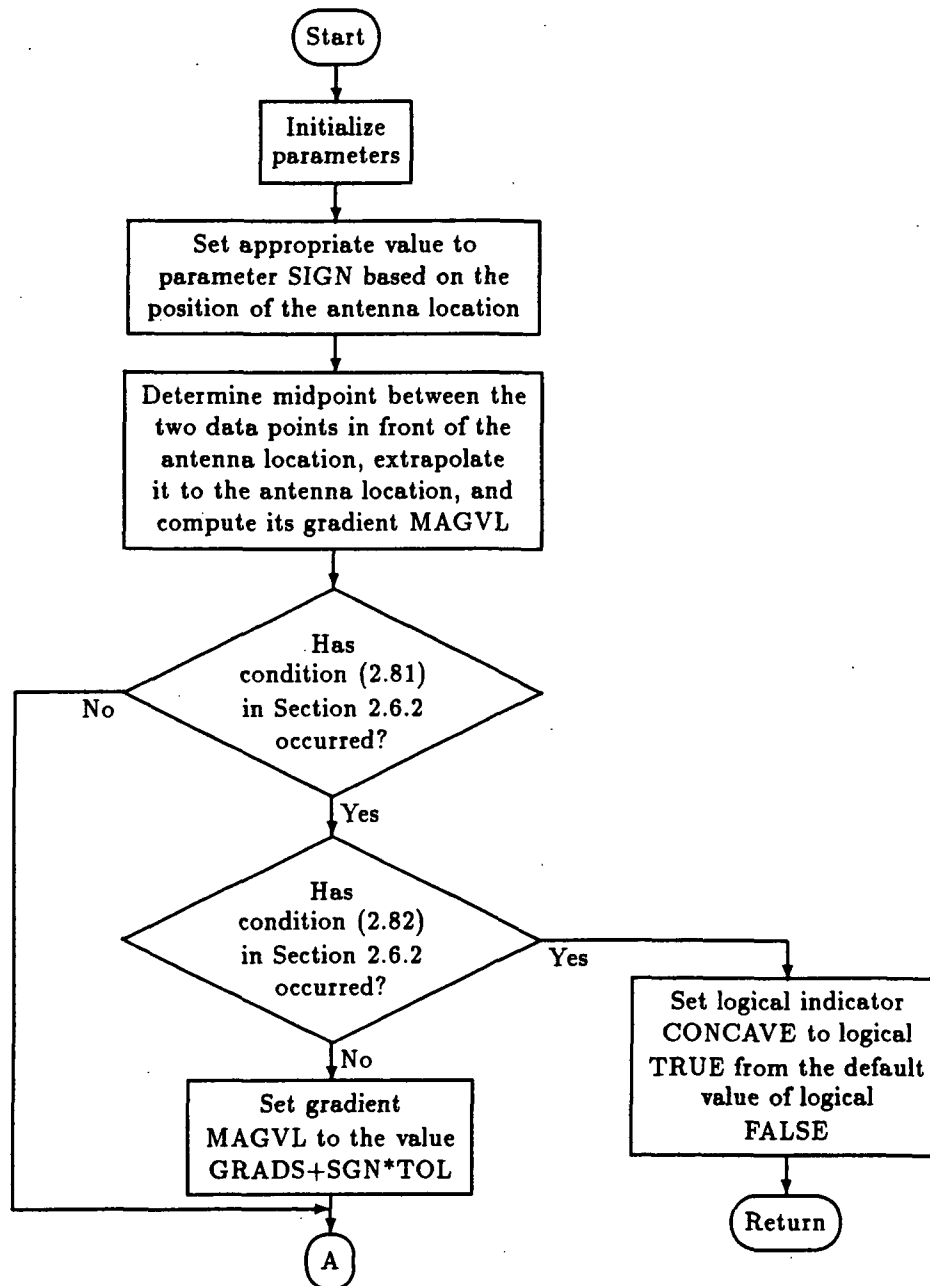
Figure 3.21: A simplified flow-chart for subroutine CONVEX.

(A)

Execute CONVX to perturb
first data point in front
of the antenna location
with parameter GRADS as
one of the input parameters

Execute CONVX to perturb
second data point in front
of the antenna location
with parameter GRADS
substituted with
parameter MAGVL

Determine midpoint between the
two data points behind the
antenna location, extrapolate
it to the antenna location, and
compute its gradient MAGVR

Has
condition (2.83)
in Section 2.6.2
occurred?

No

Yes

Has
condition (2.84)
in Section 2.6.2
occurred?

Yes

No

Set gradient
MAGVR to the value
GRADS-SGN*TOL

Set logical indicator
CONCAVE to logical
TRUE from the default
value of logical
FALSE

Return

(B)

Figure 3.22: Continuation from Figure 3.21.

96
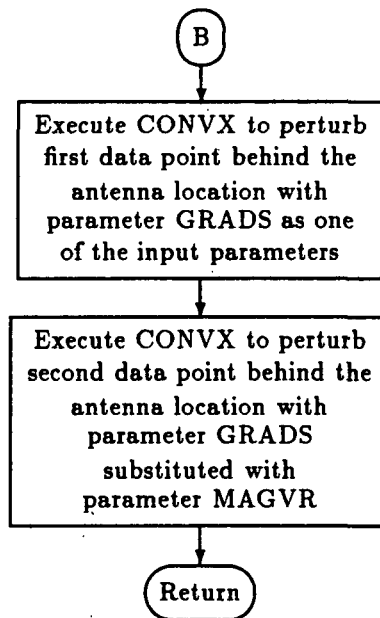
Figure 3.23: Continuation from Figure 3.22.

If the condition (2.81) were to occur, yet another decision would be arbitrated. This would be as follows. If the condition (2.82) were to occur, the problem would be formally declared as concavity by setting the logical indicator CONCAVE to logical TRUE from the default logical FALSE which indicates otherwise. Following this, statement RETURN would be executed to return the algorithm control back to the calling subroutine PTURB. Otherwise, MAVGL is assigned the value GRADS + SGN * TOL, which, in fact, is the parameter GRADS added or subtracted with a specified tolerance, and indicator CONCAVE remains as logical FALSE. The first data point (that is, $i = 1$) to the front of the antenna location is then perturbed by executing subroutine CONVX with parameter GRADS as one of the input parameters. Then, the second point (that is, $i = 2$) to the front of the antenna location is perturbed by executing subroutine CONVX again, but with parameter GRADS now substituted with parameter MAVGL.

Subsequently, the other pair of data points to the rear of the antenna location is considered. As for this pair of data points, the very same algorithm applies, only with three alterations. That is, firstly, instead of conditions (2.81) and (2.82), conditions (2.83) and (2.84) are utilized, respectively. Secondly, the expression GRADS + SGN * TOL is replaced by GRADS − SGN * TOL, and last of all, parameter MAGVL is substituted with parameter MAGVR.

3.8   Subroutine CONVX

This is, in fact, a subroutine that executes the mathematical expression (2.78), described in Section 2.6.2, on a data point provided. In other words, this subroutine perturbs the data point downwards along a vector $\hat{d}$, defined in (2.77) in Section 2.6.2, in a direction opposite to that of the outward normal of the fuselage which is assumed to be pointing directly upwards. With regards to this, the new position of the point is guaranteed to be always below the tangent line m_1 defined (2.77).

Chapter 4

Numerical Results

In this chapter, a few numerical results are presented. It should be pointed out that the numerical results generated may be acceptable, or sometimes they may not. One criterion to determine if whether a particular solution is acceptable is just by direct graphical observation by the user. Another criterion that may be employed is by checking the value of the stop-run parameter STATSTOP. STATSTOP=0 condition is an ideal solution. For other values of STATSTOP, the solution may not be ideal, but is yet acceptable. However, there are of course cases where STATSTOP would indicate an unacceptable solution, or for the worst case scenario, the entire program would come to a complete halt with an appropriate error message output by the program itself. A full list of the various values of the stop-run parameter STATSTOP and their descriptions are listed in Appendix B .

Note that for this chapter, a different set of notations and symbols is utilized in titles and labels for the figures, as well as in the contents of Appendix A through Appendix C.9. This is due to the fact that the figures, and the contents were generated through the execution of ELLC and other supporting computer codes written in FORTRAN 77 and VAX FORTRAN. In these FORTRAN languages, subscripts and superscripts cannot be employed, and special symbols are limited as well. Hence, the mathematical notations and symbols utilized in Chapter I and Chapter II were redefined for use in the codes. The outputs from these codes were

therefore the alternative notations and symbols utilized. A list of these notations and symbols is tabulated in Appendix A.

In the subsequent sections of this chapter, some examples of ideal solutions as well as of cases where $STATSTOP$s are not zeroes, are presented. Discussions and interpretations of these cases are base more on graphical observations rather than on mathematical formulations. The coordinate form (Y_s, T), discussed in Section 2.2, is employed to specify the location of the antenna on the helicopter fuselage in all the following sample runs. The cross-section plots of the fuselage in all these sample runs are consistently scaled in relative units. The computational times for these runs did not exceed 20 seconds at all. In general, they were only 10 to 12 seconds long.

4.1 Ideal solutions

As is defined previously, an ideal solution is a STATSTOP=0 condition. It should be noted that, however, such a condition does not necessarily indicate that the selected data points are actually located on the close-fit composite ellipsoid, but are within tolerable distances from it. In other words, the solution corresponds to the best solution possible, given the particular set of data points. Described mathematically, this means that, for the XZ-plane at $y = Y_s$, accurate solutions were obtained for (2.5). For the YR-plane, on the other hand, if the problem is a Case 1, exact solutions would be obtained for the system of equations (2.20) and (2.21) satisfying the constraints (2.22) through (2.24). Parameter D_0 of the composite ellipse, and hence, the composite ellipsoid, is the average value of the real roots D_{0_i}' for $i = 1, 2$ of (2.51). If the problem is a Case 2, exact solutions would be obtained for the system of equations (2.54) and (2.55) satisfying the constraints (2.56) through (2.58), and parameter C_0 is the average value of the real roots C_{0_i}' for $i = 1, 2$ of (2.73). A sample of the numerical results generated by ELLC is presented here as Sample 1.

4.1.1 Sample 1

The antenna location for this example is at $(Y_s, T) = (17.00, 0.55)$, which is at the bottom of the helicopter fuselage, as illustrated in Figure 4.1. This is in fact a Case 1 problem. Figure 4.1 and Figure 4.2 displays the graphical results of the run. The data file thus output is provided in Appendix C.1. Due to the extreme flatness of the fuselage surface at that location, the close-fit ellipse in the XZ-plane formed an enormously hugh shape, by comparison with the XZ-plane cross-section of the helicopter fuselage. Nevertheless, the ellipse generated was a perfect fit, almost entirely, to the XZ-plane in the vicinity of the antenna location. In the YR-plane, the composite ellipsoid generated was outstandingly gigantic as well for the very same reason. Again, in this plane, the composite ellipse was also an excellent fit to the fuselage surface in the proximity of the antenna location.

For this example, subroutine ELLXZ provided a close-fit ellipse in the XZ-plane at $y = Y_s = 17.00$. This ellipse possessed a semi-minor axis A_1 of value 19.809 and a semi-major axis B_1 of value 8.831 with a center (X_c, Z_c) at $(-1.634, 15.315)$

In terms of the analysis performed by the subroutine ELLYR, the parameters Y_c and C_0 are evaluated by solving the system of equations of (2.20) and (2.21). The exact solutions for Y_c and C_0 were zero and 105.738, respectively. These solutions satisfy the constraints (2.22) through (2.24). Moreover, since $C_0 > 0$ and is real, the additional functional constraint (2.47) was also satisfied automatically. Since

$$Y_c < Y_s < (Y_c + C_0),$$

the additional functional constraint (2.48) was also satisfied as well.

As for the evaluation of the parameter D_0, the real roots D'_{0_i} of (2.51) at each data point i for $(i = 1, 2)$ to the rear of the antenna location are searched. The solution D_0 obtained is the average value of the real roots D'_{0_1} and D'_{0_2}. Therefore, for this sample run, $D_0 = 83.614$. The functions f_{2_i} of (2.51) for $i = 1, 2$ are shown in Figure 4.3. Note that each of the real roots D'_{0_i} for $i = 1, 2$ is the first real

THE X-Z CROSS SECTION
YS = 17.00, T = 0.55

ELLIPSE

FUSELAGE

ANTENNA

(a)

THE X-Z CROSS SECTION
YS = 17.00, T = 0.55

ELLIPSE

FUSELAGE

ANTENNA

(b)
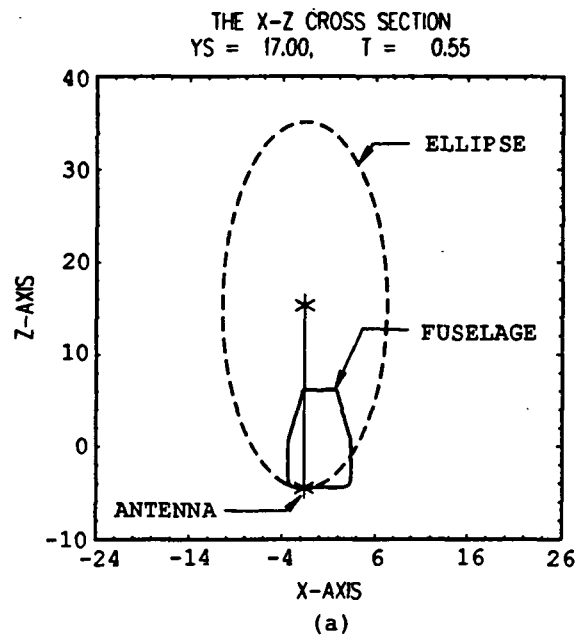
Figure 4.1: A close-fit ellipse in the XZ-plane for the antenna located at $(Y_s, T) = (17, 0.55)$.

THE Y-R CROSS SECTION
YS = 17.00, T = 0.55

● SELECTED POINT
■ ANTENNA

FUSELAGE

(a)

THE Y-R CROSS SECTION
WITH CLOSE-FIT COMPOSITE ELLIPSOID
YS = 17.00, T = 0.55

● SELECTED POINT
■ ANTENNA

COMPOSITE
ELLIPSE

FUSELAGE

(b)

Figure 4.2: A close-fit composite ellipse in the YR-plane for the antenna located at $(Y_s, T) = (17, 0.55)$.

103
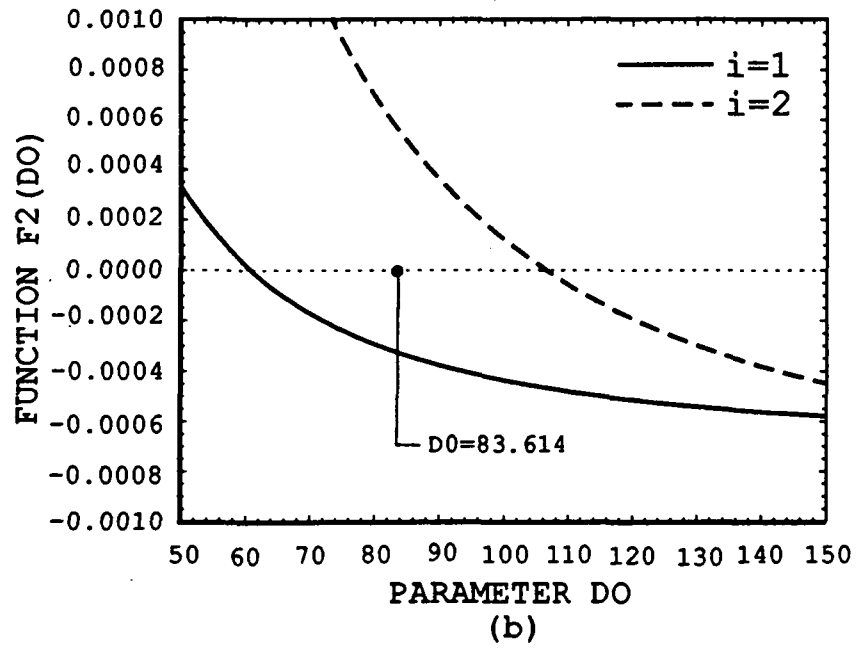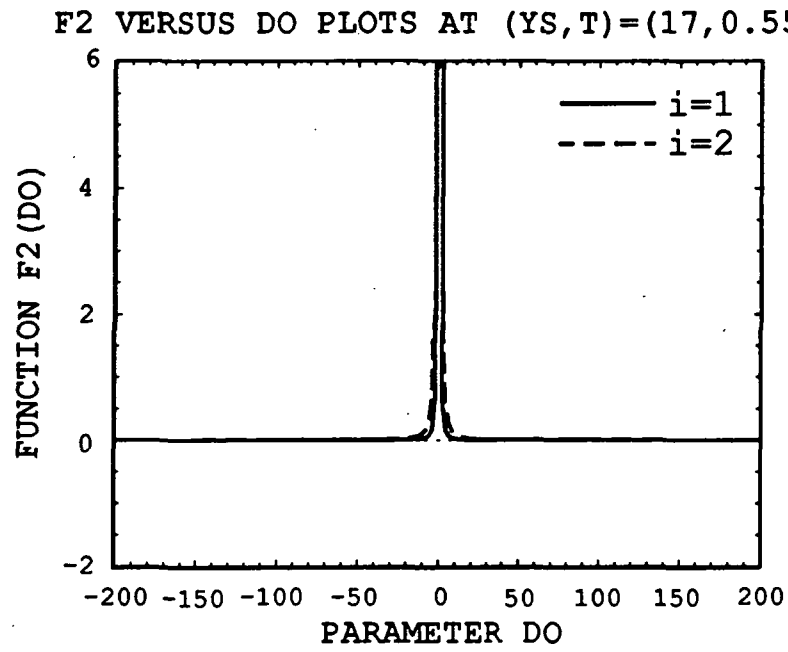
Figure 4.3: Plots of function f_{2_i} (for $i = 1, 2$) for the antenna located at $(Y_s, T) = (17, 0.55)$ prior to perturbation in the YR-plane.

root encountered, while searching downward from a value of 200, as explained in Section 3.5.

4.2 An example employing the reflection approximation

In Section 2.5 and Section 3.4, the idea of reflecting an infeasible value of Y_c on the y-component of the antenna location to approximate the solutions Y_c and C_0 for Case 1, or Y_c and D_0 for Case 2, were discussed. In this section, the results of such a procedure are presented. The values of the stop-run parameter STATSTOP that correspond to the application of the reflection concept are 11 and 12. The value 11 represents that, as an approximation, Y_c is obtained by reflection on Y_s without any perturbation of the data points. The value 12, on the other hand, represents the same status as that of value 11, but with perturbation procedures performed on the data points. For the purpose of illustrating the results of the reflection approximation, a sample run of ELLC is presented here.

4.2.1 Sample 2

For this sample run, the antenna location is at $(Y_s, T) = (12.00, 0.30)$. The resulting plots are provided in Figure 4.4 and Figure 4.5, and the numerical values output are appended in Appendix C.6. In this sample run, the stop-run condition $STATSTOP$ was 11.

From Figure 4.4, it is observed that the close-fit ellipse generated provided a fairly good fit of the surface in the XZ-plane in the vicinity of the antenna location. There was indeed a problem of fitting an ellipse to a slightly concave arc, which is in fact, the actual cross-section surface of the fuselage that is concave. Apparently, this slight concavity was within the acceptable tolerance set forth in subroutine ELLXZ. The semi-minor axis A_1 and semi-major axis B_1 of the close-fit ellipse obtained were 2.354 and 1.020, respectively.

To form a cross-section surface approximating the actual cross-section of the helicopter fuselage in the YR-plane, the surface points in the YR-plane were computed and interpolated. As can be pictured from Figure 4.5, the ellipsoid problem was undoubtedly a Case 2 problem since the first-order derivative of the surface in the YR-plane at the antenna location is negative and that the angle $\phi_s = PHIS = 91.45 > 90°$. The automatic categorization of a problem into Case 1 or Case 2 based on the first-order derivative of the surface at the antenna location was presented in Section 2.5. The angle ϕ_s, on the other hand, has been discussed in Section 2.2. A rather good fit of the composite ellipsoid was obtained, despite of the fact that the front most point at both ends of the array of selected data points did not coincide with the composite ellipse at all.

Figure 4.5 conspicuously indicates that the locus of the composite ellipse did not pass closely by the front most data point selected, which is the second data point to the front of the antenna location. This was because the solution for Y_c in the system of equations (2.54) and (2.55) corresponding to the first and second data points in front of the antenna location, respectively, was not feasible, that is, the functional constraint (2.56) was not satisfied ($Y_s - Y_c$ was positive). Nevertheless, through the reflection approximation equation (2.41), the approximated value of Y_c obtained was 18.492. For this approximation, the values of $\mid y_i - Y_s \mid$ for $i = 1$ and $i = 2$ are 1.6 and 3.2, respectively. For $\mid Y_s - Y_c \mid$, on the other hand, the value was 6.492. From these computations, it is accepted that

$$\mid y_i - Y_s \mid \ll \mid Y_s - Y_c \mid$$

for $i = 1, 2$. Hence, condition (2.46) was satisfied for $i = 1, 2$. Indeed, this approximated value of Y_c satisfied the functional constraint (2.56).

THE X-Z CROSS SECTION
YS = 12.00, T = 0.30

FUSELAGE

ANTENNA

ELLIPSE

(a)

THE X-Z CROSS SECTION
YS = 12.00, T = 0.30

FUSELAGE

ANTENNA

ELLIPSE

(b)
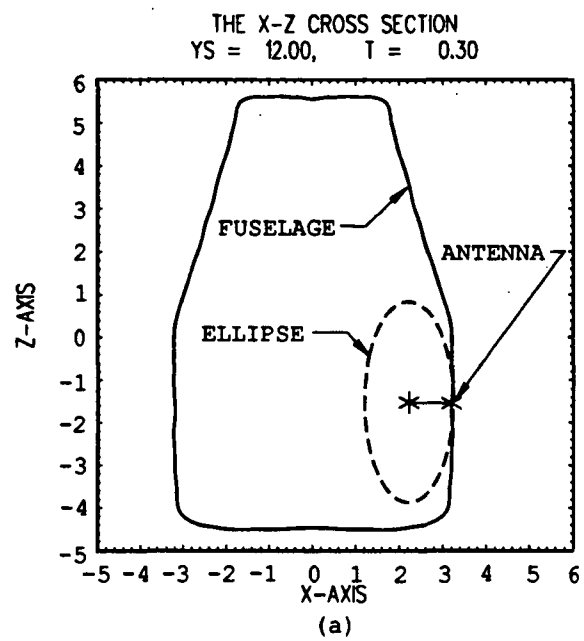
Figure 4.4: A close-fit ellipse in the XZ-plane for the antenna located at $(Y_s, T) = (12, 0.3)$.

THE Y-R CROSS SECTION
YS = 12.00,   T =   0.30

(a)

THE Y-R CROSS SECTION
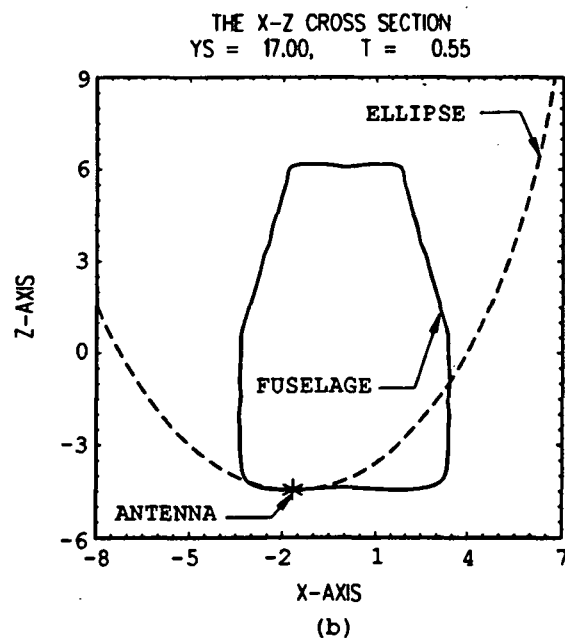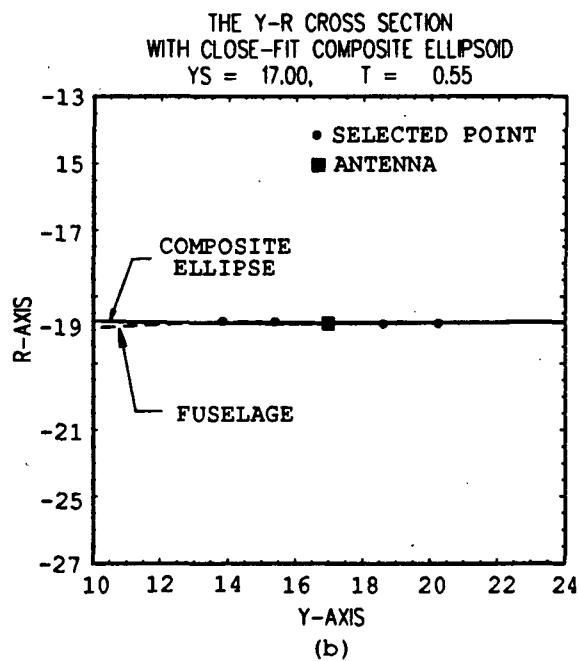## WITH CLOSE-FIT COMPOSITE ELLIPSOID
YS = 12.00,   T =   0.30

(b)

Figure 4.5: A close-fit composite ellipse in the YR-plane for the antenna located at $(Y_s, T) = (12, 0.3)$.

108

F2 VERSUS CO PLOTS AT (YS,T)=(12,0.3)

(a)

(b)
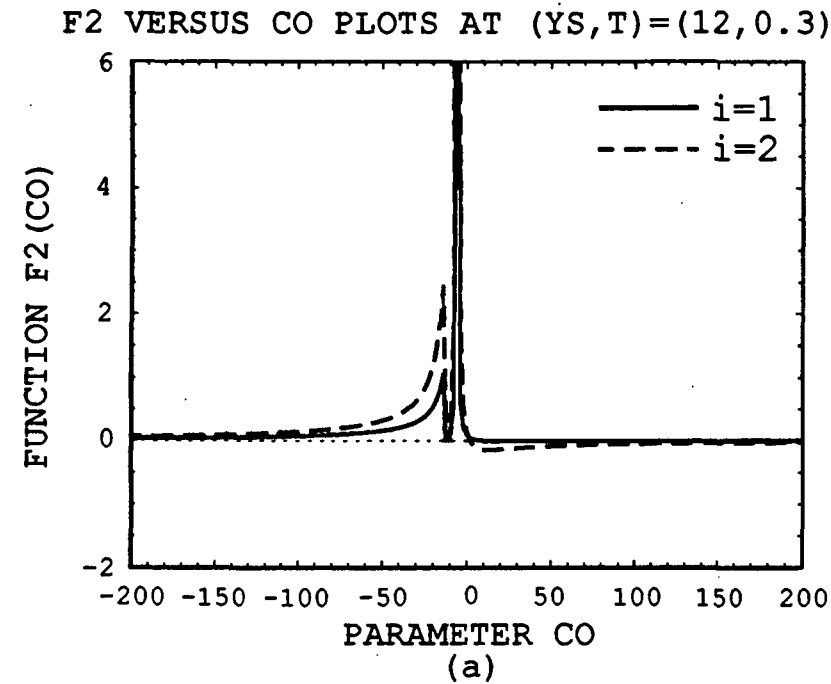
Figure 4.6: Plots of function f_{2_i} (for $i = 1, 2$) for the antenna located at $(Y_s, T) = (12, 0.3)$ prior to perturbation in the YR-plane.

109

Utilizing the value for Y_c obtained, the corresponding solution for D_0 was evaluated from (2.70) as 9.298, which is positive and real. With these solutions, the constraints (2.56) through (2.58) were all satisfied. In addition, since $D_0 > 0$ and is real, constraint (2.71) is automatically satisfied. Furthermore, since

$$Y_c > Y_s \geq (Y_c - D_0) \ ,$$

constraint (2.72) is satisfied, as well.

Having determined the values for D_0 and Y_s, the solution for C_0 was determined by applying the root searching algorithm of module RTSAFE0 in ELLC (described in Section 3.5) on (2.73). For this problem, in particular, function f_{2_i} of (2.73) is depicted in Figure 4.6. The root C_{0_i} determined for each i was indeed the first root encountered searching downwards from 200 to -200. The average of these roots was the solution for C_0, which was 4.559. Analyzing the problem geometrically, the front most data point in the Figure 4.5 is very near the $R = 0$ line, which is the axis of the composite ellipse that is orthogonal to the XZ-plane. By examining Figure 4.5, it is conspicuous that, in order for the locus to pass at least very closely to the front most point, the front end of the composite ellipse would have to be shaped like a wedge, which was unobtainable in this case. Nevertheless, considering the rear section of the composite ellipse, the locus did pass closely by the rear most data point, although not directly through it. This was due to the fact that C_0 is the averaged value of the roots C_{0_i}' for $i = 1, 2$. The explanation for this is presented subsequently in the Section 4.3.

4.3 Effects of averaging two real root solutions

In ELLC, the real root solutions D_{0_1}' and D_{0_2}' of (2.51) corresponding to the first and second data points, respectively, for Case 1, or C_{0_1}' and C_{0_2}' of (2.73) corresponding to the first and second data points, respectively, for Case 2, are averaged to obtain an approximate solution D_0 for the former, or C_0 for the latter. This is performed so

as to obtain a best possible fit of a composite ellipse to the surface of the YR-plane cross-section of the helicopter fuselage in the vicinity of the antenna location. In the following example, the effects of averaging the real roots D'_{0_i} of (2.51), or C'_{0_i} of (2.73), are demonstrated.

4.3.1 Sample 3

In this example, the antenna was located at $(Y_s, T) = (7.00, 0.41)$. Results of this sample run are plotted in Figure 4.7 and Figure 4.8 and the output appended in Appendix C.4. This was a Case 1 problem with a stop-run condition $STATSTOP = 11$, indicating that no perturbation procedure was involved. Referring to the output in Appendix C.4, one of the front data points selected initially was located across the $R = 0$ line, which would be the axis of the composite ellipse in the YR-plane that is orthogonal to the XZ-plane. Since the composite ellipse must be symmetrical along its axis, as discussed in Section 2.5, only data points on the same side as where the antenna location was would be useful. Therefore, the sampling interval DY was decreased from a value of 1.6 to a value of only 0.96. With this, the two data points to the front of the antenna location were selected without having them crossing over the $R = 0$ line, as is illustrated in Figure 4.8.

From Figure 4.7, the fitting of the ellipse onto the surface of the cross-section in the XZ-plane at $y = Y_s = 7.00$, in the proximity of the antenna location appeared to be fairly good, despite of the slightly improper fit just to the left of the antenna location in the figure. This was in fact due to a mild indentation of the actual fuselage surface just to the left of the antenna location in the figure. In spite of this, the fitting of the ellipse just to the right of the antenna location was excellent.

Analyzing the close-fit ellipse parameters in XZ-plane at $y = Y_s = 7.00$, it is noted that the semi-minor axis A_1 and the semi-major axis B_1 of the close-fit ellipse are 0.842 and 0.771, respectively, with its center at $(X_c, Y_c) = (1.431, -3.989)$.

THE X–Z CROSS SECTION
YS = 7.00, T = 0.41
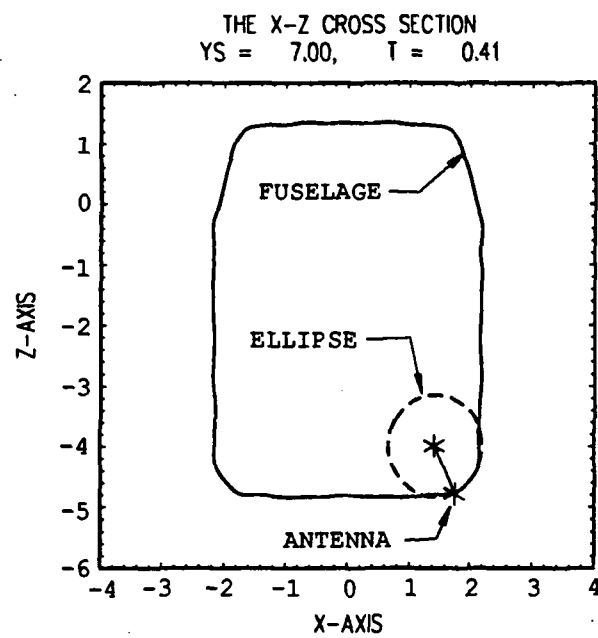
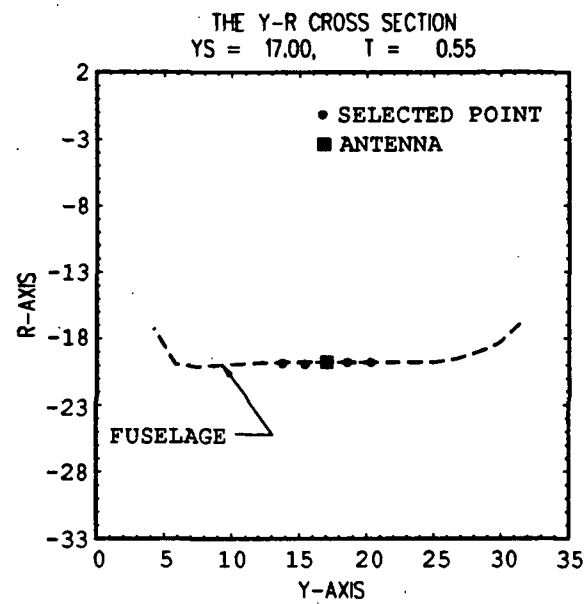Figure 4.7: A close-fit ellipse in the XZ-plane for the antenna located at $(Y_s, T) = (7, 0.41)$.

THE Y-R CROSS SECTION
YS = 7.00, T = 0.41

[figure (a): THE Y-R CROSS SECTION, YS = 7.00, T = 0.41, R-AXIS vs Y-AXIS, with FUSELAGE labeled]

(a)

THE Y-R CROSS SECTION
WITH CLOSE-FIT COMPOSITE ELLIPSOID
YS = 7.00, T = 0.41

[figure (b): THE Y-R CROSS SECTION WITH CLOSE-FIT COMPOSITE ELLIPSOID, YS = 7.00, T = 0.41, R-AXIS vs Y-AXIS, with COMPOSITE ELLIPSE and FUSELAGE labeled]
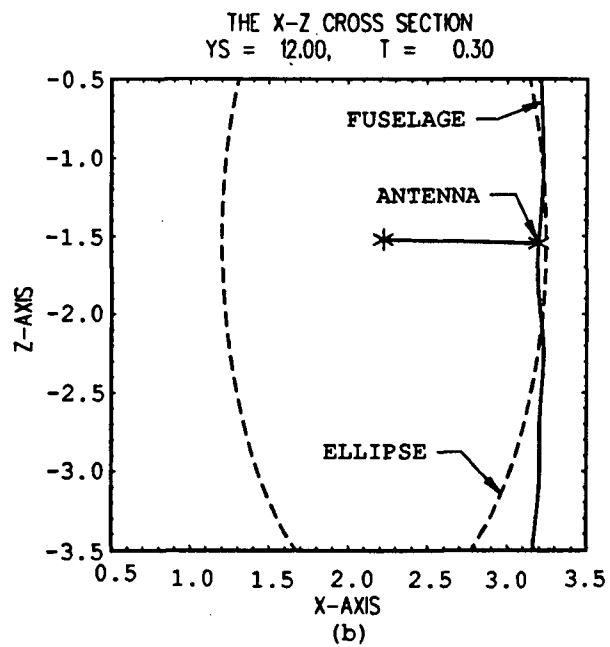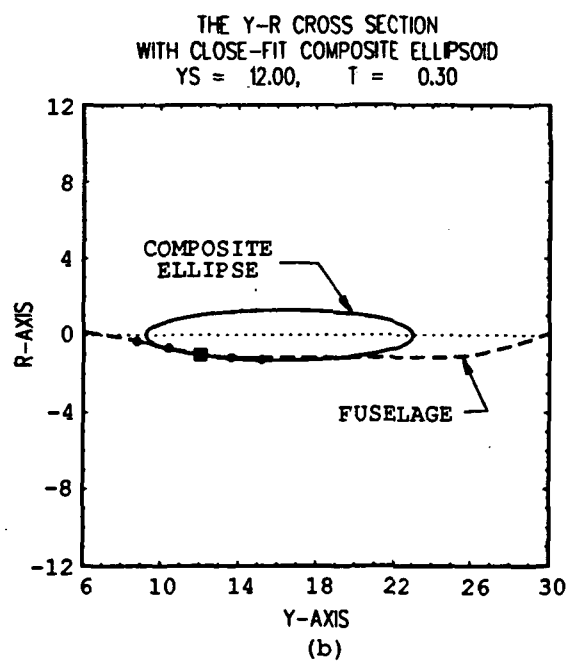
(b)
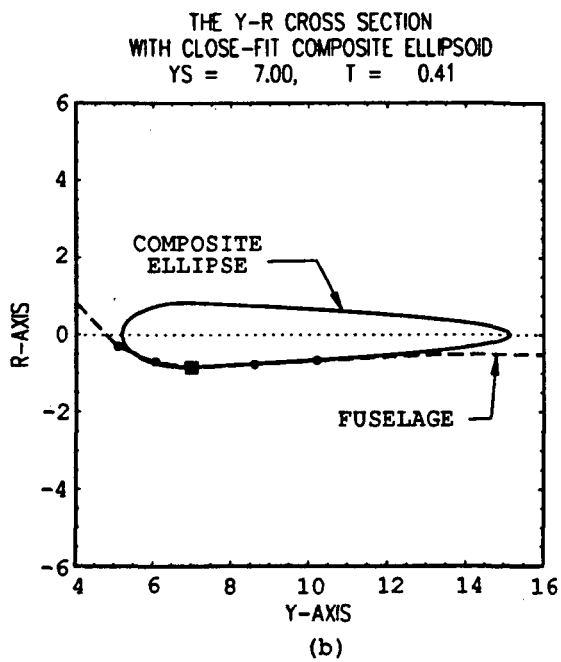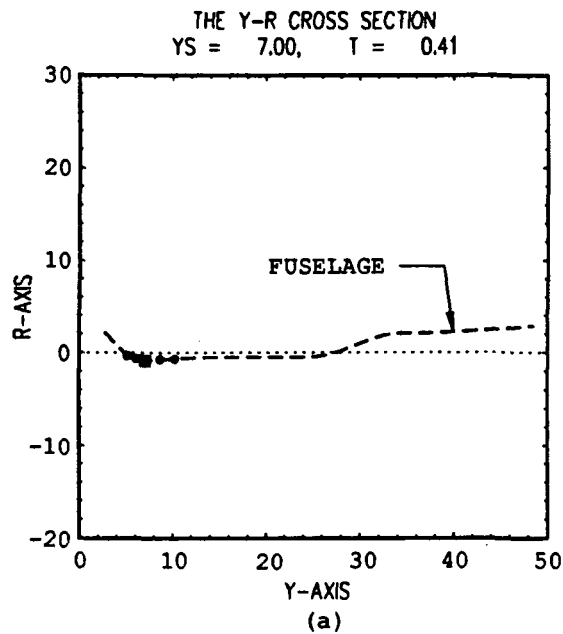
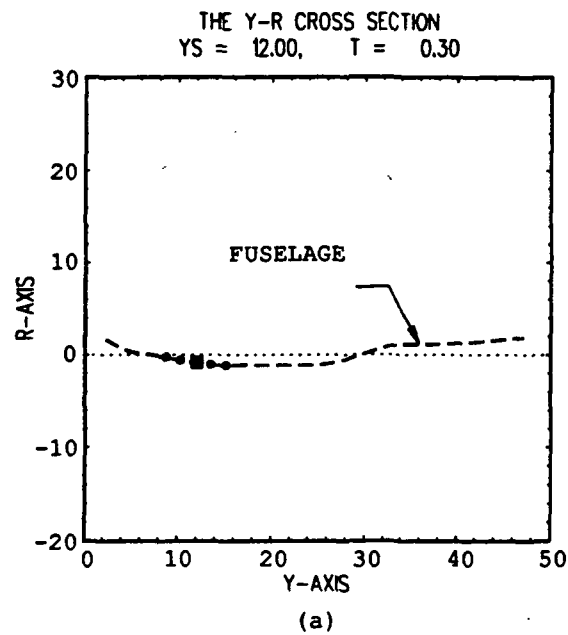Figure 4.8: A close-fit composite ellipse in the YR-plane for the antenna located at $(Y_s, T) = (7, 0.41)$.

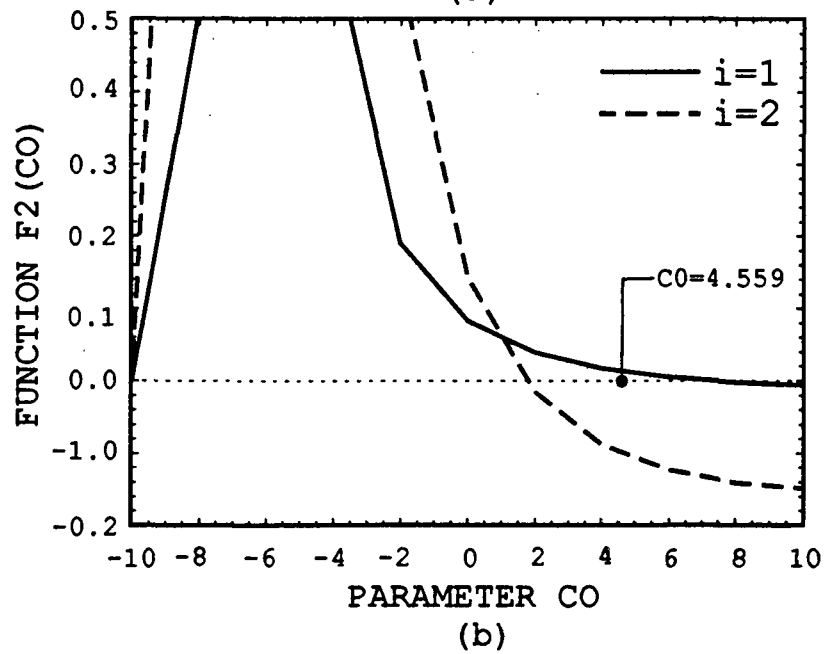113

F2 VERSUS DO PLOTS AT (YS,T)=(7,0.41)

(a)

(b)
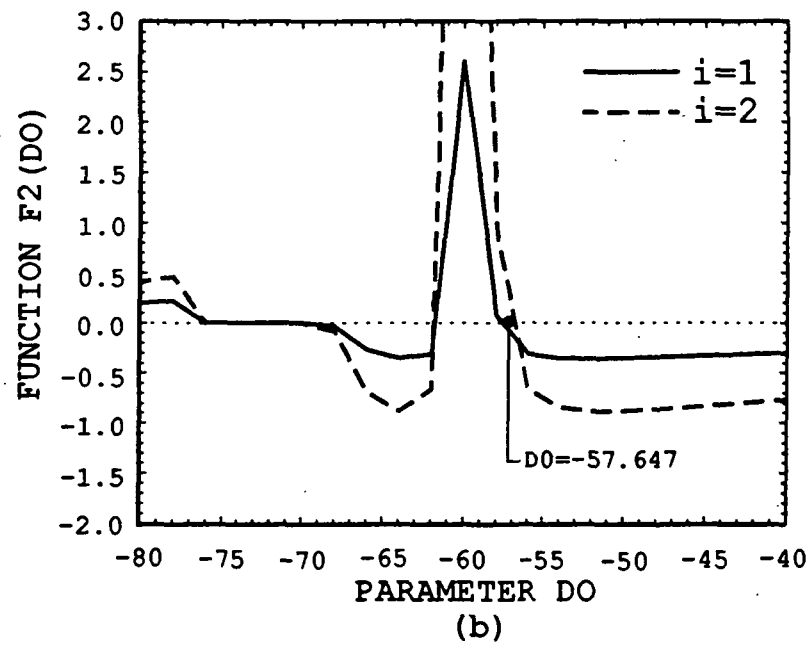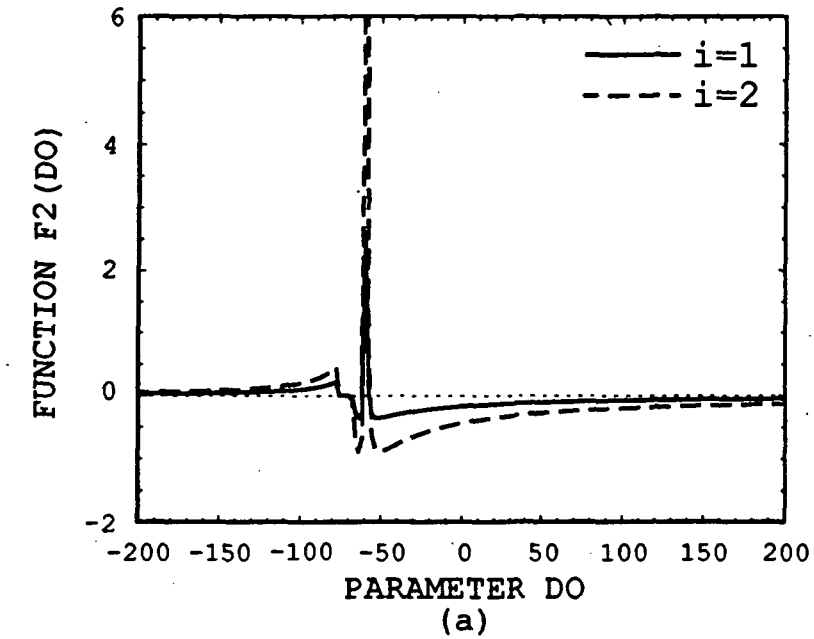
Figure 4.9: Plots of function f_{2_i} (for $i = 1, 2$) for the antenna located at $(Y_s, T) = (7, 0.41)$ prior to perturbation in the YR-plane.

114

Quite conspicuously, the ellipse was rather circular, and thus is most appropriately fitted to the particular corner of the XZ-plane cross-section.

As for the YR-plane, the composite ellipse appeared to fit the actual surface of the fuselage rather well in the vicinity of the antenna location, as illustrated in Figure 4.8. Since the value of DY was decreased due to the crossing of at least one of the front data points over the $R = 0$ line, the forward difference algorithm in subroutine ELLYR was employed to identify if the problem was a Case 1 or a Case 2, instead of the default central difference algorithm. Details of these have been discussed in Section 3.2. However, the locus of the composite ellipse did not pass closely by the front most data point, as is obvious in the figure, for the very same reason as that described in It should be noted that, since $STATSTOP = 11$ for this case, which is a Case 1 problem, as indicated in Appendix C.4, the reflection approximation equation (2.40) was employed, producing $Y_c = -52.466$. The values of $| y_i - Y_s |$ for $i = 1$ and $i = 2$ are 1.6 and 3.2,respectively, and that of $| Y_s - Y_c |$ is 59.466. Hence,

$$| y_i - Y_s | \ll | Y_s - Y_c |$$

for $i = 1, 2$, and therefore, satisfying condition (2.46). With the value of Y_c thus obtained, C_0 was evaluated as 67.623. Using similar line of reasoning as that in Sample 2 of Section 4.2, these solutions C_0 and Y_c were found to be satisfying all the constraints (2.22) through (2.24), and (2.47) and (2.48).

For an analysis of the effects of averaging two real roots D'_{0_1} and D'_{0_2}, a series of minor modifications of the module RTSAFE in subroutine ELLYR were performed so as to generate the plots illustrated in Figure 4.10 through Figure 4.12. For this analysis, all other parameters, including A_1, B_1, C_0 and Y_c, remained unchanged. In Figure 4.10, the composite ellipse was generated using only the first front data point, instead of both the first and the second front data points. This means that $D_0 = D'_{0_1}$, where D'_{0_1} is the first real root of the function f_{2_1} of (2.51) encountered by module RTSAFE. For this particular case, the ellipse was independent of the second front

data point. As such, the locus of the composite ellipse would not necessarily pass through the second data point at all, but would pass through the first. This would indicate that a perfect fit was obtained at the position of the first front data point. If, on the other hand, only the second front data point was used for the computation of the parameter D_0 of the composite ellipse, the locus of the composite ellipse would then pass through the second data point instead of the first, as illustrated in Figure 4.11. For this case, $D_0 = D'_{0_2}$, where D'_{0_2} is the first real root of the function f_{2_2} of (2.51) encountered by module RTSAFE. Nevertheless, unlike the previous case, the locus would pass rather closely by the first data point as depicted in the figure, which of course, would be most appreciated. In general, however, this may not always be the case since the composite ellipse would be independent off the first front data point. In other words, a good fit to the position at the first front data point, which is very essential to having a perfect fit in the vicinity of the antenna location, would not be guaranteed. But employing only the first data point would only provide a fit that is extremely local to the antenna location, and the use of only the second data point would provide a fit at that second data point which is a small distance away from the antenna location.

Considering all these options, a good compromise would be to utilize both the first and the second front data points simultaneously to provide the value for the parameter D_0. In this case,

$$D_0 = 0.5 \left(D'_{0_1} + D'_{0_2} \right) = -57.647.$$

Figure 4.12 illustrates the resulting locus of the composite ellipse with respect to the two front data points and the antenna location on the actual surface of the YR-plane cross-section for this implementation. As is observed from the figure, the locus of the composite ellipse would not pass directly through any of the two front data points at all. Nevertheless, the locus would pass very closely by the first front data point, a sufficiently good fit. With regards to the second front data point, the locus would pass closer by it in this implementation than in the first case where only the first

116

THE Y-R CROSS SECTION
WITH CLOSE-FIT COMPOSITE ELLIPSOID
YS = 7.00, T = 0.41
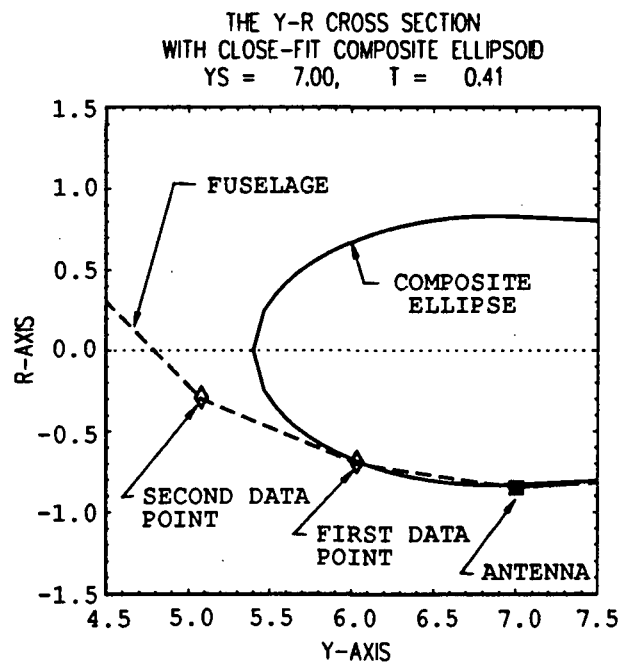
Figure 4.10: A close-fit composite ellipse in the YR-plane for the antenna located at $(Y_s, T) = (7, 0.41)$. The front portion of the composite ellipse was generated utilizing only the first data point to the front of the antenna location.

117

THE Y-R CROSS SECTION
WITH CLOSE-FIT COMPOSITE ELLIPSOID
YS = 7.00, T = 0.41
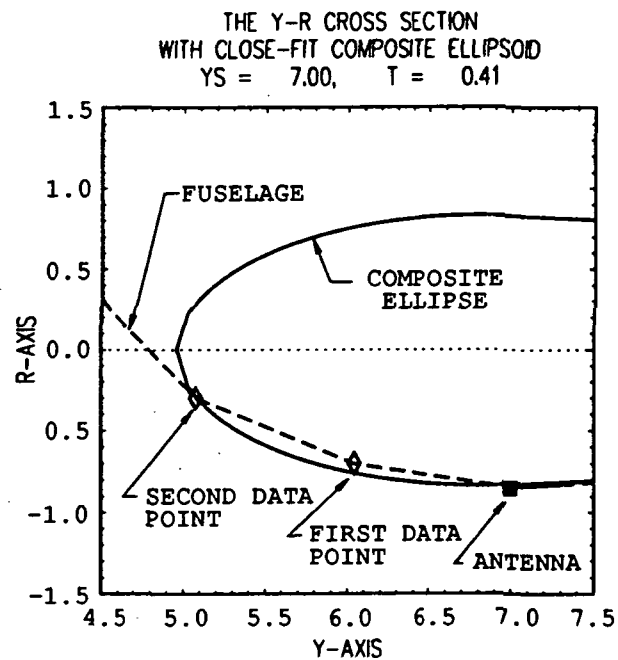
Figure 4.11: A close-fit composite ellipse in the YR-plane for the antenna located at $(Y_s, T) = (7, 0.41)$. The front portion of the composite ellipse was generated utilizing only the second data point to the front of the antenna location.

118

THE Y-R CROSS SECTION
WITH CLOSE-FIT COMPOSITE ELLIPSOID
YS = 7.00,   T = 0.41
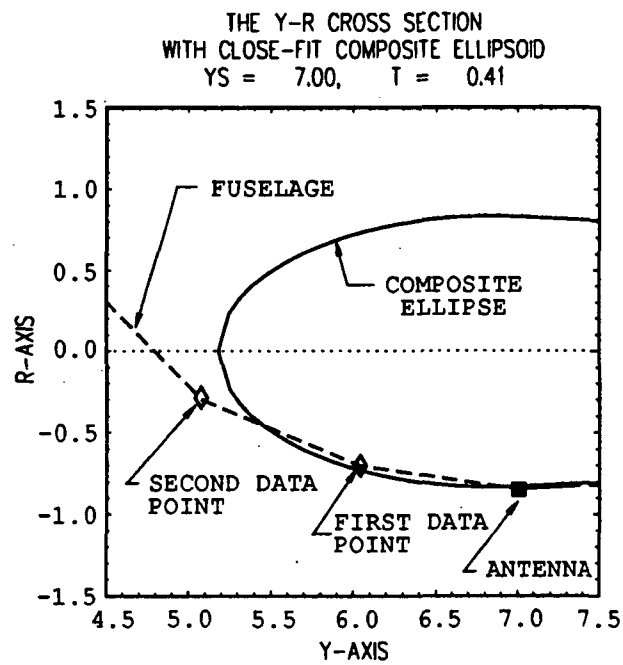
Figure 4.12: A close-fit composite ellipse in the YR-plane for the antenna located at $(Y_s, T) = (7, 0.41)$. The front portion of the composite ellipse was generated utilizing both the first and the second data points to the front of the antenna location.

data point was utilized. Mathematically, this would indicate that, at $D_0 = -57.647$, instead of trivial values, the values of function f_{2_i} of (2.51) for $i = 1$ and $i = 2$ were -0.088 and 0.249, respectively. The values -0.888 and 0.249 are in fact errors of the composite ellipse fitting corresponding to the respective data points, which ideally should be zeroes. Obviously enough, since D_0 is the average value of D'_{0_1} and D'_{0_2}, the composite ellipse was dependent on both the first, as well as the second, front data points. This was exactly what was implemented in the module RTSAFE of subroutine ELLYR, discussed in Section 3.5.

4.4   An example of perturbation in the YR-plane

Given a specific location of the antenna on the helicopter fuselage, ELLC will attempt to produce a solution for each of the parameters of the close-fit composite ellipsoid by performing the various decision making tasks at every level of the program run. If such an attempt failed in subroutine ELLYR, as would be when module RTSAFE or RTSAFEO fails, or when the first-order derivative of the surface of the XZ-plane cross-section at the antenna location is approximately zero and all the modules in subroutine ELLYR failed, ELLC would resort to perturbing the data points in the YR-plane as an attempt to create an optimal arrangement of the data points such that acceptable solutions could be generated. This perturbation process in the YR-plane would be performed by subroutine PTURB which would be called upon by subroutine ELLYR. All these has been discussed in Chapter 3. In the following, a sample of such a case is presented.

4.4.1   Sample 4

For the case where the antenna location is at $(Y_s, T) = (35.00, 0.00)$, the results illustrated in Figure 4.13 and Figure 4.14 were obtained and the output generated is appended in Appendix C.10. As stated in was 10, indicating that subroutine

PTURB was called upon to perform the perturbation procedure on the data points in the the YR-plane, at least once, before the data points were detected as being concave in the vicinity of the antenna location.

In fact, this problem was initially regarded as a Case 1 problem by subroutine ELLYR, but no acceptable solution was obtainable. This implied, among other things, a failure of module RTSAFE in determining the roots C'_{0_i} of the function f_{2_i} for $i = 1, 2$. As a result, by executing subroutine PTURB, the perturbation process in the YR-plane was performed on the data points in the YR-plane to the front of the antenna location. These data points were utilized in module RTSAFE, as has been indicated in Chapter 3. This was the first, and also the only, iteration in subroutine ELLYR for this problem. A concave surface of the cross-section in the YR-plane in the vicinity of the antenna location was detected through subroutine CONVEX. Immediately, appropriate error messages were output by ELLC, after which the program halted.

From Figure 4.13, the ellipse fitting was only fairly good in the XZ-plane. This was because of the presence of a concave notch directly at the antenna location, which is conspicuous in the figure. This notch was actually accidentally created in the process of inputting, interactively, the data points on the right half portion of the cross-section in the XZ-plane of the helicopter fuselage. The remaining other half was a symmetrical projection of the right half, as has been explained in Section 1.3. Such notches and bulges (one which, coincidentally, appeared on the bottom of the cross section of Figure 4.13) are, in fact, presently inevitable. As for the YR-plane, the composite ellipse was not generated due to a concave surface in the YR-plane in the vicinity of the antenna location. Nevertheless, the functions f_{2_i} of (2.51) for $i = 1, 2$ are plotted in Figure 4.15 to illustrate that no real root was present for $i = 1, 2$ within the search range of -200 to 200 for both functions, prior to the execution of the subroutine PTURB.

121

THE X-Z CROSS SECTION
YS = 35.00, T = 0.00
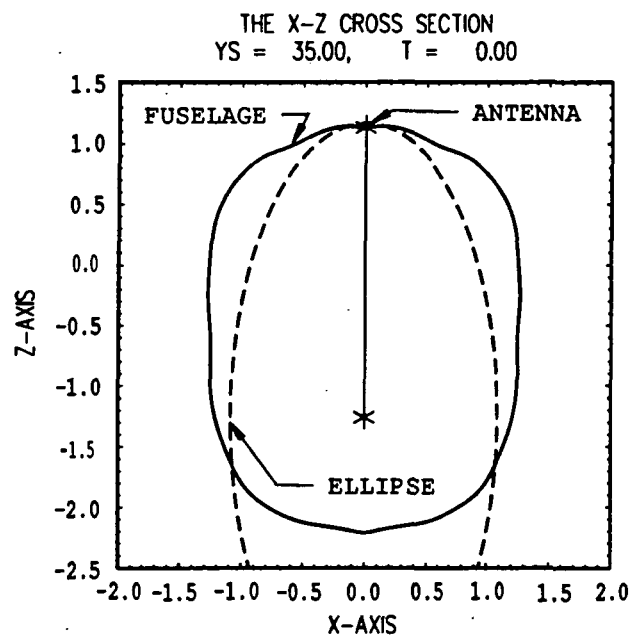
Figure 4.13: A close-fit ellipse in the XZ-plane for the antenna located at $(Y_s, T) = (35, 0)$.

122

THE Y-R CROSS SECTION
YS = 35.00,   T =   0.00

FUSELAGE

R-AXIS

Y-AXIS

(a)

THE Y-R CROSS SECTION
WITH CLOSE-FIT COMPOSITE ELLIPSOID
YS = 35.00,   T =   0.00

FUSELAGE

R-AXIS

Y-AXIS

(b)
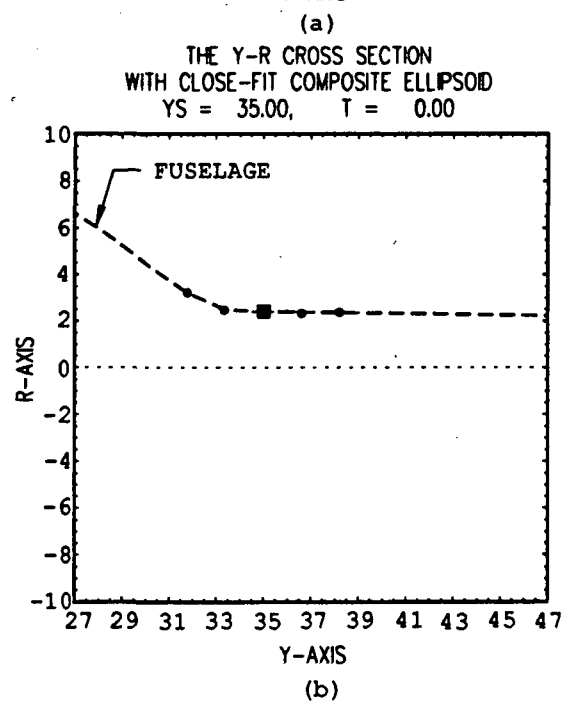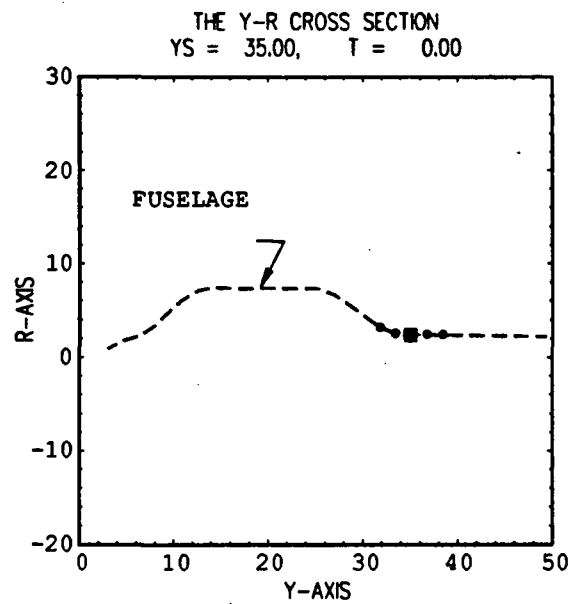
Figure 4.14: A close-fit composite ellipse in the YR-plane for the antenna located at $(Y_s, T) = (35, 0)$.

123

F2 VERSUS DO PLOTS AT (YS,T)=(35,0)

(a)

(b)
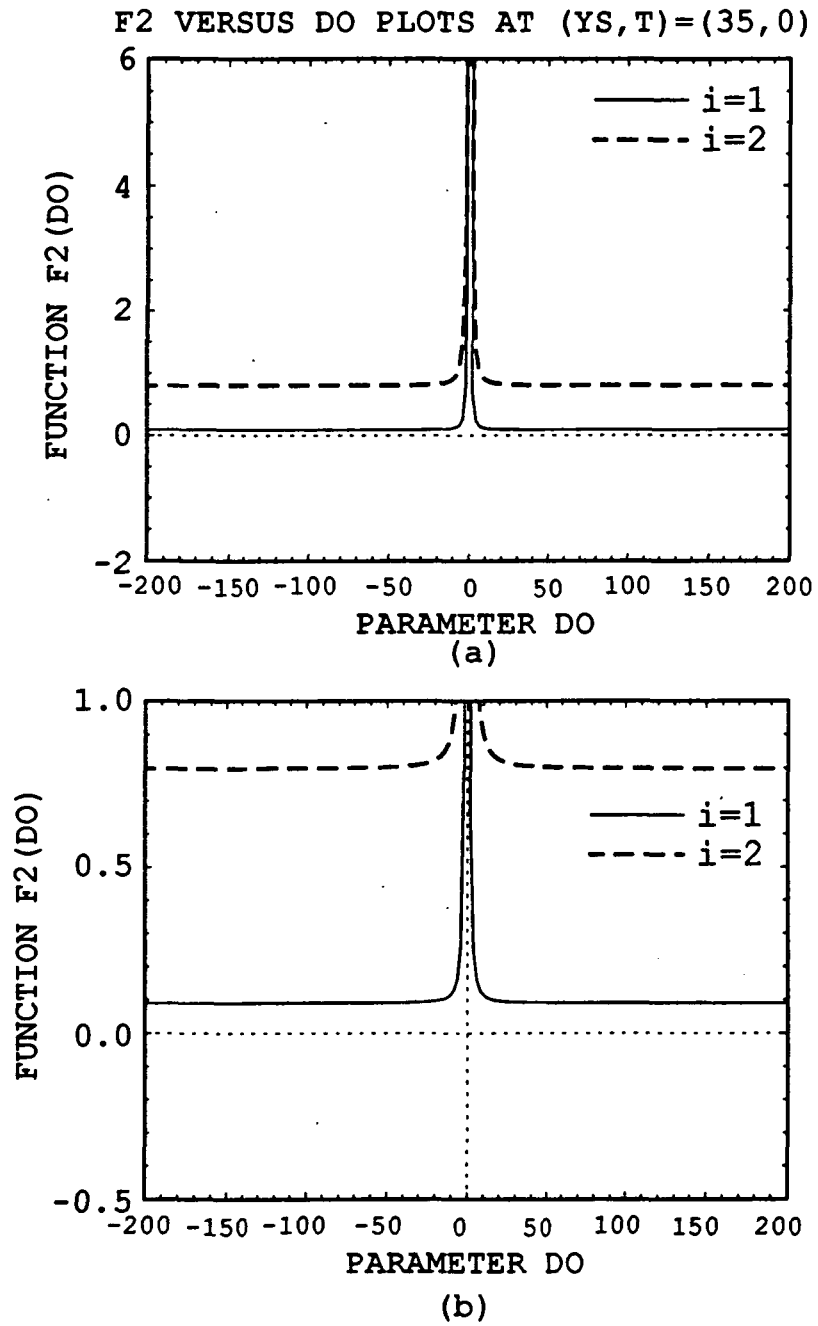
Figure 4.15: Plots of function f_{2_i} (for $i = 1, 2$) for the antenna located at $(Y_s, T) = (35, 0)$ prior to perturbation in the YR-plane.
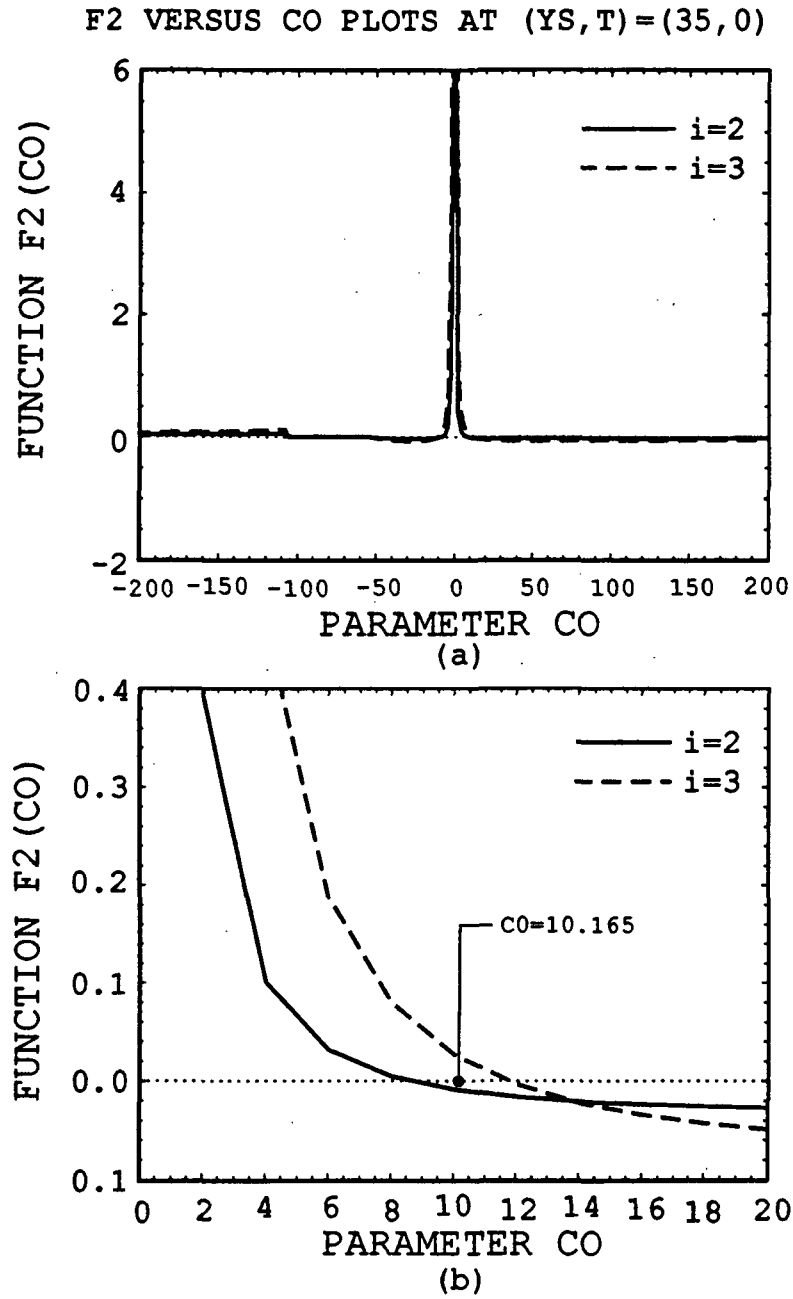
Figure 4.16: Plots of function f_{2_i} (for $i = 1, 2$) for the antenna located at $(Y_s, T) = (35, 0)$ following perturbation in the YR-plane.

4.5 Results obtained at maximum iteration count

As mentioned in Section 4.4, subroutine PTURB would be employed if module RTSAFE or RTSAFEO failed, or when the first-order derivative of the surface of the XZ-plane cross-section at the antenna location is approximately zero and no accurate solution could be obtained. However, if the perturbation process was unsuccessful in producing acceptable solutions in a particular iteration, the iteration process would be performed again in the next iteration. This would continue until an acceptable solution was found, or when the iteration count exceeded the maximum iteration allowed. When the latter occurs, for a Case 2 problem, the returned values C_0 and Y_c are values from the last iteration, and D_0 is a quarter the initial guess for $i = 2$ from the last iteration; and similarly for a Case 2 problem, the returned values D_0 and Y_c are values from the last iteration, and C_0 is a quarter the initial guess for $i = 2$ from the last iteration. In the following examples, analyses of such a such a situation were presented.

4.5.1 Sample 5

For this sample run, the antenna is located at $(Y_s, T) = (12.00, 0.05)$, which is at a top edge of the helicopter fuselage. Figure 4.17 and Figure 4.18 illustrate the results obtained from ELLC for this sample run. The output for this case is appended in Appendix C.5, which indicates a stop-run condition $STATSTOP$ of 8 and the nature of the problem being a Case 2. The data points generated to model the portion of the cross-section in the YR-plane in the vicinity of the antenna location were perturbed to maximum tolerance, to the extend that maximum iteration in subroutine ELLYR was exceeded.

Appendix C.5 indicates that this was a Case 2 problem. It should be noted that, however, the Case 2 problem here is actually based upon the perturbed data points from the final iteration, and does not reflect the actual nature of the original unper-

turbed data points. Since this was a Case 2 problem, as indicated in Appendix C.5, the returned values for D_0 and Y_s are values from the last iteration, and that for C_0 is a quarter of the initial guess value $i = 2$ utilized in module RTSAFEO in the last iteration.

With regards to Figure 4.17, the close-fit ellipse in the XZ-plane at $y = Y_s = 12.00$ for this problem was rather small as compared to the entire XZ-plane cross-section of the fuselage, although the fit appeared well in the proximity of the antenna location. For the surface a little further away from the antenna location, the fit was not as good due to the waviness of the actual surface, as has been discussed in Sample 2. of Section 4.2.

Proceeding on to the YR-plane, and referring to Figure 4.18, the close-fit composite ellipse generated did not fit the surface of the cross-section in that plane at all, even in the vicinity of the antenna location. This was due to the STATSTOP value being 8, that is, the maximum iteration was exceeded. In fact, the composite ellipse in the figure was constructed entirely on parameter values generated at the final iteration count, which was the tenth iteration. Nevertheless, it should be noted that a STATSTOP value of 8 may, in some instance, provide acceptable close-fit composite ellipse, especially if higher tolerances in functions RTSAFE and RTSAFEO were permitted. As was listed in Appendix C.5, at least one of the data points selected to the front of the antenna location crossed the $R = 0$ line, which was the axis of the composite ellipse that is orthogonal to the XZ-plane, instead of being on the same side of the line as where the antenna location is. This was indeed undesirable, as mentioned in Section 2.5. Hence, the sampling distance DY between the data points was reduced so as to avoid selecting the undesirable data points, similar to Sample 3.

As is obvious from Figure 4.18, the locus of the composite ellipse generated did not pass closely by the front most data point, which was positioned very near to the $R = 0$ line. Explanations of cases similar to this has been presented in Sample 2

127

THE X-Z CROSS SECTION
YS = 12.00,   T =   0.05
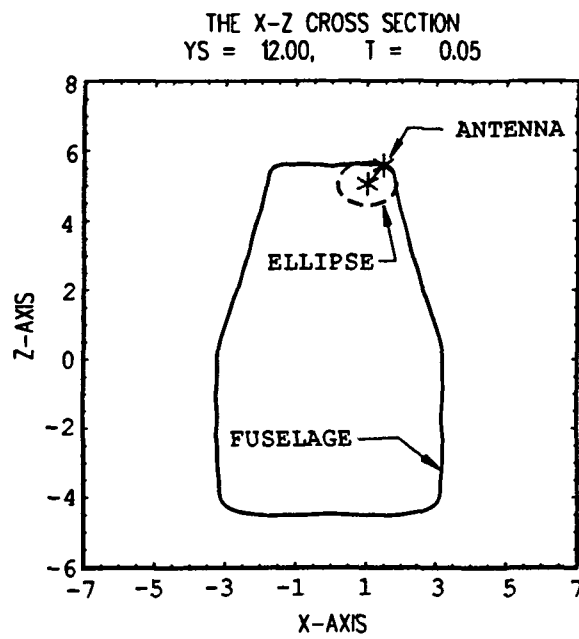
Figure 4.17: A close-fit ellipse in the XZ-plane for the antenna located at $(Y_s, T) =$ (12, 0.05).

THE Y-R CROSS SECTION
YS = 12.00,   T =   0.05

FUSELAGE

(a)

THE Y-R CROSS SECTION
WITH CLOSE-FIT COMPOSITE ELLIPSOID
YS = 12.00,   T =   0.05

FUSELAGE

COMPOSITE ELLIPSE

(b)
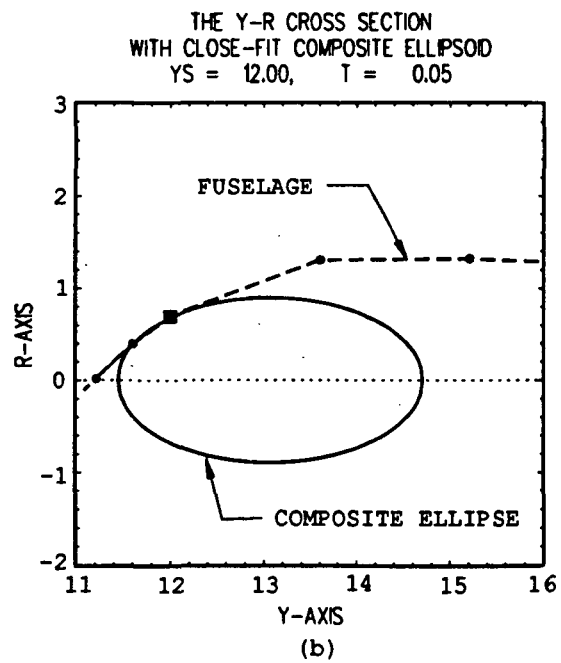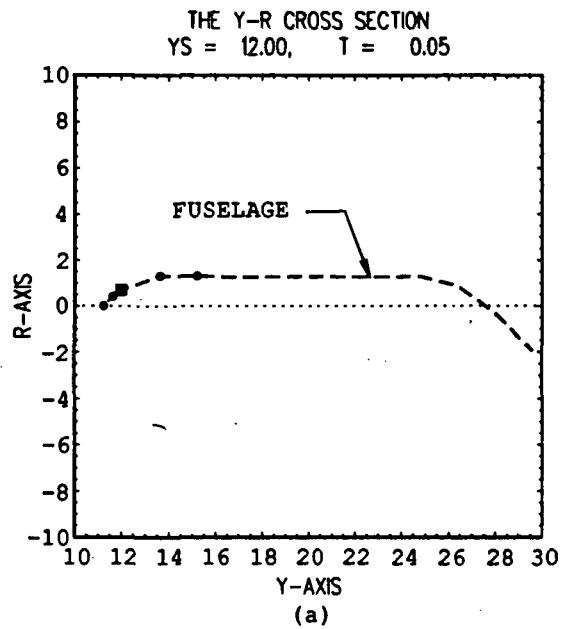
Figure 4.18: A close-fit composite ellipse in the YR-plane for the antenna located at $(Y_s, T) = (12, 0.05)$.

129

F2 VERSUS CO PLOTS AT (YS,T)=(12,0.05)

(a)

(b)

Figure 4.19: Plots of function f_{2_i} (for $i = 1, 2$) for the antenna located at $(Y_s, T) = (12, 0.05)$ prior to perturbation in the YR-plane.

Figure 4.20: Plots of function f_{2_i} (for $i = 1, 2$) for the antenna located at $(Y_s, T) = (12, 0.05)$ following perturbation in the YR-plane.

and Sample 3 of Section 4.2 and Section 4.3, respectively. However, the locus did pass through the first front data point. This implies that the solutions $D_0 = 1.515$ and $Y_c = 12.962$ were acceptable. Indeed, these solutions were obtained through the reflection approximation equation (2.41). By the same logic as that applied to Sample 2 and Sample 3, solutions could be shown to satisfy all of the governing constraints for Case 2.

In spite of this, perturbation on the data points to the rear of the antenna location was performed. This was due to the failure of module RTSAFEO to locate the zero crossings, that is, the real roots C_{0_1}' and C_{0_1}' of (2.73) within the search range of -200 to 200. The functions f_{2_i} of (2.73) is as illustrated in Figure 4.19. As can be conspicuously observed in the figure, the curve representing the second rear data point crossed the zero line at approximately $C_0 = 9$, but not that representing the first rear data point. If, however, the search was extended way beyond $C_0 = 200$, the two curves might approach close enough to the zero line such that they would be within the acceptable tolerance value. This would mean that C_0 would be extremely large, and so would the composite ellipse. Apparently, with perturbation performed on the rear data points for each successive iteration until the tenth, the f_{2_i} curves did not improve at all, if not worse. The results for the tenth iteration is depicted in Figure 4.20, which in fact, appeared somewhat similar to those in Figure 4.19. Without any doubt, the final value of 1.75 returned for C_0 was a quarter of the initial guess for inputting into subroutine RTSAFEO in the tenth iteration. Indeed, the functions f_{2_i} for $i = 1, 2$ were enormously large when $C_0 = 1.75$ was substituted into (2.73) for $i = 1, 2$, implying that the value $C_0 = 1.75$ was far from being accurate.

For the purpose of analyzing the perturbation process of the rear data points for this antenna location as executed by subroutine PTURB, the algorithm of which has been presented in Section 4.4, Figure 4.21 through Figure 4.24 were plotted. In Figure 4.21, $M1$ represents the tangent line to the surface of the YR-plane cross-section at the antenna location, evaluated through a difference algorithm implemented in in

the beginning portion of the algorithm in ELLYR, prior to any perturbation procedure. $M2$, on the other hand, represents the extrapolation of a line from the antenna location to the midpoint between the first and second original (unperturbed) data points to the rear of that antenna location. Line 1 and Line 2 are lines through the same first and second original data points, respectively. They are, respectively, perpendicular to $M1$ and $M2$. Such a set up was performed by subroutine CONVEX, which then called subroutine CONVX to evaluated the new perturbed positions of the respective data points. In fact, in the figure, subroutine CONVX relocated the first data point a factor of only $0.25\,\alpha$ into the fuselage from $M1$ along Line 1, where $\alpha = 0.2$ in this iteration. Similarly, the second data point was relocated a factor of α into the fuselage from $M2$ along Line 2. All other data points remained unperturbed.

Unfortunately, again, the perturbation did not successfully produce any acceptable solutions at all. Therefore, in the next iteration, a similar perturbation was performed all over again, as illustrated in Figure 4.22. In this figure, the original positions of the data points from Figure 4.21 were placed into the figure as reference points. In this iteration, $M1$ represents the tangent line to the presently perturbed surface at the antenna location, whereas $M2$ represents the extrapolation line from the antenna location to the midpoint between the perturbed locations of the first and second data points. Line 1 and Line 2 are lines through the perturbed locations of the first and second data points, respectively. These lines are also, respectively, perpendicular to $M1$ and $M2$, similar to Figure 4.21. For this iteration, α was incremented to 0.4. Nonetheless, similar to the previous iteration, the perturbed location for the first data point was relocated a factor of $0.25\,\alpha$ into the fuselage from $M1$ along Line 1, and that for the second data point, a factor of α into the fuselage from $M2$ along Line 2.

Particularly for this antenna location, the iteration was executed until the maximum iteration count was reached without any acceptable solutions at all, as indicated by the STATSTOP value of 8. Figure 4.23 and Figure 4.24 are perturbation
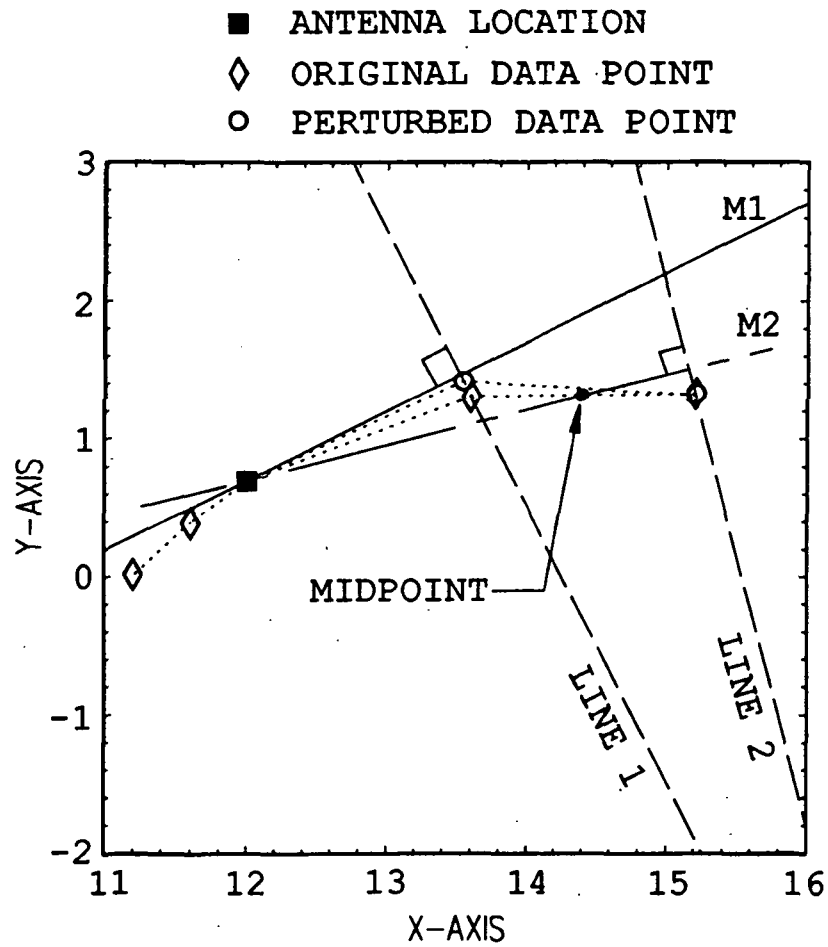
Figure 4.21: A geometrical description of the perturbation process in the YR-plane on data points to the rear of the antenna location $(Y_s, T) = (12, 0.05)$: First iteration.

ANTENNA LOCATION

ORIGINAL DATA POINT

PERTURBED DATA POINT

Figure 4.22: A geometrical description of the perturbation process in the YR-plane on data points to the rear of the antenna location $(Y_s, T) = (12, 0.05)$: Second iteration.
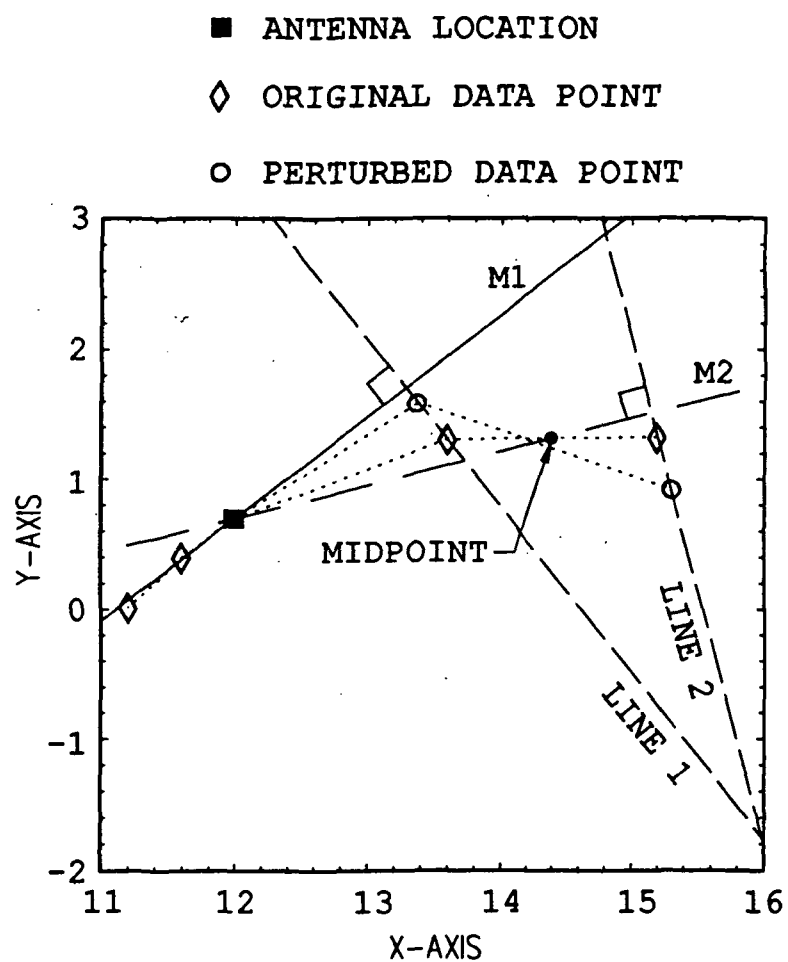
Figure 4.23: A geometrical description of the perturbation process in the YR-plane on data points to the rear of the antenna location $(Y_s, T) = (12, 0.05)$: Third iteration.
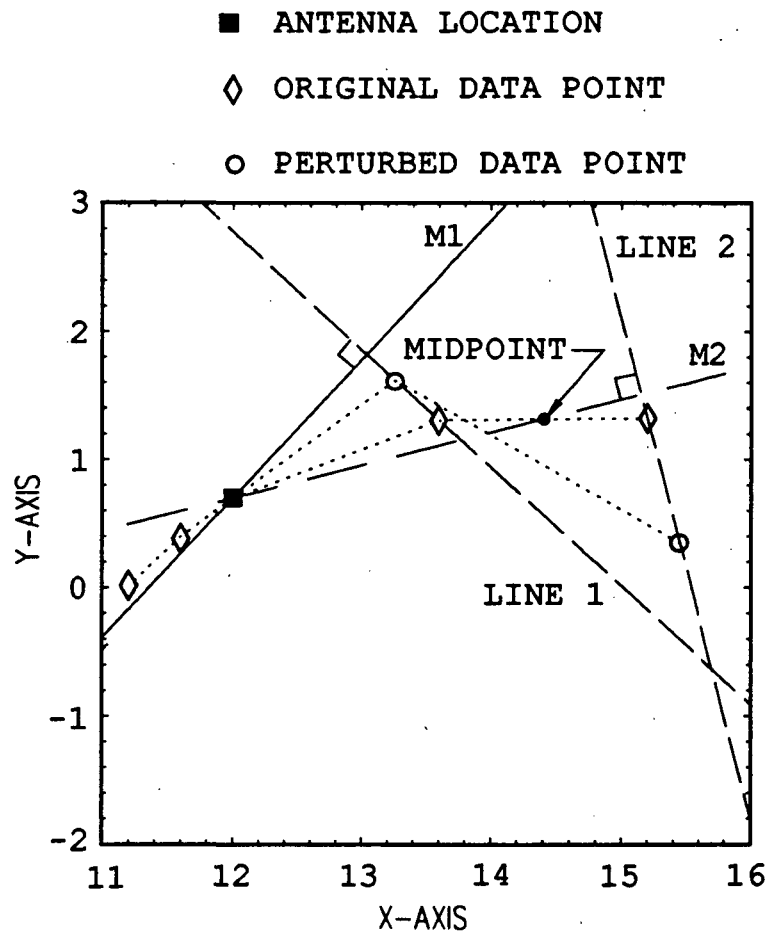
Figure 4.24: A geometrical description of the perturbation process in the YR-plane on data points to the rear of the antenna location $(Y_s, T) = (12, 0.05)$: Final iteration.

137

schematics for the third and last (tenth) iterations, respectively, whereby $\alpha = 0.6$ for the former, and $\alpha = 1.2$ for the latter. In fact, the points in Figure 4.24 were perturbed too far apart, to the extend that $M1$ was no longer accurate in representing the tangent line of the original surface at the antenna location at all. At this stage, the difference algorithms in subroutine ELLYR would have to be recalibrated.

4.6 Some cases of antenna locations close to end points of the helicopter fuselage

It should be noted that the present version of ELLC was not developed to handle antenna locations close to the end points of the helicopter fuselage. This was because, for the current algorithm of ELLC, data points on the cross-section in the YR-plane must be selected, two to the front and two to the rear of the antenna location. Nevertheless, the separation DY between any two adjacent data points in the YR-plane, or between the antenna location and the data point in the YR-plane adjacent to the antenna location, may be decreased, if necessary, to accommodate these data points. The solutions generated may actually be acceptable if the spacing between the data points were within the tolerance range whereby the difference algorithm in subroutine ELLYR would provide accurate computations, as has been discussed in Section 3.1 and Section 3.2. Otherwise, the solutions would generally be unacceptable. The stop-run condition STATSTOP for such antenna locations are 7, 13, 14, 15, 16 and 17.

4.6.1 Sample 6

For this sample run, the antenna was located at $(Y_s, T) = (49.00, 0.30)$, that is, on the right side of the tail end of the helicopter fuselage. The graphical results of this run are depicted in Figure 4.25 and Figure 4.26. The output of this sample run is appended in Appendix C.11. Conspicuously, this is a Case 1 problem, as is implied in the figures, as well as indicated in the appendix. Since the antenna was located

THE X-Z CROSS SECTION
YS =   49.00,   T = . 0.30
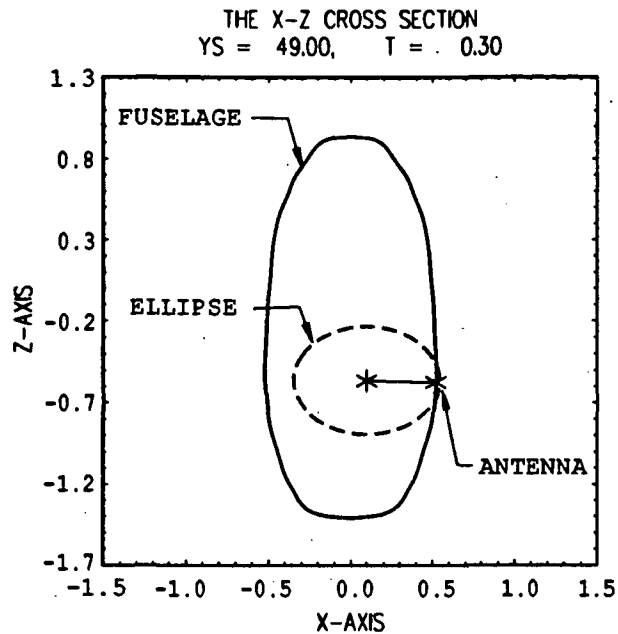
Figure 4.25: A close-fit ellipse in the XZ-plane for the antenna located at $(Y_s, T) = (49, 0.3)$.

very near the tail end of the helicopter fuselage, where $y = 50.00$, no data point on

the YR-plane cross-section that was located to the rear of the antenna location could

be obtained, if the parameter $DY1$ in ELLC, discussed in Section 3.2 was set to the

default value of 1.6. Therefore, in order to accommodate the two necessary rear data

points, the value for $DY1$ was decreased to 0.5. As a result, the $STATSTOP$ value

for this run is 7, as indicated in Appendix C.11.

From Figure 4.25, the close fit ellipse generated appeared to be an acceptable

solution for the cross-section in the XZ-plane, although the fit was localized to the

surface in that cross-section at the antenna location. It should be noted that the

scaling in 4.25 was enlarged, compared to all other XZ-plane plots provided in the

previous examples. The very minor misfit at the antenna location appears distinctive

on this enlarged diagram. Despite of this misfit, there was no detectable error in
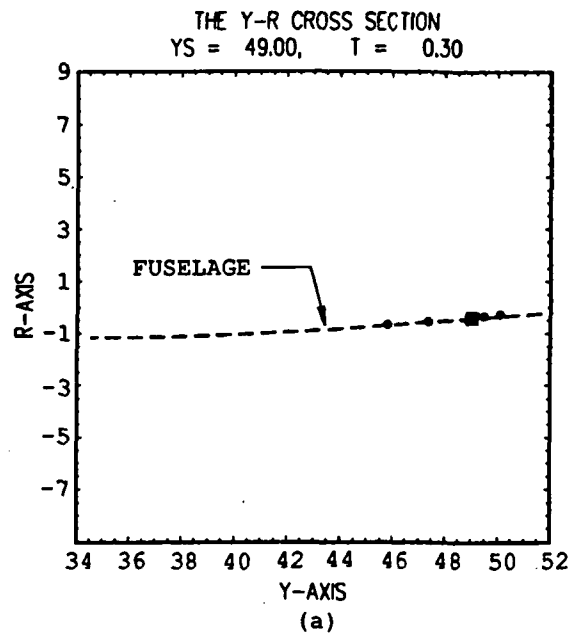
Figure 4.26: A close-fit composite ellipse in the YR-plane for the antenna located at $(Y_s, T) = (49, 0.3)$.
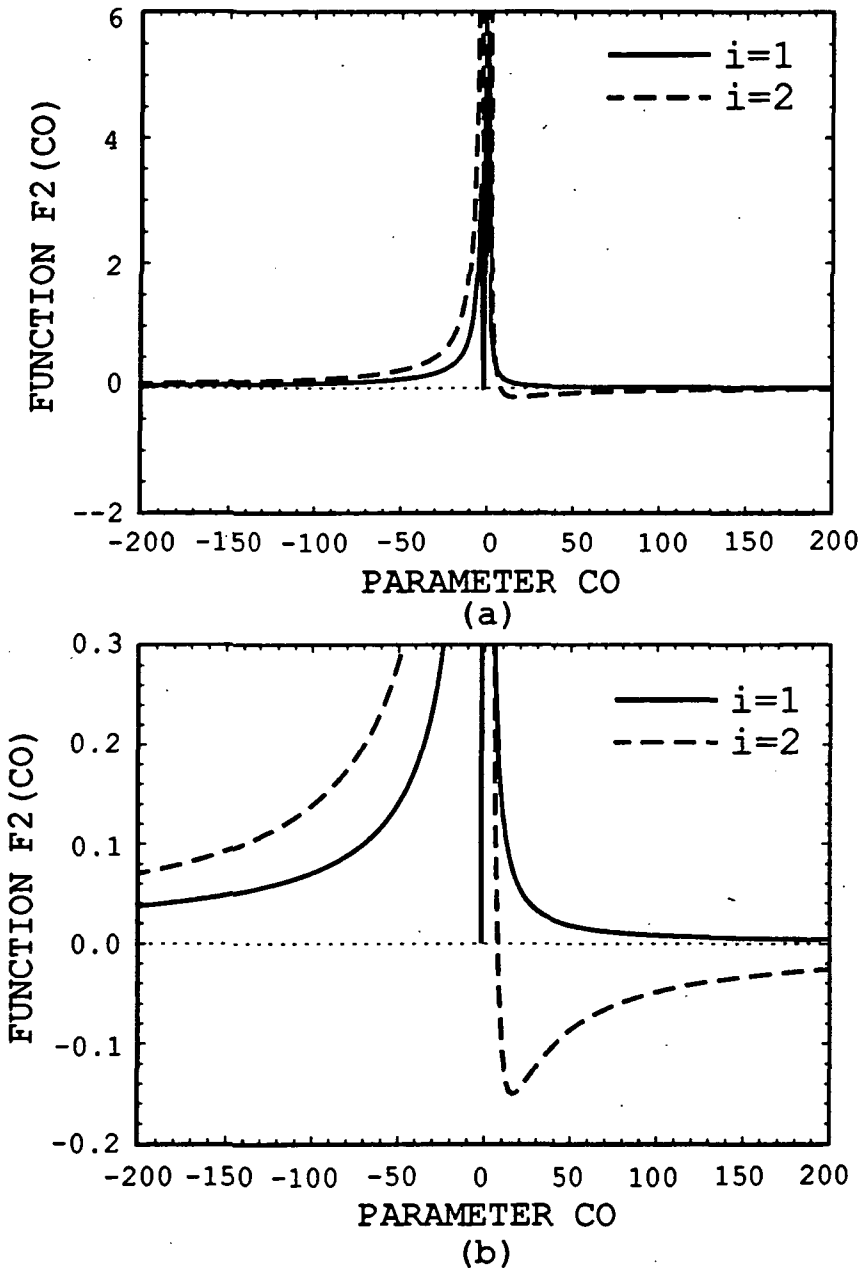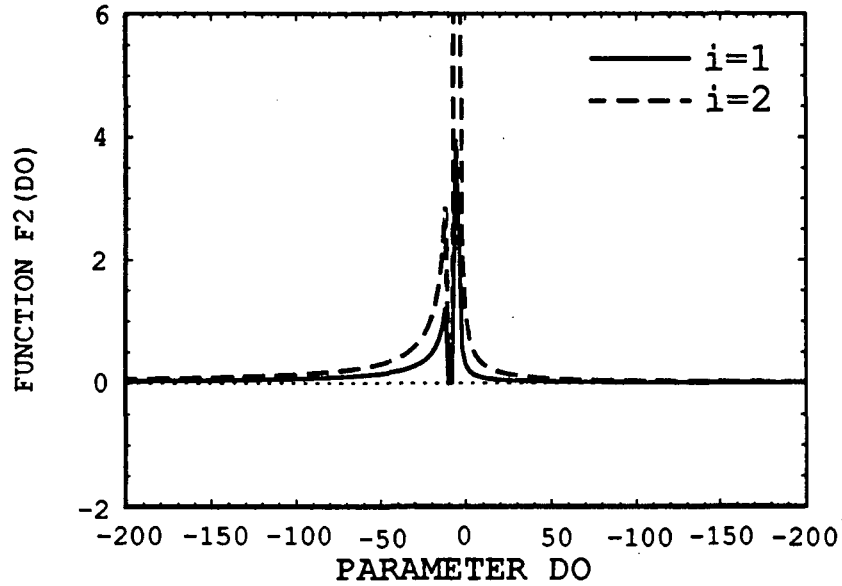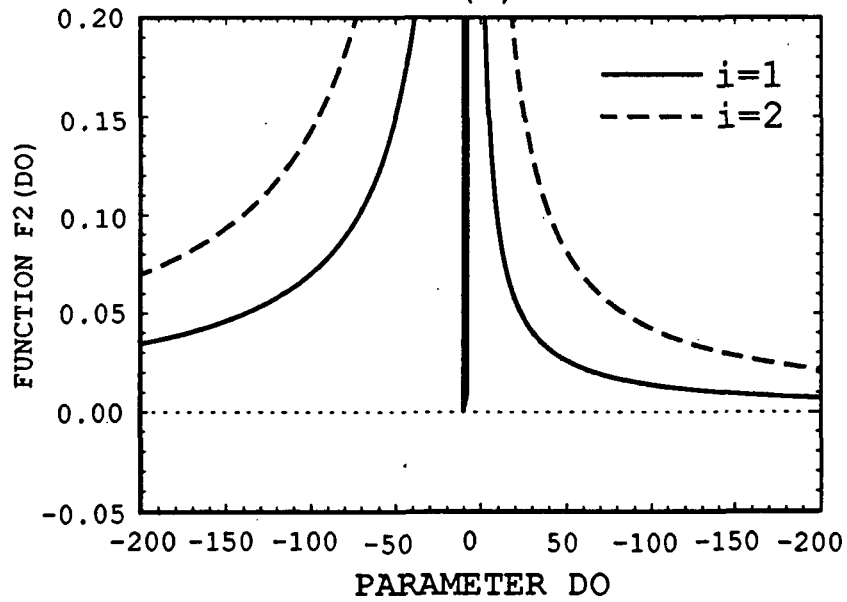
Figure 4.27: Plots of function f_{2_i} (for $i = 1, 2$) for the antenna located at $(Y_s, T) = (49, 0.3)$ prior to perturbation in the YR-plane.
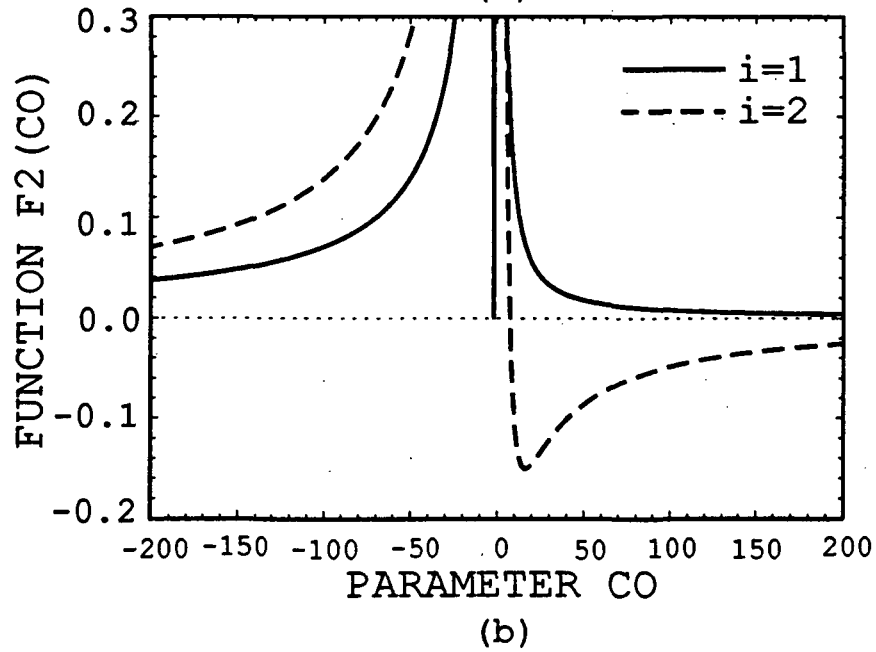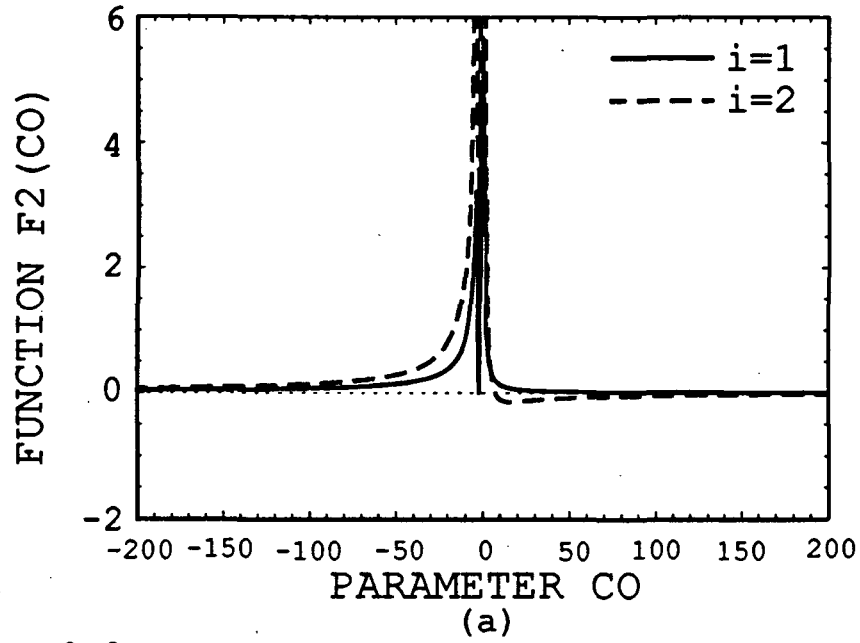
141

F2 VERSUS DO PLOTS AT (YS,T)=(49,0.3)

(a)

(b)
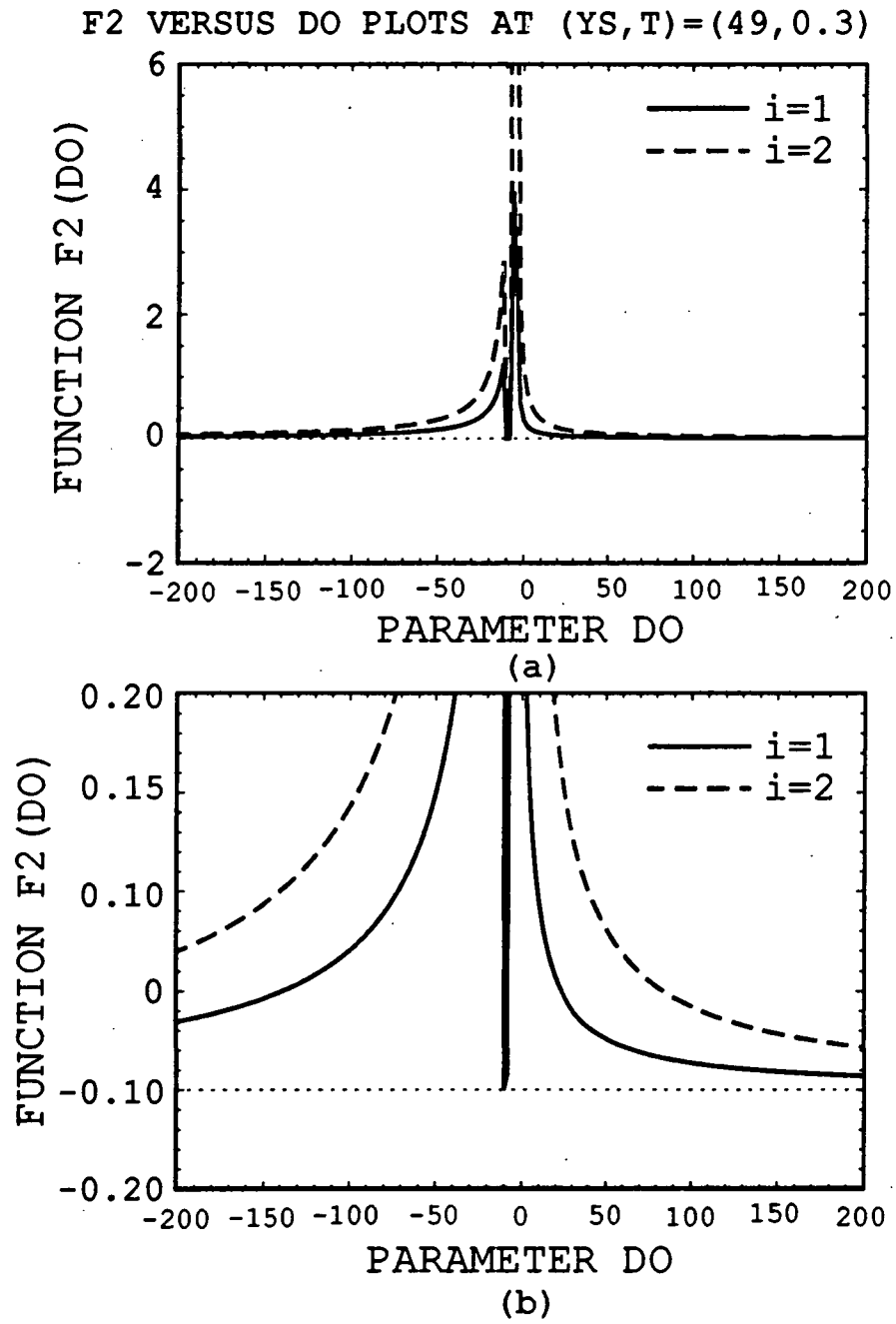
Figure 4.28: Plots of function f_{2_i} (for $i = 1, 2$) for the antenna located at $(Y_s, T) = (49, 0.3)$ following perturbation in the YR-plane.

142

the execution of subroutine ELLXZ. Indeed, this implied that the fit was acceptable within the maximum tolerance defined in subroutine ELLXZ.

In the YR-plane, as is observed in Figure 4.26, the cross-section surface was rather straight at the proximity of the antenna location. Since the sampling interval $DY1$ for data points to the rear of the antenna location was adjusted, the backward difference algorithm was utilized for computing the first-order derivative of the surface at the antenna location, so as to determine that this was a Case 1 problem. Details of this procedure has been discussed in Section 3.1 and Section 3.2. In the first iteration, module RTSAFE in subroutine ELLYR failed to provide accurate solution for D_0. Indeed, there was no zero crossing of the the function f_{2_i} for $i = 1, 2$ within the search range of -200 to 200, as was illustrated in Figure 4.27. In fact, f_2 was not even within the tolerance range that would regard it as zero, implying that the at least one of the real roots of f_2, $i = 1, 2$ did not exist within this domain. Analyzing this geometrically, such a problem might be attributed to the actual surface of the fuselage being too linear in the vicinity of the antenna location, and that the absolute value of the R-component, $|R_s|$, at the cross section of the antenna location, $Y_s = 49$ was restricted to a small value of only -0.424.

Therefore, subroutine PTURB was executed to perturb the data points to the rear of the antenna location. Fortunately enough, for this second iteration, and due to the fact that module SOLVR would always guarantee a solution if the surface gradient at the antenna location was not within the tolerance range of being zero, as was in this case, module RTSAFE successfully obtained a value for D_0. Although, again, none of the curves of functions f_2, $i = 1, 2$ crossed the zero line, they were both within the tolerance range of being considered as zeroes at some regions within the search range of $D_0 = -200$ to $D_0 = 200$. (Note that the tolerance range for this was $|DX| < 1.0 \times 10^{-6}$, where DX is $f_2(D_0)/\frac{d}{dD_0}f_2(D_0)$ [9].) For the first point, the real root was 0.779, and that for the second, was 0.906. Hence, averaging these, the value of D_0 was evaluated to be 0.842. For this second iteration, module SOLVR

had produced the solutions $C_0 = 7.558$ and $Y_c = 43.7$ by the method of reflection, prior to the execution of module RTSAFE.

In general, the composite ellipse was acceptable, even though its locus did not pass by close to the front most selected data point, as expected, due to perturbation performed on the front data points. In spite of this, the locus did pass closely by the first front data point, and almost directly on both the right data points. As a matter of fact, the composite ellipse thus obtained protruded a little beyond the edge of the fuselage end, as was obvious in Figure 4.26. As such, the completed close-fit composite ellipsoid produced would protrude out of the tail end of the helicopter fuselage. This, of course, would not be a problem when the parameters were input into NEWAIR, since NEWAIR would be able to handle such a problem by chopping off the protruding portion of the composite ellipsoid [1].

4.6.2 Sample 7

The antenna location for this sample run was at $(Y_s, T) = (5, 0.85)$, at the slanted surface on the side of the helicopter fuselage. The stop-run condition STATSTOP for this case was 13, indicating that the antenna location was being too close to one end of the fuselage, and that the required data points could not be selected in the YR-plane since they are indeterminate. Therefore, no composite ellipse was generated. The run was halted at this point. The output file of this run is appended in Appendix C.3.

Figure 4.29 illustrates the XZ-plane cross section of the helicopter fuselage with a close-fit ellipse at the antenna location. The degree of acceptability of this fitting to the slanted surface of fuselage was similar to those of samples 7 and 8, even though it does not appear to be so in the figure due to the smaller scaling factor of the plot. Moreover, the region of the ellipse utilized for close-fitting the actual surface was much flatter than those of the previous cases.

THE X-Z CROSS SECTION
YS =   5.00,   T = . 0.85
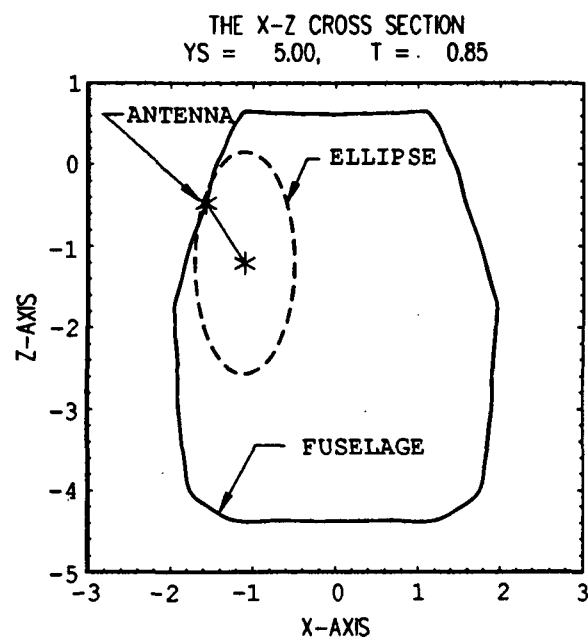
Figure 4.29: A close-fit ellipse in the XZ-plane for the antenna located at $(Y_s, T) = (5, 0.85)$.

4.7 Failures in routine ELLXZ

There are indeed five causes of program halting in routine ELLXZ, which are stop-run conditions STATSTOPs of values 1 through 5 listed in Appendix B. Of these, the most frequently encountered are $STATSTOP = 1$ and $STATSTOP = 2$, indicating that the surface at the antenna location is not convex in the proper direction of the outward normal of the fuselage for the former, and the exceeding of maximum iteration count for latter. Somewhat rare is the case for which $STATSTOP = 3$, indicating a line search failure had occurred. Interestingly, $STATSTOP = 4$ and $STATSTOP = 5$ are yet to be observed to occur. These stop-run conditions indicate, respectively, that failure in QR solution of the Newton-Raphson equation had occurred, and that a square-root of a negative value had occurred. In this section, two of these cases are presented.

4.7.1 Sample 8

For this sample run, the antenna is positioned at $(Y_s, T) = (16.00, 0.00)$, directly above the fuselage of the helicopter, as illustrated in Figure 4.30. As is observed from the enlarged view of the antenna location in the XZ-plane, the antenna location in question was in fact a small notch at the top of the fuselage, very possibly caused by the inaccurate inputting of the fuselage surface points interactively, as discussed in Sample 2. In fact, such notches are very often encountered throughout the entire cross sections of the helicopter fuselage. For this particular case, the notch was too deep to the extend that routine ELLXZ regarded it as a convex surface not in the proper direction of the outward normal of the fuselage. As such, the stop-run condition STATSTOP was 1, as listed in the output appended in Appendix C.12.

4.7.2 Sample 9

The antenna location for this sample run was at $(Y_s, T) = (2.1, 0.9)$, presumably extremely close to the front tip of the helicopter fuselage, which was $Y_s = 2.0$. As is

146

THE X-Z CROSS SECTION
YS = 16.00,   T =   0.00

(a)

THE X-Z CROSS SECTION
YS = 16.00,   T =   0.00

(b)
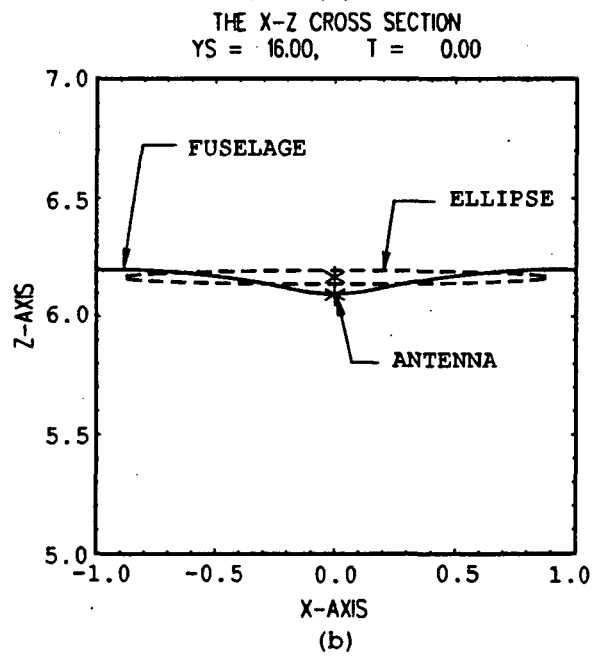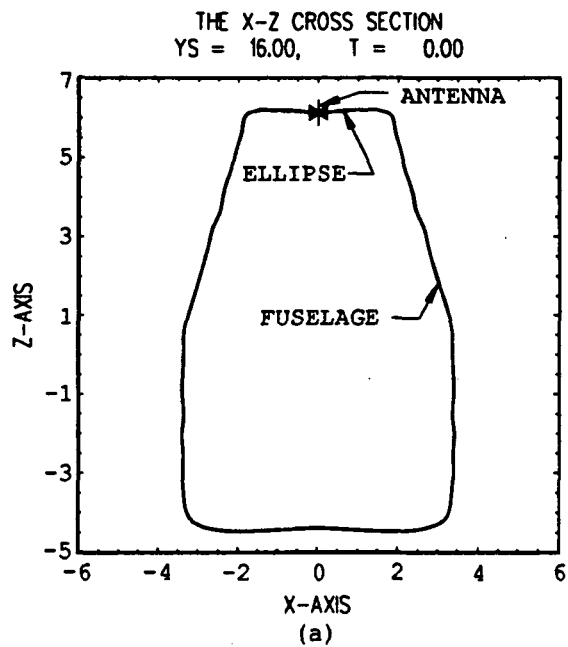
Figure 4.30: A close-fit ellipse in the XZ-plane for the antenna located at $(Y_s, T) =$ (16,0).

147

observed from Figure 4.31, the actual surface in the vicinity of the antenna location was rather irregular, again, possibly due to the inaccurate inputting of the surface points interactively, as discussed in Sample 2. This was indeed the suspected cause of the stop-run condition STATSTOP being 3, indicating that a line search failure had occurred in ELLXZ. The short output file of this run is included in Appendix C.9.

THE X-Z CROSS SECTION
YS = 2.10,   T =   0.90

(a)

THE X-Z CROSS SECTION
YS = 2.10,   T =   0.90

(b)
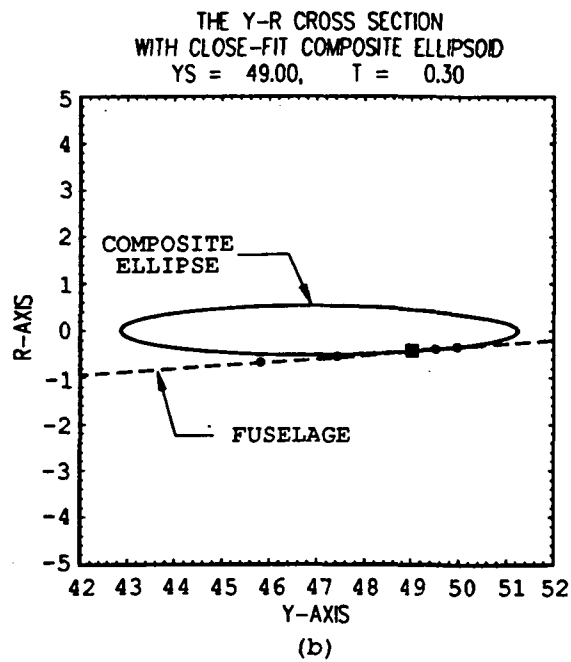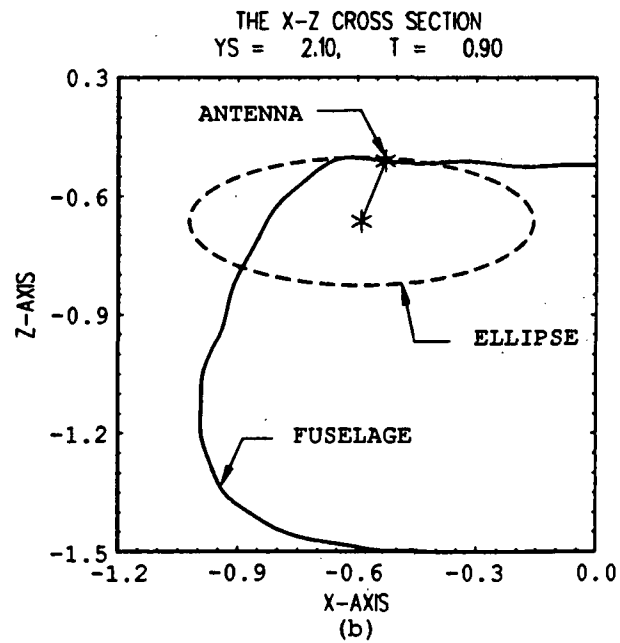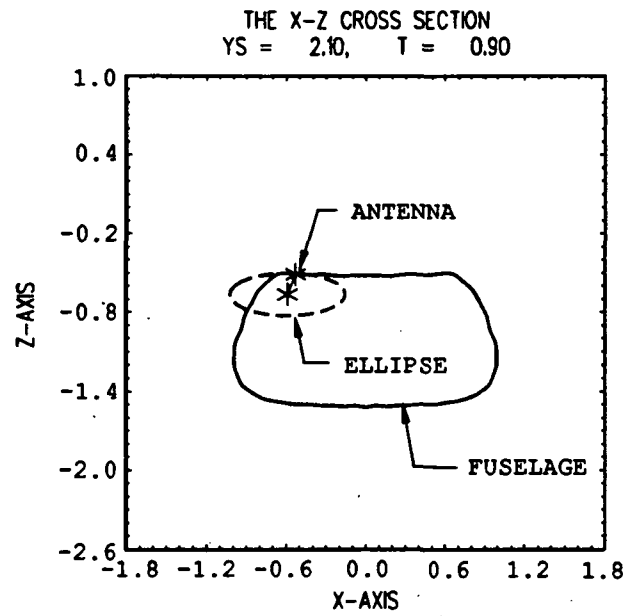
Figure 4.31: A close-fit ellipse in the XZ-plane for the antenna located at $(Y_s, T) =$ (2.1, 0.9).

Chapter 5

Summary

In summary, three computer codes were described in this report. The first was the *H*elicopter *A*ntenna *R*adiation *P*rediction (HARP) Code. This is a software package still under development at the ElectroScience Laboratory of The Ohio State University. This is in fact a computer code capable of displaying advance computer graphics. Integrated into it are the GTD and MM techniques for analyzing, respectively, the high and low frequency spectrum of the radiation emitted from an antenna mounted on a helicopter fuselage. The second code mentioned in this report is NEWAIR3. This code is written in FORTRAN 77 for high frequency GTD analysis of antennae mounted on aircraft. This code will be integrated into HARP to provide for the high frequency analysis of an antenna mounted on a helicopter fuselage. For this code to be executed, the helicopter must be modelled in terms of a composite ellipsoid and a set of flat, finite polygonal plates. In order to perform the modelling of the composite ellipsoid automatically, a computer code known as the *ELL*ipsoid *C*ode (ELLC) was developed, hence, the third and final code to be described here.

With the successful development of ELLC, the automatic fitting of the composite ellipsoid to the surface of the helicopter fuselage was made possible. In most of the sample runs presented in Chapter 4, the composite ellipsoids were generally good fits of the fuselage surface in the vicinity of the antenna location. In fact, in ELLC, the

actual 3-dimensional problem of fitting a composite ellipsoid to the fuselage surface was separated into two 2-dimensional problems:

1. The problem of fitting an ellipse to the surface of the cross-section in the XZ-plane.

2. The problem of fitting a composite ellipse to the surface of the cross-section in the YR-plane.

The subroutines necessary for solving the first 2-dimensional problem were developed by Scheick and Klevenow and a brief description is presented in Section 2.3. The other 2-dimensional problem in the Y-R plane, however, were completely described in this report. The method utilized here is only a preliminary result which requires further improvement. For this method, only a minimum number of points along the surface of the helicopter fuselage was used. Indeed, to obtain a good fit to the fuselage surface, more points would have to be utilized. A method has been developed by Scheick and Klevenow that uses more points on the surface. This latter technique will be discussed in a future report. Numerous sample runs of ELLC were analyzed in Chapter 4 utilizing the theories and concepts presented in Chapter 2. A concise description of the algorithm utilized in ELLC was presented in Chapter III, together with some flow-charts illustrating the nature of the logic in ELLC.

One of the limitations of ELLC is being incapable of fitting a composite ellipsoid to surfaces near the ends of the helicopter fuselage. In addition, computational runs of ELLC for antenna locations on concave surfaces of the fuselage may not be successful, depending on the severity of the concavity of the surface in question and the tolerance desired by the user. Nevertheless, ELLC is very efficient, with a general CPU time of less than 20 seconds on a VAX 8550 computer.

Appendix A

Notations and Symbols in ELLC

Notations and symbols utilized in ELLC	Notations and symbols in Chapter 1 and Chapter 2
$F1$ for $i = 1, 2$	f_{1_i} for $i = 1, 2$
$F2$ for $i = 1, 2$	f_{2_i} for $i = 1, 2$
XS, YS, ZS, RS	X_s, Y_s, Z_s, R_s
T	T
$PHIS$	ϕ_s
X, Y, Z, R	x, y, z, R
$A0, B0, C0, D0$	A_0, B_0, C_0, D_0
$A1, B1$	A_1, B_1
XC, YC, ZC	X_c, Y_c, Z_c
YSH	Y_{sh}
$C01P, C02P$	C'_{0_1}, C'_{0_2}
$D01P, D02P$	D'_{0_1}, D'_{0_2}

Table A.1: Alternative notations and symbols for utilization in ELLC.

Appendix B

Stop-run Conditions

```
STOP-RUN STATUS:
---------------

STATSTOP = 0   GOOD CLOSE-FIT COMPOSITE ELLIPSOID
               SOLUTION IS OBTAINED.
STATSTOP = 1   ELLIPSE CANNOT BE FITTED IN THE XZ-PLANE AT
               THE YS CROSS-SECTION BY "ELLXZ" MODULE; SURFACE
               POINTS ARE NOT CONVEX IN THE PROPER DIRECTION.
STATSTOP = 2 MAXIMUM ITERATIONS IN "ELLXZ" MODULE EXCEEDED;
               CLOSE-FIT ELLIPSE MAY NOT BE GOOD.
STATSTOP = 3 LINE SEARCH FAILURE IN "ELLXZ" MODULE.
STATSTOP = 4 FAILURE IN QR SOLUTION OF THE NEWTON-RAHPSON
               EQUATION IN THE "ELLXZ" MODULE.
STATSTOP = 5   SQUARE-ROOT OF A NEGATIVE VALUE OCCURRED IN
               "ELLXZ" MODULE.
STATSTOP = 6   BOTH SPACINGS DY1 (FOR CROSS SECTIONS BEHIND
               THE ANTENNA LOCATION) AND DY2 (FOR CROSS
               SECTION IN FRONT OF THE ANTENNA LOCATION)
               ARE CHANGED BEYOND THE ACCEPTABLE TOLERANCE
               WHEREBY THE DIFFERENCE ALGORITHM WOULD PROVIDE
               ACCURATE COMPUTATIONS FOR THE YR-PLANE.
STATSTOP = 7   ANTENNA LOCATION IS TOO CLOSE TO AN END
               POINT OF THE HELICOPTER FUSELAGE. MAXIMUM
               SPACING BETWEEN POINTS IN THE YR-PLANE
               REQUIRED FOR COMPUTATIONS IS ADJUSTED. HOWEVER,
               THE CLOSE-FIT COMPOSITE ELLIPSOID GENERATED MAY
               NOT BE GOOD.
STATSTOP = 8   MAXIMUM ITERATIONS IN "ELLYR" MODULE EXCEEDED.
               SURFACE POINTS IN THE YR-PLANE ARE PERTURBED
```

TO MAXIMUM TOLERANCE. FOR "CASE 1" PROBLEM,
THE RETURNED VALUES FOR CO AND YC ARE VALUES
FROM LAST ITERATION, AND FOR DO, THE RETURNED
VALUE IS A QUARTER THE INITIAL GUESS FOR I=2 FROM
LAST ITERATION, WHICH MAY NOT BE GOOD. FOR "CASE 2"
PROBLEM, THE RETURNED VALUES FOR DO AND YC ARE
VALUES FROM LAST ITERATION, AND FOR CO, THE
RETURNED VALUE IS A QUARTER THE INITIAL GUESS
FOR I=2 FROM LAST ITERATION, WHICH MAY NOT
BE GOOD.

STATSTOP = 9   IN "ELLYR" MODULE, SURFACE POINTS IN THE YR-PLANE
ARE PERTURBED TO OBTAIN SOLUTIONS; PERTURBED POINTS
ARE CONVEX.

STATSTOP = 10   IN "ELLYR" MODULE, SURFACE POINTS IN THE YR-PLANE
ARE PERTURBED TO OBTAIN SOLUTIONS; PERTURBED POINTS
ARE CONCAVE.

STATSTOP = 11   AS AN APPROXIMATION, YC IN "ELLYR" MODULE
IS OBTAINED BY REFLECTION ON YS, WITHOUT
PERTURBATION OF SURFACE POINTS IN THE YR-PLANE.

STATSTOP = 12   AS AN APPROXIMATION, YC IN "ELLYR" MODULE
IS OBTAINED BY REFLECTION ON YS, AFTER
PERTURBATION OF SURFACE POINTS IN THE YR-PLANE.

STATSTOP = 13   STATSTOP=7 CONDITION, BUT THE REQUIRED POINTS
IN THE YR-PLANE ARE INDETERMINATE; CLOSE-FIT
COMPOSITE ELLIPSOID CANNOT BE GENERATED.

STATSTOP = 14   STATSTOP=7 CONDITION, BUT SOLUTIONS ARE
STATSTOP=9 TYPE.

STATSTOP = 15   STATSTOP=7 CONDITION, BUT SOLUTIONS ARE
STATSTOP=10 TYPE.

STATSTOP = 16   STATSTOP=7 CONDITION, BUT SOLUTIONS ARE
STATSTOP=11 TYPE.

STATSTOP = 17   STATSTOP=7 CONDITION, BUT SOLUTIONS ARE
STATSTOP=12 TYPE.

Appendix C

Output Files from ELLC

C.1 For $Y_s = 17.00$, $T = 0.55$

```
NAME OF THIS FILE: Y17T55    .DAT
THIS DATA FILE IS GENERATED BY "ELLC.FOR"
NAME OF EXTERNAL MASTER DATA FILE READ: LH.MASTER
NUMBER OF SURFACE POINTS USED: 5 (2 EACH, IN THE FRONT
   AND IN THE REAR OF THE ANTENNA LOCATION, RESPECTIVELY)

HELICOPTER FUSELAGE STARTS FROM Y =   2.000 TO Y =   50.000
ANTENNA LOCATION (IN THE XZ-PLANE CROSS-SECTION)
      = (YS,TINIT) = (   17.000 ,   0.550 )
ANTENNA LOCATION IN RECTANGULAR COORDINATES
      = (XS,YS,ZS) = (   -1.664 ,   17.000 ,   -4.468 )

AT YS =   17.000 :
   SEMI-MINOR AXIS OF THE BEST-FIT
         ELLIPSE IN THE XZ-PLANE = A1 =   19.809
   SEMI-MAJOR AXIS OF THE BEST-FIT
         ELLIPSE IN THE XZ-PLANE = B1 =    8.831
   CENTER OF BEST-FIT ELLIPSE = (XC,ZC) = (   -1.634 ,   15.315 )

FUSELAGE CROSS-SECTION SAMPLING:
-------------------------------

ANTENNA LOCATION IN YR-COORDINATES
      = (YS,RS) = (   17.000 ,  -19.783 )

TO THE REAR OF THE ANTENNA LOCATION AT SPACING DY =   1.6000
```

i-th CROSS SECTION	RECTANGULAR COORDINATES			YR-COORDINATES AT PHIS = -179.91 DEG	
	X	Y	Z	Y	R
2	-1.664	18.600	-4.465	18.600	-19.781
3	-1.664	20.200	-4.466	20.200	-19.781
4	-1.664	21.800	-4.461	21.800	-19.776
5	-1.664	23.400	-4.458	23.400	-19.774
6	-1.664	25.000	-4.465	25.000	-19.780
7	-1.664	26.600	-4.232	26.600	-19.547
8	-1.663	28.200	-3.746	28.200	-19.061
9	-1.662	29.800	-3.075	29.800	-18.390
10	-1.660	31.400	-1.593	31.400	-16.908

TO THE FRONT OF THE ANTENNA LOCATION AT SPACING DY =   1.6000

i-th CROSS SECTION	RECTANGULAR COORDINATES			YR-COORDINATES AT PHIS = -179.91 DEG	
	X	Y	Z	Y	R
2	-1.664	15.400	-4.461	15.400	-19.776
3	-1.664	13.800	-4.459	13.800	-19.774
4	-1.664	12.200	-4.509	12.200	-19.824
5	-1.664	10.600	-4.598	10.600	-19.913
6	-1.665	9.000	-4.677	9.000	-19.992
7	-1.665	7.400	-4.792	7.400	-20.108
8	-1.664	5.800	-4.587	5.800	-19.902
9	-1.660	4.200	-1.914	4.200	-17.229

THIS IS A "CASE 1" PROBLEM
STOP-RUN STATUS = STATSTOP = 0

PARAMETER VALUES FOR CLOSE-FIT COMPOSITE ELLIPSOID:

    AO =   19.809
    BO =   8.831
    CO =   105.738
    DO =   83.614
    YSH =   0.000
    (XC,YC,ZC) = (-1.634 ,   17.000 ,   15.315)
    STOP-RUN STATUS = STATSTOP = 0

```
RUN COMPLETED!
CPU TIME:  12.89 SECONDS
```

C.2   For $Y_s = 3.00$, $T = 0.50$

```
NAME OF THIS FILE: Y03T50   .DAT
THIS DATA FILE IS GENERATED BY "ELLC.FOR"
NAME OF EXTERNAL MASTER DATA FILE READ: LH.MASTER
NUMBER OF SURFACE POINTS USED: 5 (2 EACH, IN THE FRONT
    AND IN THE REAR OF THE ANTENNA LOCATION, RESPECTIVELY)


HELICOPTER FUSELAGE STARTS FROM Y =   2.000 TO Y =   50.000
ANTENNA LOCATION (IN THE XZ-PLANE CROSS-SECTION)
       = (YS,TINIT) = (    3.000 ,    0.500 )
ANTENNA LOCATION IN RECTANGULAR COORDINATES
       = (XS,YS,ZS) = (    0.000 ,    3.000 ,   -1.884 )


AT YS =    3.000 :
   SEMI-MINOR AXIS OF THE BEST-FIT
        ELLIPSE IN THE XZ-PLANE = A1 =    1.177
   SEMI-MAJOR AXIS OF THE BEST-FIT
        ELLIPSE IN THE XZ-PLANE = B1 =    0.526
   CENTER OF BEST-FIT ELLIPSE = (XC,ZC) = (    0.000 ,   -0.729 )


FUSELAGE CROSS-SECTION SAMPLING:
--------------------------------


ANTENNA LOCATION IN YR-COORDINATES
       = (YS,RS) = (    3.000 ,   -1.155 )


TO THE REAR OF THE ANTENNA LOCATION AT SPACING DY =    1.6000
```

i-th CROSS SECTION	RECTANGULAR COORDINATES			YR-COORDINATES AT PHIS = -180.00 DEG	
	X	Y	Z	Y	R
2	0.000	4.600	-4.032	4.600	-3.303
3	0.000	6.200	-4.757	6.200	-4.028
4	0.000	7.800	-4.799	7.800	-4.069
5	0.000	9.400	-4.702	9.400	-3.973
6	0.000	11.000	-4.555	11.000	-3.826

7	0.000	12.600	-4.426	12.600	-3.697
8	0.000	14.200	-4.374	14.200	-3.645
9	0.000	15.800	-4.386	15.800	-3.657
10	0.000	17.400	-4.392	17.400	-3.663
11	0.000	19.000	-4.388	19.000	-3.659
12	0.000	20.600	-4.389	20.600	-3.660
13	0.000	22.200	-4.382	22.200	-3.653
14	0.000	23.800	-4.385	23.800	-3.656
15	0.000	25.400	-4.361	25.400	-3.632
16	0.000	27.000	-4.077	27.000	-3.348
17	0.000	28.600	-3.603	28.600	-2.874
18	0.000	30.200	-3.061	30.200	-2.332
19	0.000	31.800	-2.572	31.800	-1.843
20	0.000	33.400	-2.260	33.400	-1.531
21	0.000	35.000	-2.213	35.000	-1.484
22	0.000	36.600	-2.205	36.600	-1.476
23	0.000	38.200	-2.166	38.200	-1.437
24	0.000	39.800	-2.101	39.800	-1.372
25	0.000	41.400	-2.015	41.400	-1.285
26	0.000	43.000	-1.909	43.000	-1.180
27	0.000	44.600	-1.789	44.600	-1.060
28	0.000·	46.200	-1.657	46.200	-0.928
29	0.000	47.800	-1.517	47.800	-0.788
30	0.000	49.400	-1.372	49.400	-0.643

ANTENNA LOCATION TOO CLOSE TO AN END POINT OF THE HELICOPTER FUSELAGE.
ADJUSTING ...

TO THE FRONT OF THE ANTENNA LOCATION AT SPACING DY =   0.5000

i-th CROSS SECTION		RECTANGULAR COORDINATES Y		YR-COORDINATES AT PHIS = -180.00 DEG Y	
	X	Y	Z	Y	R
2	0.000	2.500	-1.536	2.500	-0.807
3	0.000	2.000	-1.536	2.000	-0.807

THIS IS A "CASE 2" PROBLEM
STOP-RUN STATUS = STATSTOP = 15

WARNING: ANTENNA LOCATION IS TOO CLOSE TO AN END POINT
         IN THE YR-PLANE. CLOSE-FIT COMPOSITE ELLIPSOID

MAY NOT BE GOOD.

SURFACE POINTS ARE NOT CONVEX IN THE PROPER DIRECTION.

RUN HALTED: STATSTOP = 15
            CLOSE-FIT COMPOSITE ELLIPSOID CANNOT BE GENERATED.

RUN COMPLETED!
CPU TIME: 21.27 SECONDS

C.3   For $Y_s = 5.00$, $T = 0.85$

NAME OF THIS FILE: Y05T85   .DAT
THIS DATA FILE IS GENERATED BY "ELLC.FOR"
NAME OF EXTERNAL MASTER DATA FILE READ: LH.MASTER
NUMBER OF SURFACE POINTS USED: 5 (2 EACH, IN THE FRONT
    AND IN THE REAR OF THE ANTENNA LOCATION, RESPECTIVELY)

HELICOPTER FUSELAGE STARTS FROM Y =   2.000 TO Y =   50.000
ANTENNA LOCATION (IN THE XZ-PLANE CROSS-SECTION)
        = (YS,TINIT) = (5.000 ,   0.850)
ANTENNA LOCATION IN RECTANGULAR COORDINATES
        = (XS,YS,ZS) = (-1.572 ,   5.000 ,   -0.473)

AT YS =   5.000 :
    SEMI-MINOR AXIS OF THE BEST-FIT
        ELLIPSE IN THE XZ-PLANE = A1 =   1.361
    SEMI-MAJOR AXIS OF THE BEST-FIT
        ELLIPSE IN THE XZ-PLANE = B1 =   0.603
    CENTER OF BEST-FIT ELLIPSE = (XC,ZC) = (-1.103 ,   -1.210)

FUSELAGE CROSS-SECTION SAMPLING:

ANTENNA LOCATION IN YR-COORDINATES
        = (YS,RS) = (5.000 ,   0.874)

TO THE REAR OF THE ANTENNA LOCATION AT SPACING DY =   1.6000

i-th		RECTANGULAR		YR-COORDINATES	
CROSS		COORDINATES		AT PHIS = -32.50 DEG	
SECTION	X	Y	Z	Y	R

2	-1.969	6.600	0.150	6.600	1.612
3	-2.170	8.200	0.465	8.200	1.987
4	-2.374	9.800	0.785	9.800	2.366
5	-2.710	11.400	1.312	11.400	2.990
6	-2.983	13.000	1.741	13.000	3.499
7	-3.056	14.600	1.856	14.600	3.635
8	-3.018	16.200	1.796	16.200	3.564
9	-3.013	17.800	1.788	17.800	3.555
10	-3.024	19.400	1.805	19.400	3.575
11	-3.022	21.000	1.802	21.000	3.572
12	-3.016	22.600	1.793	22.600	3.560
13	-3.025	24.200	1.806	24.200	3.576
14	-2.969	25.800	1.719	25.800	3.473
15	-2.720	27.400	1.327	27.400	3.009
16	-2.349	29.000	0.746	29.000	2.320
17	-1.933	30.600	0.092	30.600	1.544
18	-1.503	32.200	-0.582	32.200	0.745
19	-1.261	33.800	-0.962	33.800	0.295
20	-1.253	35.400	-0.975	35.400	0.279
21	-1.235	37.000	-1.003	37.000	0.245
22	-1.182	38.600	-1.085	38.600	0.148
23	-1.075	40.200	-1.253	40.200	-0.051

```
ANTENNA LOCATION TOO CLOSE TO AN END POINT OF THE HELICOPTER FUSELAGE.
ADJUSTING ...

RUN HALTED: STATSTOP = 13
            CLOSE-FIT COMPOSITE ELLIPSOID CANNOT BE GENERATED.

RUN COMPLETED!
CPU TIME:  17.31 SECONDS
```

C.4   For $Y_s = 7.00$, $T = 0.41$

```
NAME OF THIS FILE: Y07T41    .DAT
THIS DATA FILE IS GENERATED BY "ELLC.FOR"
NAME OF EXTERNAL MASTER DATA FILE READ: LH.MASTER
NUMBER OF SURFACE POINTS USED: 5 (2 EACH, IN THE FRONT
    AND IN THE REAR OF THE ANTENNA LOCATION, RESPECTIVELY)

HELICOPTER FUSELAGE STARTS FROM Y =   2.000 TO Y =   50.000
```

```
ANTENNA LOCATION (IN THE XZ-PLANE CROSS-SECTION)
        = (YS,TINIT) = (    7.000 ,    0.410 )
ANTENNA LOCATION IN RECTANGULAR COORDINATES
        = (XS,YS,ZS) = (    1.752 ,    7.000 ,    -4.774 )

AT YS =    7.000 :
    SEMI-MINOR AXIS OF THE BEST-FIT
         ELLIPSE IN THE XZ-PLANE = A1 =    0.842
    SEMI-MAJOR AXIS OF THE BEST-FIT
         ELLIPSE IN THE XZ-PLANE = B1 =    0.771
    CENTER OF BEST-FIT ELLIPSE = (XC,ZC) = (    1.431 ,    -3.989 )


FUSELAGE CROSS-SECTION SAMPLING:
---------------------------------


ANTENNA LOCATION IN YR-COORDINATES
        = (YS,RS) = (    7.000 ,    -0.849 )


TO THE REAR OF THE ANTENNA LOCATION AT SPACING DY =    1.6000
```

i-th CROSS SECTION	X	RECTANGULAR COORDINATES Y	Z	YR-COORDINATES AT PHIS = 157.77 DEG Y	R
2	1.720	8.600	-4.697	8.600	-0.766
3	1.686	10.200	-4.614	10.200	-0.675
4	1.652	11.800	-4.530	11.800	-0.585
5	1.625	13.400	-4.464	13.400	-0.514
6	1.622	15.000	-4.457	15.000	-0.506
7	1.626	16.600	-4.466	16.600	-0.516
8	1.626	18.200	-4.465	18.200	-0.515
9	1.625	19.800	-4.465	19.800	-0.514
10	1.624	21.400	-4.462	21.400	-0.512
11	1.622	23.000	-4.456	23.000	-0.505
12	1.628	24.600	-4.472	24.600	-0.522
13	1.565	26.200	-4.317	26.200	-0.354
14	1.392	27.800	-3.893	27.800	0.103
15	1.161	29.400	-3.328	29.400	0.714
16	0.923	31.000	-2.747	31.000	1.342
17	0.731	32.600	-2.277	32.600	1.849
18	0.645	34.200	-2.065	34.200	2.078
19	0.648	35.800	-2.074	35.800	2.069

```
20        0.637     37.400    -2.048    37.400    2.097
21        0.616     39.000    -1.996    39.000    2.153
22        0.586     40.600    -1.922    40.600    2.233
23        0.548     42.200    -1.828    42.200    2.334
24        0.503     43.800    -1.719    43.800    2.452
25        0.453     45.400    -1.596    45.400    2.585
26        0.398     47.000    -1.463    47.000    2.729
27        0.341     48.600    -1.321    48.600    2.882
```

SELECTED DATA POINT CROSSES THE ZERO LINE IN THE YR-PLANE.
ADJUSTING SPACING DY...

SELECTED DATA POINT CROSSES THE ZERO LINE IN THE YR-PLANE.
ADJUSTING SPACING DY...

SELECTED DATA POINT CROSSES THE ZERO LINE IN THE YR-PLANE.
ADJUSTING SPACING DY...

TO THE FRONT OF THE ANTENNA LOCATION AT SPACING DY =   0.9600

i-th CROSS SECTION	RECTANGULAR COORDINATES			YR-COORDINATES AT PHIS = 157.77 DEG	
	X	Y	Z	Y	R
2	1.696	6.040	-4.638	6.040	-0.702
3	1.544	5.080	-4.266	5.080	-0.300
4	0.410	2.200	-1.490	2.200	2.699

THIS IS A "CASE 1" PROBLEM
STOP-RUN STATUS = STATSTOP = 11

PARAMETER VALUES FOR CLOSE-FIT COMPOSITE ELLIPSOID:

```
    AO =     1.768
    BO =     1.618
    CO =    67.623
    DO =   -57.647
    YSH =   59.309
    (XC,YC,ZC) = (     1.431 ,  -52.466 ,   -3.989 )
    STOP-RUN STATUS = STATSTOP = 11
```

```
RUN COMPLETED!
CPU TIME:  14.13 SECONDS
```

C.5   For $Y_s = 12.00$, $T = 0.05$

```
NAME OF THIS FILE: Y12T05    .DAT
THIS DATA FILE IS GENERATED BY "ELLC.FOR"
NAME OF EXTERNAL MASTER DATA FILE READ: LH.MASTER
NUMBER OF SURFACE POINTS USED: 5 (2 EACH, IN THE FRONT
    AND IN THE REAR OF THE ANTENNA LOCATION, RESPECTIVELY)

HELICOPTER FUSELAGE STARTS FROM Y =   2.000 TO Y =    50.000
ANTENNA LOCATION (IN THE XZ-PLANE CROSS-SECTION)
        = (YS,TINIT) = (   12.000 ,    0.050 )
ANTENNA LOCATION IN RECTANGULAR COORDINATES
        = (XS,YS,ZS) = (   1.469 ,   12.000 ,    5.588 )

AT YS =  12.000 :
    SEMI-MINOR AXIS OF THE BEST-FIT
          ELLIPSE IN THE XZ-PLANE = A1 =    0.607
    SEMI-MAJOR AXIS OF THE BEST-FIT
          ELLIPSE IN THE XZ-PLANE = B1 =    0.838
    CENTER OF BEST-FIT ELLIPSE = (XC,ZC) = (    1.022 ,    5.054 )

FUSELAGE CROSS-SECTION SAMPLING:
---------------------------------


ANTENNA LOCATION IN YR-COORDINATES
        = (YS,RS) = (   12.000 ,    0.696 )

TO THE REAR OF THE ANTENNA LOCATION AT SPACING DY =    1.6000
```

i-th CROSS SECTION	RECTANGULAR COORDINATES			YR-COORDINATES AT PHIS = 39.96 DEG	
	X	Y	Z	Y	R
2	1.860	13.600	6.054	13.600	1.305
3	1.870	15.200	6.067	15.200	1.320
4	1.827	16.800	6.016	16.800	1.254
5	1.836	18.400	6.026	18.400	1.268
6	1.845	20.000	6.037	20.000	1.282
7	1.838	21.600	6.028	21.600	1.271

```
8        1.833    23.200    6.023    23.200    1.263
9        1.848    24.800    6.041    24.800    1.287
10       1.589    26.400    5.732    26.400    0.884
11       0.818    28.000    4.812    28.000   -0.317
12      -0.230    29.600    3.561    29.600   -1.948
```

SELECTED DATA POINT CROSSES THE ZERO LINE IN THE YR-PLANE.
ADJUSTING SPACING DY...

SELECTED DATA POINT CROSSES THE ZERO LINE IN THE YR-PLANE.
ADJUSTING SPACING DY...

SELECTED DATA POINT CROSSES THE ZERO LINE IN THE YR-PLANE.
ADJUSTING SPACING DY...

SELECTED DATA POINT CROSSES THE ZERO LINE IN THE YR-PLANE.
ADJUSTING SPACING DY...

SELECTED DATA POINT CROSSES THE ZERO LINE IN THE YR-PLANE.
ADJUSTING SPACING DY...

SELECTED DATA POINT CROSSES THE ZERO LINE IN THE YR-PLANE.
ADJUSTING SPACING DY...

SELECTED DATA POINT CROSSES THE ZERO LINE IN THE YR-PLANE.
ADJUSTING SPACING DY...

SELECTED DATA POINT CROSSES THE ZERO LINE IN THE YR-PLANE.
ADJUSTING SPACING DY...

TO THE FRONT OF THE ANTENNA LOCATION AT SPACING DY =   0.4000

```
i-th                RECTANGULAR          YR-COORDINATES
CROSS               COORDINATES          AT PHIS =   39.96 DEG
SECTION     X         Y        Z           Y          R


2        1.276    11.600    5.357    11.600    0.395
3        1.029    11.200    5.064    11.200    0.012
```

THIS IS A "CASE 2" PROBLEM
STOP-RUN STATUS = STATSTOP = 8

```
WARNING: MAXIMUM ITERATIONS IN "ELLYR" MODULE EXCEEDED.
         CLOSE-FIT COMPOSITE ELLIPSOID MAY NOT BE GOOD.

PARAMETER VALUES FOR CLOSE-FIT COMPOSITE ELLIPSOID:
---------------------------------------------------

     AO =     0.786
     BO =     1.085
     CO =     1.750
     DO =     1.515
     YSH =     0.112
     (XC,YC,ZC) = (     1.022 ,    12.962 ,     5.054 )
     STOP-RUN STATUS = STATSTOP =  8


RUN COMPLETED!
CPU TIME:  11.60 SECONDS
```

C.6   For $Y_s = 12.00$, $T = 0.30$

```
NAME OF THIS FILE: Y12T30    .DAT
THIS DATA FILE IS GENERATED BY "ELLC.FOR"
NAME OF EXTERNAL MASTER DATA FILE READ: LH.MASTER
NUMBER OF SURFACE POINTS USED: 5 (2 EACH, IN THE FRONT
     AND IN THE REAR OF THE ANTENNA LOCATION, RESPECTIVELY)


HELICOPTER FUSELAGE STARTS FROM Y =    2.000 TO Y =    50.000
ANTENNA LOCATION (IN THE XZ-PLANE CROSS-SECTION)
       = (YS,TINIT) = (    12.000 ,     0.300 )
ANTENNA LOCATION IN RECTANGULAR COORDINATES
       = (XS,YS,ZS) = (     3.200 ,    12.000 ,    -1.548 )

AT YS =    12.000 :
   SEMI-MINOR AXIS OF THE BEST-FIT
        ELLIPSE IN THE XZ-PLANE = A1 =     2.354
   SEMI-MAJOR AXIS OF THE BEST-FIT
        ELLIPSE IN THE XZ-PLANE = B1 =    1.020
   CENTER OF BEST-FIT ELLIPSE = (XC,ZC) = (    2.224 ,    -1.523 )

FUSELAGE CROSS-SECTION SAMPLING:
-----------------------------------


ANTENNA LOCATION IN YR-COORDINATES
```

= (YS,RS) = (12.000 ,   -0.976)

TO THE REAR OF THE ANTENNA LOCATION AT SPACING DY =   1.6000

i-th CROSS SECTION	X	RECTANGULAR COORDINATES Y	Z	YR-COORDINATES AT PHIS = 91.45 DEG Y	R
2	3.379	13.600	-1.552	13.600	-1.156
3	3.387	15.200	-1.552	15.200	-1.164
4	3.357	16.800	-1.552	16.800	-1.134
5	3.363	18.400	-1.552	18.400	-1.140
6	3.370	20.000	-1.552	20.000	-1.146
7	3.364	21.600	-1.552	21.600	-1.140
8	3.359	23.200	-1.552	23.200	-1.136
9	3.373	24.800	-1.552	24.800	-1.149
10	3.196	26.400	-1.548	26.400	-0.973
11	2.792	28.000	-1.537	28.000	-0.568
12	2.277	29.600	-1.524	29.600	-0.053
13	1.740	31.200	-1.511	31.200	0.484
14	1.302	32.800	-1.500	32.800	0.922
15	1.128	34.400	-1.495	34.400	1.096
16	1.137	36.000	-1.496	36.000	1.087
17	1.104	37.600	-1.495	37.600	1.120
18	1.041	39.200	-1.493	39.200	1.183
19	0.953	40.800	-1.491	40.800	1.271
20	0.841	42.400	-1.488	42.400	1.383
21	0.707	44.000	-1.485	44.000	1.517
22	0.542	45.600	-1.481	45.600	1.682
23	0.362	47.200	-1.476	47.200	1.862

TO THE FRONT OF THE ANTENNA LOCATION AT SPACING DY =   1.6000

i-th CROSS SECTION	X	RECTANGULAR COORDINATES Y	Z	YR-COORDINATES AT PHIS = 91.45 DEG Y	R
2	2.895	10.400	-1.540	10.400	-0.672
3	2.524	8.800	-1.531	8.800	-0.300
4	2.208	7.200	-1.523	7.200	0.016
5	2.018	5.600	-1.518	5.600	0.206
6	1.570	4.000	-1.507	4.000	0.654

```
    7          0.601      2.400      -1.482       2.400       1.623
```

THIS IS A "CASE 2" PROBLEM
STOP-RUN STATUS = STATSTOP = 11

PARAMETER VALUES FOR CLOSE-FIT COMPOSITE ELLIPSOID:

```
    AO =    3.288
    BO =    1.425
    CO =    4.559
    DO =    9.298
    YSH =   -2.270
    (XC,YC,ZC) = (    2.224 ,    18.492 ,    -1.523 )
    STOP-RUN STATUS = STATSTOP = 11
```


RUN COMPLETED!
CPU TIME: 14.74 SECONDS

C.7   For $Y_s = 16.00$, $T = 0.00$

NAME OF THIS FILE: Y16T00   .DAT
THIS DATA FILE IS GENERATED BY "ELLC.FOR"
NAME OF EXTERNAL MASTER DATA FILE READ: LH.MASTER
NUMBER OF SURFACE POINTS USED: 5 (2 EACH, IN THE FRONT
    AND IN THE REAR OF THE ANTENNA LOCATION, RESPECTIVELY)

HELICOPTER FUSELAGE STARTS FROM Y =   2.000 TO Y =   50.000
ANTENNA LOCATION (IN THE XZ-PLANE CROSS-SECTION)
        = (YS,TINIT) = (16.000 ,   0.000)
ANTENNA LOCATION IN RECTANGULAR COORDINATES
        = (XS,YS,ZS) = (0.000 ,   16.000 ,   6.093)

AT YS =   16.000 :
    SEMI-MINOR AXIS OF THE BEST-FIT
        ELLIPSE IN THE XZ-PLANE = A1 =   0.029
    SEMI-MAJOR AXIS OF THE BEST-FIT
        ELLIPSE IN THE XZ-PLANE = B1 =   0.889
    CENTER OF BEST-FIT ELLIPSE = (XC,ZC) = (0.000 ,   6.166)

RUN HALTED: STATSTOP = 1
            ELLIPSE FIT IN THE XZ-PLANE CANNOT BE GENERATED.

RUN COMPLETED!
CPU TIME: 3.30 SECONDS

C.8   For $Y_s = 16.00$, $T = 0.03$

NAME OF THIS FILE: Y16T03   .DAT
THIS DATA FILE IS GENERATED BY "ELLC.FOR"
NAME OF EXTERNAL MASTER DATA FILE READ: LH.MASTER
NUMBER OF SURFACE POINTS USED: 5 (2 EACH, IN THE FRONT
    AND IN THE REAR OF THE ANTENNA LOCATION, RESPECTIVELY)

HELICOPTER FUSELAGE STARTS FROM Y =   2.000 TO Y =   50.000
ANTENNA LOCATION (IN THE XZ-PLANE CROSS-SECTION)
        = (YS,TINIT) = (16.000 ,   0.030)
ANTENNA LOCATION IN RECTANGULAR COORDINATES
        = (XS,YS,ZS) = (0.950 ,   16.000 ,   6.200)

AT YS =   16.000 :
    SEMI-MINOR AXIS OF THE BEST-FIT
        ELLIPSE IN THE XZ-PLANE = A1 =   0.200
    SEMI-MAJOR AXIS OF THE BEST-FIT
        ELLIPSE IN THE XZ-PLANE = B1 =   0.969
    CENTER OF BEST-FIT ELLIPSE = (XC,ZC) = (0.941 ,   6.006)

FUSELAGE CROSS-SECTION SAMPLING:

ANTENNA LOCATION IN YR-COORDINATES
        = (YS,RS) = (16.000 ,   0.194)

TO THE REAR OF THE ANTENNA LOCATION AT SPACING DY =   1.6000

i-th		RECTANGULAR		YR-COORDINATES	
CROSS		COORDINATES		AT PHIS =	2.59 DEG
SECTION	X	Y	Z	Y	R
2	0.948	17.600	6.171	17.600	0.165
3	0.950	19.200	6.203	19.200	0.197
4	0.950	20.800	6.202	20.800	0.196
5	0.949	22.400	6.182	22.400	0.176
6	0.950	24.000	6.200	24.000	0.194

.7	0.945	25.600	6.088	25.600	0.081
8	0.911	27.200	5.349	27.200	-0.658
9	0.859	28.800	4.197	28.800	-1.811
10	0.801	30.400	2.908	30.400	-3.101
11	0.746	32.000	1.713	32.000	-4.298
12	0.714	33.600	1.002	33.600	-5.009
13	0.712	35.200	0.945	35.200	-5.066
14	0.711	36.800	0.929	36.800	-5.082
15	0.710	38.400	0.899	38.400	-5.113
16	0.708	40.000	0.859	40.000	-5.152
17	0.705	41.600	0.804	41.600	-5.208
18	0.701	43.200	0.718	43.200	-5.294
19	0.695	44.800	0.583	44.800	-5.429
20	0.683	46.400	0.309	46.400	-5.703

TO THE FRONT OF THE ANTENNA LOCATION AT SPACING DY =   1.6000

i-th CROSS SECTION	X	RECTANGULAR COORDINATES Y	Z	YR-COORDINATES AT PHIS = 2.59 DEG Y	R
2	0.954	14.400	6.300	14.400	0.294
3	0.941	12.800	6.015	12.800	0.008
4	0.899	11.200	5.080	11.200	-0.927
5	0.835	9.600	3.673	9.600	-2.336
6	0.766	8.000	2.137	8.000	-3.873
7	0.716	6.400	1.030	6.400	-4.982
8	0.695	4.800	0.571	4.800	-5.441
9	0.652	3.200	-0.379	3.200	-6.392

THIS IS A "CASE 1" PROBLEM
STOP-RUN STATUS = STATSTOP =   8

WARNING: MAXIMUM ITERATIONS IN "ELLYR" MODULE EXCEEDED.
         CLOSE-FIT COMPOSITE ELLIPSOID MAY NOT BE GOOD.

PARAMETER VALUES FOR CLOSE-FIT COMPOSITE ELLIPSOID:

       AO =   0.208
       BO =   1.011
       CO =   5.466

```
DO =     0.250
YSH =     1.404
(XC,YC,ZC) = (     0.941 ,     14.442 ,     6.006 )
STOP-RUN STATUS = STATSTOP =   8
```

RUN COMPLETED!
CPU TIME: 11.44 SECONDS

C.9   For $Y_s = 2.10$, $T = 0.90$

```
NAME OF THIS FILE: Y21T90    .DAT
THIS DATA FILE IS GENERATED BY "ELLC.FOR"
NAME OF EXTERNAL MASTER DATA FILE READ: LH.MASTER
NUMBER OF SURFACE POINTS USED: 5 (2 EACH, IN THE FRONT
    AND IN THE REAR OF THE ANTENNA LOCATION, RESPECTIVELY)

HELICOPTER FUSELAGE STARTS FROM Y =   2.000 TO Y =   50.000
ANTENNA LOCATION (IN THE XZ-PLANE CROSS-SECTION)
      = (YS,TINIT) = (    2.100 ,     0.900 )
ANTENNA LOCATION IN RECTANGULAR COORDINATES
      = (XS,YS,ZS) = (   -0.529 ,     2.100 ,    -0.511 )

AT YS =    2.100 :
   SEMI-MINOR AXIS OF THE BEST-FIT
        ELLIPSE IN THE XZ-PLANE = A1 =     0.162
   SEMI-MAJOR AXIS OF THE BEST-FIT
        ELLIPSE IN THE XZ-PLANE = B1 =     0.432
   CENTER OF BEST-FIT ELLIPSE = (XC,ZC) = (   -0.590 ,    -0.665 )

RUN HALTED: STATSTOP =   3
            ELLIPSE FIT IN THE XZ-PLANE CANNOT BE GENERATED.
```

RUN COMPLETED!
CPU TIME: 7.37 SECONDS

C.10   For $Y_s = 35.00$, $T = 0.00$

```
NAME OF THIS FILE: Y35T00    .DAT
THIS DATA FILE IS GENERATED BY "ELLC.FOR"
NAME OF EXTERNAL MASTER DATA FILE READ: LH.MASTER
NUMBER OF SURFACE POINTS USED: 5 (2 EACH, IN THE FRONT
```

AND IN THE REAR OF THE ANTENNA LOCATION, RESPECTIVELY)

HELICOPTER FUSELAGE STARTS FROM Y =   2.000 TO Y =   50.000
ANTENNA LOCATION (IN THE XZ-PLANE CROSS-SECTION)
       = (YS,TINIT) = (35.000 ,   0.000)
ANTENNA LOCATION IN RECTANGULAR COORDINATES
       = (XS,YS,ZS) = (0.000 ,   35.000 ,   1.132)

AT YS =   35.000 :
   SEMI-MINOR AXIS OF THE BEST-FIT
        ELLIPSE IN THE XZ-PLANE = A1 =   2.428
   SEMI-MAJOR AXIS OF THE BEST-FIT
        ELLIPSE IN THE XZ-PLANE = B1 =   1.085
   CENTER OF BEST-FIT ELLIPSE = (XC,ZC) = (0.000 ,   -1.262)

FUSELAGE CROSS-SECTION SAMPLING:

ANTENNA LOCATION IN YR-COORDINATES
       = (YS,RS) = (35.000 ,   2.395)

TO THE REAR OF THE ANTENNA LOCATION AT SPACING DY =   1.6000

i-th CROSS SECTION	RECTANGULAR COORDINATES X	 Y	 Z	YR-COORDINATES AT PHIS = Y	 0.00 DEG R
2	0.000	36.600	1.125	36.600	2.387
3	0.000	38.200	1.103	38.200	2.365
4	0.000	39.800	1.080	39.800	2.343
5	0.000	41.400	1.057	41.400	2.319
6	0.000	43.000	1.033	43.000	2.295
7	0.000	44.600	1.008	44.600	2.270
8	0.000	46.200	0.983	46.200	2.245
9	0.000	47.800	0.957	47.800	2.220
10	0.000	49.400	0.932	49.400	2.194

TO THE FRONT OF THE ANTENNA LOCATION AT SPACING DY =   1.6000

i-th CROSS SECTION	RECTANGULAR COORDINATES X	 Y	 Z	YR-COORDINATES AT PHIS = Y	 0.00 DEG R

171

2	0.000	33.400	1.239	33.400	2.501
3	0.000	31.800	1.951	31.800	3.213
4	0.000	30.200	3.064	30.200	4.327
5	0.000	28.600	4.301	28.600	5.564
6	0.000	27.000	5.383	27.000	6.646
7	0.000	25.400	6.032	25.400	7.294
8	0.000	23.800	6.087	23.800	7.349
9	0.000	22.200	6.077	22.200	7.340
10	0.000	20.600	6.097	20.600	7.360
11	0.000	19.000	6.093	19.000	7.356
12	0.000	17.400	6.064	17.400	7.327
13	0.000	15.800	6.106	15.800	7.368
14	0.000	14.200	6.182	14.200	7.445
15	0.000	12.600	5.844	12.600	7.107
16	0.000	11.000	4.902	11.000	6.164
17	0.000	9.400	3.499	9.400	4.761
18	0.000	7.800	1.979	7.800	3.241
19	0.000	6.200	0.941	6.200	2.203
20	0.000	4.600	0.475	4.600	1.737
21	0.000	3.000	-0.377	3.000	0.885

THIS IS A "CASE 1" PROBLEM
STOP-RUN STATUS = STATSTOP = 10

SURFACE POINTS ARE NOT CONVEX IN THE PROPER DIRECTION.

RUN HALTED: STATSTOP = 10
          CLOSE-FIT COMPOSITE ELLIPSOID CANNOT BE GENERATED.

RUN COMPLETED!
CPU TIME: 16.28 SECONDS

C.11   For $Y_s = 49.00$, $T = 0.30$

NAME OF THIS FILE: ay49t30   .DAT
THIS DATA FILE IS GENERATED BY "ELLC.FOR"
NAME OF EXTERNAL MASTER DATA FILE READ: LH.MASTER
NUMBER OF SURFACE POINTS USED: 5 (2 EACH, IN THE FRONT
    AND IN THE REAR OF THE ANTENNA LOCATION, RESPECTIVELY)

HELICOPTER FUSELAGE STARTS FROM Y =   2.000 TO Y =   50.000

```
ANTENNA LOCATION (IN THE XZ-PLANE CROSS-SECTION)
        = (YS,TINIT) = (   49.000 ,     0.300 )
ANTENNA LOCATION IN RECTANGULAR COORDINATES
        = (XS,YS,ZS) = (      0.521 ,    49.000 ,    -0.574 )


AT YS =   49.000 :
    SEMI-MINOR AXIS OF THE BEST-FIT
        ELLIPSE IN THE XZ-PLANE = A1 =    0.329
    SEMI-MAJOR AXIS OF THE BEST-FIT
        ELLIPSE IN THE XZ-PLANE = B1 =    0.445
    CENTER OF BEST-FIT ELLIPSE = (XC,ZC) = (     0.097 ,    -0.564 )


FUSELAGE CROSS-SECTION SAMPLING:
--------------------------------


ANTENNA LOCATION IN YR-COORDINATES
        = (YS,RS) = (   49.000 ,    -0.424 )


ANTENNA LOCATION TOO CLOSE TO AN END POINT OF THE HELICOPTER FUSELAGE.
ADJUSTING ...


TO THE REAR OF THE ANTENNA LOCATION AT SPACING DY =    0.5000
```

i-th CROSS SECTION	RECTANGULAR COORDINATES			YR-COORDINATES AT PHIS = 91.40 DEG	
	X	Y	Z	Y	R
2	0.479	49.500	-0.573	49.500	-0.381
3	0.436	50.000	-0.572	50.000	-0.338

```
TO THE FRONT OF THE ANTENNA LOCATION AT SPACING DY =    1.6000
```

i-th CROSS SECTION	RECTANGULAR COORDINATES			YR-COORDINATES AT PHIS = 91.40 DEG	
	X	Y	Z	Y	R
2	0.653	47.400	-0.578	47.400	-0.556
3	0.777	45.800	-0.581	45.800	-0.680
4	0.645	47.500	-0.577	47.500	-0.548
5	0.685	47.000	-0.578	47.000	-0.587
6	0.724	46.500	-0.579	46.500	-0.626
7	0.762	46.000	-0.580	46.000	-0.665

8	0.799	45.500	-0.581	45.500	-0.702
9	0.836	45.000	-0.582	45.000	-0.739
10	0.872	44.500	-0.583	44.500	-0.774
11	0.906	44.000	-0.584	44.000	-0.809
12	0.940	43.500	-0.585	43.500	-0.843
13	0.972	43.000	-0.585	43.000	-0.875
14	1.004	42.500	-0.586	42.500	-0.907
15	1.034	42.000	-0.587	42.000	-0.937
16	1.062	41.500	-0.588	41.500	-0.965
17	1.089	41.000	-0.588	41.000	-0.992
18	1.115	40.500	-0.589	40.500	-1.018
19	1.138	40.000	-0.589	40.000	-1.041
20	1.160	39.500	-0.590	39.500	-1.063
21	1.180	39.000	-0.591	39.000	-1.083
22	1.198	38.500	-0.591	38.500	-1.101
23	1.213	38.000	-0.591	38.000	-1.116
24	1.226	37.500	-0.592	37.500	-1.129
25	1.237	37.000	-0.592	37.000	-1.140
26	1.245	36.500	-0.592	36.500	-1.148
27	1.251	36.000	-0.592	36.000	-1.154
28	1.254	35.500	-0.592	35.500	-1.157
29	1.251	35.000	-0.592	35.000	-1.154
30	1.245	34.500	-0.592	34.500	-1.148

THIS IS A "CASE 1" PROBLEM
STOP-RUN STATUS = STATSTOP = 17

WARNING: ANTENNA LOCATION IS TOO CLOSE TO AN END POINT
         IN THE YR-PLANE. CLOSE-FIT COMPOSITE ELLIPSOID
         MAY NOT BE GOOD.

PARAMETER VALUES FOR CLOSE-FIT COMPOSITE ELLIPSOID:

     AO =   0.462
     BO =   0.624
     CO =   7.558
     DO =   -0.605
     YSH =   3.817
     (XC,YC,ZC) = (0.097 ,   43.700 ,   -0.564)
     STOP-RUN STATUS = STATSTOP = 17

RUN COMPLETED!
CPU TIME: 16.66 SECONDS

C.12   For $Y_s = 16.00$, $T = 0.00$

NAME OF THIS FILE: ay16t00   .DAT
THIS DATA FILE IS GENERATED BY "ELLC.FOR"
NAME OF EXTERNAL MASTER DATA FILE READ: LH.MASTER
NUMBER OF SURFACE POINTS USED: 5 (2 EACH, IN THE FRONT
    AND IN THE REAR OF THE ANTENNA LOCATION, RESPECTIVELY)

HELICOPTER FUSELAGE STARTS FROM Y =   2.000 TO Y =   50.000
ANTENNA LOCATION (IN THE XZ-PLANE CROSS-SECTION)
       = (YS,TINIT) = (16.000 ,   0.000)
ANTENNA LOCATION IN RECTANGULAR COORDINATES
       = (XS,YS,ZS) = (0.000 ,   16.000 ,   6.093)

AT YS =   16.000 :
   SEMI-MINOR AXIS OF THE BEST-FIT
       ELLIPSE IN THE XZ-PLANE = A1 =   0.029
   SEMI-MAJOR AXIS OF THE BEST-FIT
       ELLIPSE IN THE XZ-PLANE = B1 =   0.889
   CENTER OF BEST-FIT ELLIPSE = (XC,ZC) = (0.000 ,   6.166)

RUN HALTED: STATSTOP = 1
            ELLIPSE FIT IN THE XZ-PLANE CANNOT BE GENERATED.

RUN COMPLETED!
CPU TIME: 3.55 SECONDS

175

Bibliography

[1] W. D. Burnside; J. J. Kim; B. Grandchamp; R. G. Rojas; P. H. Law; "Airborne Antenna Radiation Pattern Code User's Manual;" Technical Report 716199-4; The Ohio State University, ElectroScience Laboratory, Department of Electrical Engineering, Columbus, Ohio; September 1985.

[2] F. T. Klevenow; B. G. Lynch; E. H. Newman; R. G. Rojas; J. T. Scheick; H. T. Shamansky; K. Y. Sze; "The Helicopter Antenna Radiation Prediction Code (HARP);" Technical Report 722792-1; The Ohio State University, ElectroScience Laboratory, Department of Electrical Engineering, Columbus, Ohio; August 1990.

[3] R. G. Kouyoumjian; P. H. Pathak; "A Uniform Geometrical Theory of Diffraction for an Edge in a Perfectly-Conducting Surface;" Proc. IEEE, vol. 62, pp. 1448-1461; November 1974.

[4] P. H. Pathak; N. Wang; W. D. Burnside; R. G. Kouyoumjian; "A Uniform GTD Solution for the Radiation from Sources on a Convex Surface;" IEEE Trans. on Antennas and Propagation, vol. AP-29, No. 4, pp. 609-622; July 1981.

[5] R. G. Kouyoumjian; P. H. Pathak; W. D. Burnside; "A Uniform GTD for the Diffraction by Edges, Vertices, and Convex Surfaces;" *Acoustic, Electromagnetic and Elastic Wave Scattering - Focus on the T-Matrix Approach;* V. K. Varadan, V. V. Varadan, Eds.; Pergamon Press, New York; 1980; pp. 373-397.

[6] B. R. Levy; J. B. Keller; "Part I: Applications of the Geometrical Theory of Diffraction;" Communications on Pure and Applied Mathematics, vol. XII, pp. 159-209; 1959.

[7] R. G. Rojas; W. D. Burnside; "GTD Analysis of Airborne Antennas Radiating in the Presence of Lossy Dielectric Layers;" Technical Report 710964-8; The Ohio State University, ElectroScience Laboratory, Department of Electrical Engineering, Columbus, Ohio; August 1981.

[8] R. F. Harrington; *Field Computations by Moment Methods;* MacMillan Publishing Company, New York; 1984.

[9] W. H. Press; B. P. Flannery; S. A. Teukolsky; W. T. Vetterling; *Numerical Recipes: The Art of Scientific Computing*; Cambridge University Press, Cambridge; 1986.

[10] D. L. Luenberger; *Linear and Nonlinear Programming*, 2nd. ed.; Addison-Wesley Publishing Company, Reading, Massachusetts; 1984.

[11] C. F. Gerald; *Applied Numerical Analysis*, 2nd. ed.; Addison-Wesley Publishing Company, Reading, Massachusetts; 1980.

722792-2, "Automated Composite Ellipsoid Modelling for High Frequency GTD Analysis," K. Sze, R. Rojas, F. Kevenow & Scheick, September 1991